



This document was prepared for the ETI by third parties under contract to the ETI. The ETI is making these documents and data available to the public to inform the debate on low carbon energy innovation and deployment.

Programme Area: Marine

Project: PerAWAT

Title: Tidal Array Scale Numerical Modelling Interactions within a Farm (Steady Flow)

Abstract:

This report describes the formulation of and results obtained from an actuator disk model of a tidal turbine. The presented work falls into the first category of farm scaled models, namely blade modelled/turbine resolved three dimensional Reynolds averaged Navier-Stokes (RANS) simulations. Output from these models will be used for the development of shallow water equation models of turbines which are to be incorporated into basin scale models in WG2 WP3. The advantages of using a model of this type in a RANS simulation is that the time to solution is much faster than for blade-resolved models allowing small arrays of turbines to be modelled.

Context:

The Performance Assessment of Wave and Tidal Array Systems (PerAWaT) project, launched in October 2009 with £8m of ETI investment. The project delivered validated, commercial software tools capable of significantly reducing the levels of uncertainty associated with predicting the energy yield of major wave and tidal stream energy arrays. It also produced information that will help reduce commercial risk of future large scale wave and tidal array developments.

Disclaimer:

The Energy Technologies Institute is making this document available to use under the Energy Technologies Institute Open Licence for Materials. Please refer to the Energy Technologies Institute website for the terms and conditions of this licence. The Information is licensed 'as is' and the Energy Technologies Institute excludes all representations, warranties, obligations and liabilities in relation to the Information to the maximum extent permitted by law. The Energy Technologies Institute is not liable for any errors or omissions in the Information and shall not be liable for any loss, injury or damage of any kind caused by its use. This exclusion of liability includes, but is not limited to, any direct, indirect, special, incidental, consequential, punitive, or exemplary damages in each case such as loss of revenue, data, anticipated profits, and lost business. The Energy Technologies Institute does not guarantee the continued supply of the Information. Notwithstanding any statement to the contrary contained on the face of this document, the Energy Technologies Institute confirms that the authors of the document have consented to its publication by the Energy Technologies Institute.

PerAWaT (MA 1003) Report

WG3 WP2 D5a

**Tidal array scale numerical modelling.
Interactions within a farm (Steady Flow).**

Participant lead on the deliverable: DM Ingram

Other participant: DA Olivieri

Institute for Energy Systems

School of Engineering

The University of Edinburgh

King's Buildings, Edinburgh EH9 3JL

Not to be disclosed other than in line with the terms of the
Technology Contract

August 2012

Executive summary	3
Chapter 1. Actuator disk models	7
1. Implementation	11
Chapter 2. Depth averaged analysis	13
1. Shallow water equations	13
Chapter 3. Results	19
1. Single turbine flume test	19
2. Array of turbines in series	36
3. Staggered array of turbines	60
Appendix A. Production of Depth averaged data using VisIt	83
Appendix B. Contents of the Accompanying CD	89
Appendix C. usinv.f90	91
Appendix D. ustsns.f90	107
Appendix. Bibliography	121
Contents	

Executive summary

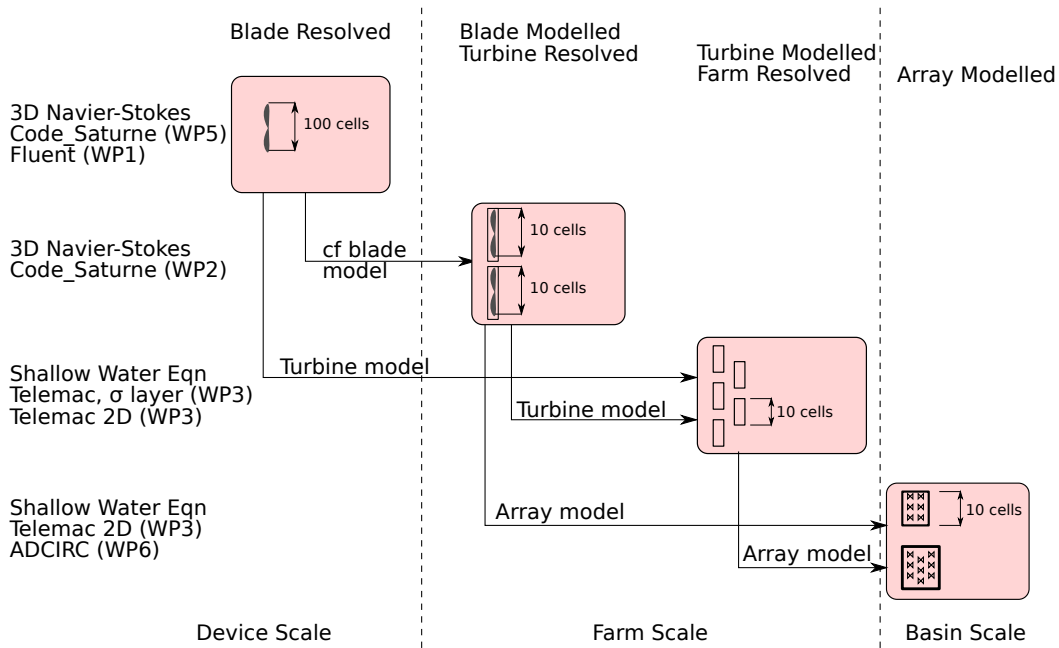


FIGURE 1. Interaction of the various scales of turbine model within the WG3 of the PerAWAT project

This report describes the formulation of and results obtained from an actuator disk model of a tidal turbine. The presented work falls into the first category of farm scaled models, namely *blade modelled/turbine resolved* three dimensional Reynolds averaged Navier-Stokes (RANS) simulations. Output from these models will be used for the development of shallow water equation models of turbines which are to be incorporated into basin scale models in WG2 WP3. The advantages of using a model of this type in a RANS simulation is that the time-to solution is much faster than for blade-resolved models allowing small arrays of turbines to be modelled.

In addition to describing the formulation of the model it has been applied to the simulation of three test cases. The first case is for a single three bladed horizontal axis tidal turbine in a flume. This test case is based on the experiments performed in the EDF flume in Chattou which have previously been modelled by the University of Oxford. Comparisons to the predicted thrust and power coefficient distributions as functions of tip-speed ratio are made with these results and with the results from the EDF experiments. The coefficients used for the actuator disk model are drawn from information derived from blade resolved simulations performed in Edinburgh (in WP5) and from lift/drag data from Garad-Hassan's `Tidal-Bladed` programme.

The second and third cases model experiments performed on arrays of turbines by Manchester University. In these simulations the centre rows of a very wide array are modelled and the two cases considered represent rotors in series (i.e. directly downstream of each other) and in a staggered grid. Comparisons of predicted thrust and power coefficient distributions as functions of tip-speed ratio are made against data from the Manchester tests.

Finally, following discussions at sub-project technical meetings, a depth averaging analysis has been performed on the results obtained from the simulations. By presenting the velocity and turbulence information in this way models of turbine for shallow water simulations can be checked and calibrated, providing for the first time, detailed information for this purpose. The depth averaging analysis of the three dimensional RANS results is only possible because of recent advances in flow visualisation tools which allow statistical information, including mean values, to be derived from fully three dimensional data.

The work presented in D5a concentrates on steady-state cases where the mean upstream turbulent flow onto the turbine (or array) is of constant and uniform velocity. The subsequent deliverable D5b will examine unsteady flow. It is important to note that the blade element momentum (BEM) model used to model the rotor makes an assumption of steady flow onto the rotor disk. In the unsteady simulations this assumption will be violated, but such a violation is acceptable provided that the time scales inherent in the unsteady flow are slower than that associated with the blade passing frequency of the turbine.

Deliverable D5a comprises:

- (1) input files for chosen configurations (on the accompanying CD)
- (2) report on the implementation of the parametric model and the simulation of the selected farm layouts, and an assessment of the models ability to characterise the farm, under steady turbulent flow conditions (this report).
- (3) report on the structure of the parametric description of the wake of an array of horizontal axis turbines (to be provided to WG3 WP3 D3 and WG3 WP6 D5) for steady turbulent flow (see the depth averaged analysis presented in chapter 3).

The acceptance criteria for this report are:

- (1) `Code_Saturne` input and output files for the selected configurations.

These are on the accompanying CD, the file structure on the CD is described in Appendix B and also in the README file on the CD's top level directory.

- (2) Report describes the following (for steady turbulent flow conditions)
 - (a) Describe chosen farm configurations

The chosen farm configurations are discussed in the results chapter in §3.1 for the single turbine case, §3.2 for two rows of turbines in series, and §3.3 for two rows of turbines in a staggered arrangement.

- (b) assumptions and algorithms behind the model; guidance on interpretation of results including assessment of farm performance; interpretation and discussion of results; discussion of applications and limitations.

The actuator disk model is described in detail in chapter 1, this chapter also includes details of the implementation of the model within `Code_saturne` and details of the model's limitations

- (3) The basic structure of the parametric description of the wake of an array of horizontal axis will be defined (i.e. number and identification of key parameters, and the relationships between them).

The approach taken to parameterise the wake for use in shallow water models is described in chapter 2. A detailed tabular presentation of the depth averaged results, together with summary pseudo-colour mosaic plots, are presented in §3.1 for the single turbine case, §3.2 for two rows of turbines in series, and §3.3 for two rows of turbines in a staggered arrangement.

CHAPTER 1

Actuator disk models

Actuator disk models make it possible to simulate the effects of a rotor within a three dimensional Reynolds averaged Navier-Stokes simulation without the need to resolve the individual blades of the rotor. As such the actuator disk models are much more computationally efficient than blade resolved models, requiring an order of magnitude less mesh points. The actuator disk region is a part of the computational domain where the presence of the rotor is accounted for by adding momentum to (in the case of a fan) or removing momentum from (in the case of a turbine) the fluid explicitly using a source term. Actuator disk models can be used when we have information about how the rotor behaves on its own and we want to know how it affects its surroundings. These models have been widely applied to wind turbines (e.g. Mikkelsen [2003]). They are based on an extension of the Froude momentum theory and can be applied to a range of problems where a sudden discontinuities in flow properties occurs [Horlock, 1978].

The actuator disk model approximates the forces the turbine device applies to the flow, by spreading the rotor blade forces over the swept disk volume with the same diameter as that of the rotor in question. The solution to the flow problem is captured in a Reynolds Averaged Navier-Stokes (RANS) equation as a contributing source term S_i . The RANS equations are time-averaged equations of motion for fluid flow, which used together with approximations based on knowledge of the properties of flow turbulence, give approximate time-averaged solutions to the NavierStokes equations. For a stationary, incompressible Newtonian fluid, these equations can be written in Einstein notation as:

$$(1) \quad \rho \overline{u_j} \frac{\partial \overline{u_i}}{\partial x_j} = \rho \overline{f_i} + \frac{\partial}{\partial x_j} \left[-\overline{p} \delta_{ij} + \mu \left(\frac{\partial \overline{u_i}}{\partial x_j} + \frac{\partial \overline{u_j}}{\partial x_i} \right) - \overline{\rho u'_i u'_j} \right] + \overline{S_i},$$

where $\overline{u_i}$ and $\overline{u_j}$ are the time averaged velocity components in the x_i and x_j coordinate directions, \overline{p} is the time averaged pressure, ρ is the constant fluid density, δ_{ij} is the Kronecker delta function, $\overline{S_i}$ is the time averaged value of the source term due to the forces experienced on a fluid element within the actuator disk (see figure 1) and $\overline{\rho u'_i u'_j}$ is the time average of the fluctuating (turbulent) momentum. This last term cannot be determined analytically and must be modelled using an empirical turbulence model.

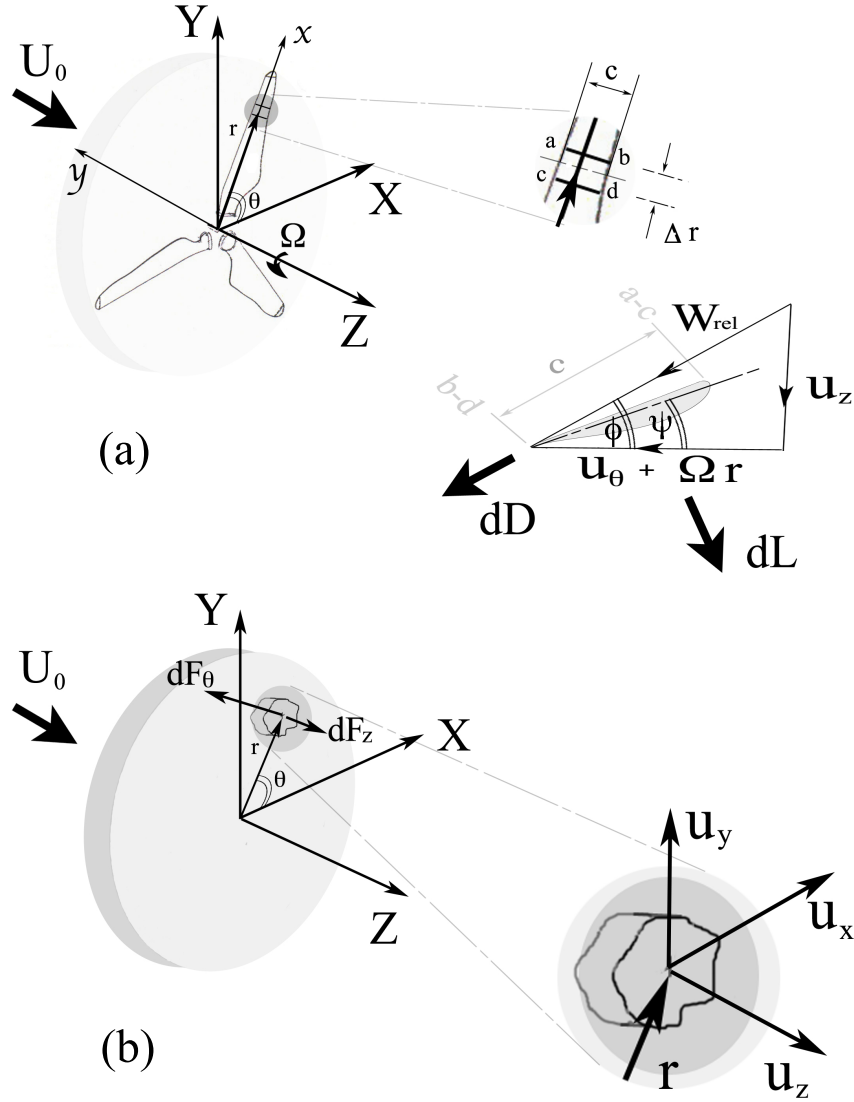


FIGURE 1. Details of the actuator disk model involving (a) a view of a Blade Element at r from the rotating blades and its equivalent effect (b) seen as a RANS source term S_i at r and θ .

The source term S_i is derived from considering the forces experienced on a fluid element within the actuator disk, see figure 1. The source term is defined as:

$$(2) \quad S_i = -\frac{dF_i}{V_{cell}},$$

where V_{cell} is the volume of the particular finite volume in the disc region, at a radial position r and an azimuthal coordinate θ .

The force dF_i is derived using blade element momentum theory [Hansen, 2001]. Here the theory is applied to compute the forces on the fluid element arising from an N bladed tidal turbine, rotating at a speed Ω . The rotor plane is split into a number of finite annuli of width δr , located at a radius, r , with the effects of the N blades smeared out of the 2π radians of the rotor plane (Figure 1). Writing the blade element forces $dF_{L,Dcell} = \{-dF_\theta \sin \theta, dF_\theta \cos \theta, dF_z\}$ in blade fixed coordinates at r , (Figure1(b)) leads to

$$(3) \quad dF_{L,Dcell} = \frac{N\delta A f_{L,D}}{(2\pi r)},$$

where δA is the frontal area of the disc element and $f_{L,D}$ is instantaneous sectional rotor forces due to local lift dL and drag dD of each blade of the N rotating blades of the rotor. The sectional rotor force $f_{L,D}$ is derived from the two dimensional α vs C_L/C_D tables for the particular airfoil blade section design involved in the blade design at radial position r . If we considered the fact that $f_{L,D} = f(dF_\theta, dF_z)$, then for dF_θ and dF_z we get

$$(4) \quad dF_\theta = 0.5\rho c W_{rel}^2 F(C_L \sin \phi - C_D \cos \phi)$$

$$(5) \quad dF_z = 0.5\rho c W_{rel}^2 F(C_L \cos \phi + C_D \sin \phi)$$

where W_{rel} , c , ρ and F are the blade element relative flow velocity, local blade chord, density ρ and Prandtl tip loss factor [Prandtl and Betz, 1927]. This expressed mathematically as

$$(6) \quad F = \frac{2}{\pi} \arccos \left[\exp\left(-\frac{N(R-r)}{2r \sin \phi}\right) \right]$$

where R is the tip radius of the rotor. The blade element flow velocity W_{rel} is the flow velocity experienced by each sweeping blade in the plane of the disc and can be accounted for by the simple flow analysis shown in figure1(a), involving u_z , Ωr and u_θ . Where u_θ is the circumferential velocity at r and θ which is simply

$$(7) \quad u_\theta = -u_x \sin \theta + u_y \cos \theta$$

As the model proceeds the values of u_z and u_θ , provided by the solution of the Navier Stokes equation(1), will change for a given free stream velocity U_0 and rotor rotational speed Ω until the flow field has converged to steady state condition. The angle of attack, α , of the blade elements will also change during flow calculation, since $\alpha = \phi - \psi$. This is found using the given blade element blade twist angle, ψ , and the calculated local blade element flow angle ϕ (Figure1(a)). This dependency also means that the forces on

the rotor change as the solution converges, since both the coefficients of lift and drag, (C_L and C_D) also depend on the local angle of attack, α .

In setting up the `Code_Saturne` simulations for all the cases presented in this report employed, the `usinv.f90`, `ustsns.f90` user subroutines must be modified to incorporate the actuator disk model. The `Code_Saturne` user manual [EDF, 2012] details of the procedure for implementing both explicit and implicit source terms for the u_x , u_y and u_z momentum equations. The implicit and explicit components of the source term are linearised by using a first-order Taylor expansion. Considering (1):

$$(8) \quad \rho \frac{\partial u_i}{\partial t} + \dots = \dots + f(u_i).$$

The source $f(u_i)$ can be expressed as non-linear source term of the form $f(u_i) = -K_i u_i^2$. Note K_i is effectively a force resistance coefficient equivalent to

$$(9) \quad K_i \equiv \frac{(dF_{L,Dcell})_i}{V_{cell} W_{rel}^2}.$$

With reference to (3) for the terms employed in (9). As a result the source term $f(u_i)$ must decompose into an implicit $crvimp_i$ part and an explicit $crvexp_i$ part in accordance with `Code_Saturne` finite volume solver [EDF, 2012] such that

$$(10) \quad crvimp_i = V_{cell} \frac{df}{du_i} \left(u_i^{(n)} \right), \text{ and}$$

$$(11) \quad crvexp_i = V_{cell} \left[f \left(u_i^{(n)} \right) - \frac{df}{du_i} \left(u_i^{(n)} \right) u_i^{(n)} \right].$$

Applying each of these decompositions to the three, u_x , u_y and u_z , momentum equations we obtain:

$$(12) \quad \begin{aligned} crvimp_x &= 2K_x(\Omega r + u_\theta) \sin \theta \\ crvexp_x &= -K_x (W_{rel}^2 + 2(\Omega r + u_\theta)u_x \sin \theta) \end{aligned}$$

$$(13) \quad \begin{aligned} crvimp_y &= -2K_y(\Omega r + u_\theta) \cos \theta \\ crvexp_y &= -K_y (W_{rel}^2 - 2(\Omega r + u_\theta)u_y \cos \theta) \end{aligned}$$

and

$$(14) \quad \begin{aligned} crvimp_z &= -2K_x u_z \\ crvexp_z &= K_x (u_z^2 - (\Omega r + u_\theta)^2) \end{aligned} \cdot$$

Furthermore, it is necessary that the computation grid used resolves the rotor plane with sufficient fidelity that the actuator disk model influences the overall flow field. The best results are obtained when nacelle of the turbine (and possibly the supporting structure)

are gridded as solid volumes within the computational grid. Chapter 3 discusses the computational setup for both the single and multi-array turbine models.

1. Implementation

This model is implemented in the `ustsns.f90` and `usinv.f90` user routines to enable the solver to effectively model the flow around the actuator disk. Full listings of the Fortran-90 code for both of the user routines (for the two turbines in series case) are presented in appendices C and D. The `usinv.f90` subroutines are called when the solver first starts up and are used to initialise the actuator disk model. `usinv.f90` reads `blade.txt`, a data file which describes the blade section of the rotor.

The following data is taken from the `blade.txt` file for the case with two turbines in series.

```
0.001 38.3667 0.015 1.0 Circle Circle
0.015 38.3667 0.015 1.0 Circle Circle
0.0325 22.8758 0.02 0.04 Goe804 Goe804
0.045 16.0 0.03 0.04 Goe804 Goe804
0.059 11.3441 0.0275 0.04 Goe804 Goe804
0.0725 8.96169 0.025 0.04 Goe804 Goe804
0.085 7.4854 0.022326 0.04 Goe804 Goe804
0.099 5.77244 0.019486 0.04 Goe804 Goe804
0.1125 4.12977 0.0175 0.04 Goe804 Goe804
0.125 3.08001 0.015454 0.04 Goe804 Goe804
0.135 2.57973 0.013 0.04 Goe804 Goe804
-1 -1 -1 -1 -1 -1
```

Each line of the file describes a particular slice through the rotor: The first column of the data file contains the radial ordinate of the section (in meters), the second contains the twist angle (in degrees), the third the chord length (in meters), the fourth the relative thickness and the final two columns contain the

file names of the tables containing the lift and drag data. The last row of the input file is indicated by the entry of -1 in each column.

When information is needed for a radial station not found in the file, the information needed to compute the forces on the actuator disk element are found by interpolating between the two nearest radial stations.

The lift/drag data files follow a similar format, for example the `Circle.txt` contains:

```
-90 0.0 3.00E-01
2 0.0 3.00E-01
4 0.0 3.00E-01
6 0.0 3.00E-01
8 0.0 3.00E-01
10 0.0 3.00E-01
12 0.0 3.00E-01
```

```
14 0.0 3.00E-01
16 0.0 3.00E-01
18 0.0 3.00E-01
180 0.0 3.00E-01
-999 -999 -999
```

In this file each line contains an angle of attack (in degrees) followed by the lift and drag coefficients. The file is terminated by the entry of -999 in each column. As with the `blade.txt` data, if an angle of attack is needed which is not explicitly given in the file the required lift and drag values are interpolated from the nearest entries in the table.

CHAPTER 2

Depth averaged analysis

1. Shallow water equations

Shallow water flow codes, like those in the TELEMAC suite [Moulinec et al., 2011], are based on a depth-averaged model of the fluid equations. This approach is taken to reduce the computational costs associated with flow simulations over large geographic areas, as even with modern high performance computers it is inconceivable that basin scale three dimensional Reynolds averaged Navier-Stokes models could be applied to engineering applications.

The depth-averaged two-dimensional flow equations (the so-called shallow water equations) are obtained, as the name suggests, by averaging the Reynolds equations over the depth. The following conditions have to be met in order for the shallow water equations to be applicable:

- vertical momentum exchange is negligible and the vertical velocity component w is a lot smaller than the horizontal components u and v , i.e.

$$w \ll u \text{ and } w \ll v.$$

- the pressure gain is linear with the depth (i.e. there is a hydrostatic pressure distribution), i.e.

$$p \approx \rho g z.$$

For simplicity of exposition we will consider the one-dimensional form of the shallow water equations (some times called the St. Venant equations):

$$(15) \quad \frac{\partial}{\partial t} \begin{pmatrix} \phi \\ \phi u \end{pmatrix} + \frac{\partial}{\partial x} \begin{pmatrix} \phi u \\ \phi u^2 + \frac{1}{2} \phi^2 \end{pmatrix} = \begin{pmatrix} 0 \\ g(S_0 - S_f) - T \end{pmatrix}$$

where $\phi = gh$ is the geopotential, u is the velocity, S_0 is the slope of the channel, S_f is the Chezy friction term, and T is the momentum sink associated with the presence of a turbine. The equations can be simplified even further by writing them in their homogeneous form;

$$(16) \quad \frac{\partial}{\partial t} \begin{pmatrix} \phi \\ \phi u \end{pmatrix} + \frac{\partial}{\partial x} \begin{pmatrix} \phi u \\ \phi \bar{u}^2 + \frac{1}{2} \phi^2 \end{pmatrix} = 0.$$

The first equation conserves energy, measured in terms of the local head of water, ρgh and the second equation conserved momentum, $\rho gh u$. Since these equations have been

obtained by averaging the Navier-Stokes equations over the water column, the velocity, u , should properly be written as

$$\bar{u} = \frac{1}{h} \int_{-h}^0 u(z) dz,$$

where h is the, local, water depth. Giving,

$$(17) \quad \frac{\partial}{\partial t} \left(\frac{\phi}{\phi \bar{u}} \right) + \frac{\partial}{\partial x} \left(\phi u^2 + \frac{1}{2} \phi^2 \right) = 0.$$

Although it is unlikely that these conditions hold in the neighbourhood of a tidal turbine it has been found that the shallow water equations can give acceptable solutions for other problems which violate the assumptions (for example wave overtopping of breakwaters, see Richardson et al. [2002, 2003]) and they can also provide useful engineering design information. Furthermore the time-to-solution for models based on the shallow water equation is several orders of magnitude faster than three-dimensional Navier-Stokes simulations with free surfaces [Ingram et al., 2005].

Shallow water models for tidal current interactions can prove highly effective for domains in which the lateral dimensions greatly exceed the vertical [Bryden et al., 2007] where they represent solutions of a simplified form of the Navier-Stokes equations. In many locations, there is unlikely to be sufficient boundary condition information to justify a full 3D analysis, even if such an approach were practical computationally. Modellers generally have to be content with a combination of outputs from acoustic depth profilers and, in the best described environments, with surface radar measurements. Regrettably, depth profilers do not give comprehensive area information and are limited in the accuracy of their output as a result of spatial uncertainty, while radar gives no indication of conditions below the surface. Neither profilers nor surface radar, even in combination, will give a comprehensive boundary description.

Shallow water models can be extended using a multi-layer interpretation, when there is a need to consider issues associated with depth velocity profiles in the absence of significant upwelling. In such cases, it becomes inappropriate to simply represent the energy extraction process through an artificial increase in the bed friction over a defined area of the sea bed. However, the actuator disk approach remains applicable.

In the following section a method for depth averaging three dimensional, Reynolds averaged, Navier-Stokes simulation results is described. This approach was discussed in a technical meeting of WG3 at Chattou in Paris and it was agreed that the results would be post-processed to produced depth averaged output which could be used for the development of boundary conditions and actuator disk models for shallow water solvers. Data presented in this way can also be used for direct validation of shallow water simulations.

1.1. Depth averaging. In designing source terms to model tidal turbines in shallow water flows, based on either three-dimensional Navier-Stokes simulations or on experimental data, it is thus necessary to examine the depth averaged quantities such as: the velocity components \bar{u} , \bar{v} ; the depth averaged total pressure (which can be equated

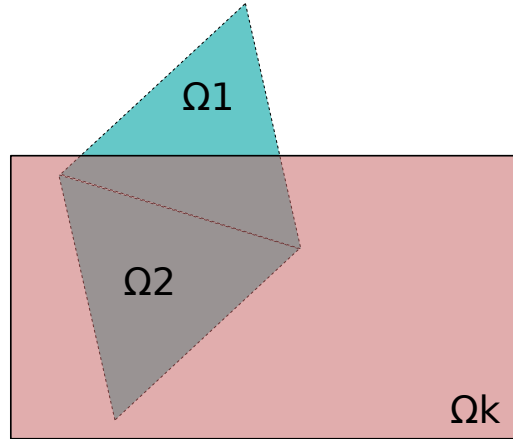


FIGURE 1. Volume weighted averaging inclusion condition for two computation cells ($j = 1$ and $j = 2$). Cell $j = 1$ is not included in the volume weighted average for bin k computed using equation (18), while cell $j = 2$ is.

to total head), \bar{P} ; and, depth averaged measures of turbulence, \bar{k} . Fortunately modern scientific visualisation and analysis tools now include routines for performing statistical analysis on three dimensional data from simulations and experiments.

In the present analysis the methodology described by Joy et al. [2007] has been applied, using the VisIt flow analysis tool [Childs et al., 2005]. In this approach the stream-wise and cross-flow directions are divided into a number of discrete bins over the domain of interest (Figure 3). The flow variable under consideration is then averaged for all computational cells contained within the bin using a volume weighted average, i.e.

$$(18) \quad \bar{q}_k = \frac{1}{\sum_j v_j} \sum_j v_j q_j \quad \forall j \text{ st } \Omega_j \in \Omega_k$$

where Ω_j is the j^{th} control volume and Ω_k is the discrete bin. Figure 1 illustrates the selection criteria for including computation cells in the volume weighted average for a given bin.

Figures 2 and 3 show the three dimensional velocity magnitude field and the binned depth averaged data from one of the simulations of the single turbine tested in the EDF flume. In this case results are presented for a tip-speed ratio of 4.0, a more detailed depth averaged analysis is presented later. Figure 3 is a mosaic plot where each of the discrete bins is coloured using a pseudo-colour to represent the exact value of the depth averaged velocity magnitude. In each of the mosaic plots presented in this report the bin colour is found by linear interpolation of the hue from 240° (blue) to 0° (red) using

TABLE 1. Depth averaged velocity magnitude data for the single turbine tested in the EDF fume at a TSR of 4.0, using 9 stream wise bins and 21 cross flow bins. The value for the cell containing the turbine has been underlined and only the right hand half of the flow domain is show.

stream wise direction \rightarrow								
0.2420	0.2441	0.2432	0.2422	0.2415	0.2415	0.2415	0.2415	0.2415
0.2579	0.2584	0.2576	0.2579	0.2575	0.2574	0.2574	0.2574	0.2574
0.2596	0.2599	0.2587	0.2586	0.2581	0.2581	0.2580	0.2580	0.2580
0.2613	0.2617	0.2603	0.2601	0.2596	0.2596	0.2596	0.2595	0.2595
0.2682	0.2714	0.2689	0.2674	0.2670	0.2669	0.2669	0.2669	0.2669
0.2641	0.2674	0.2633	0.2630	0.2627	0.2627	0.2626	0.2626	0.2626
0.2679	0.2707	0.2685	0.2677	0.2678	0.2678	0.2678	0.2678	0.2678
0.2659	0.2657	0.2666	0.2657	0.2660	0.2661	0.2661	0.2661	0.2661
0.2700	0.2704	0.2717	0.2705	0.2712	0.2714	0.2714	0.2714	0.2714
0.2659	<u>0.2671</u>	0.2660	0.2669	0.2691	0.2692	0.2692	0.2692	0.2692

the HSV colour model [Foley and Van Dam, 1982]. The hue of the cell is

$$H_{cell} = u_{cell} \frac{240}{u_{min} - u_{max}},$$

while the saturation and value of the cell are both set to 1. Plots of this kind are widely used for the representation of discrete data and are closely related to the pseudo-colour plots used to present the three dimensional results in this report and to the voxel techniques used in medical imaging [Foley and Van Dam, 1982; Halse et al., 1991; Ihaka and Gentleman, 1996; Larkin, 1992]. They are implemented in statistical packages such as R [Crawley, 2007] and in CFD visualisation tools such as VisIt [Childs et al., 2005].

The bins need to be sufficiently large to contain a number of cells, but since the grids associated with basin scale shallow water simulations will be much coarser than those used in the high-resolution three dimensional simulations this is not an issue. If the bins are too small then larger computational grid cells will not be contained entirely within them, and therefore not included in the volume weighted average, leading to missing values. In cases where the flow field is expected to be symmetric in the cross-flow direction (for example with single turbines and turbines in series) it is important that there is an odd number of bins in that direction.

Binned data can be plotted (Fig 3) or exported in tabular form (Table 1). Once the depth averaged fields have been computed depth-averaged velocity distributions down stream of the array can be extracted and plotted if required. For coarser grain shallow water models the depth averaged quantities in the table can be aggregated to estimate source terms and provided validation data.

Appendix A contains instructions for the production of depth averaged data using the VisIt program.

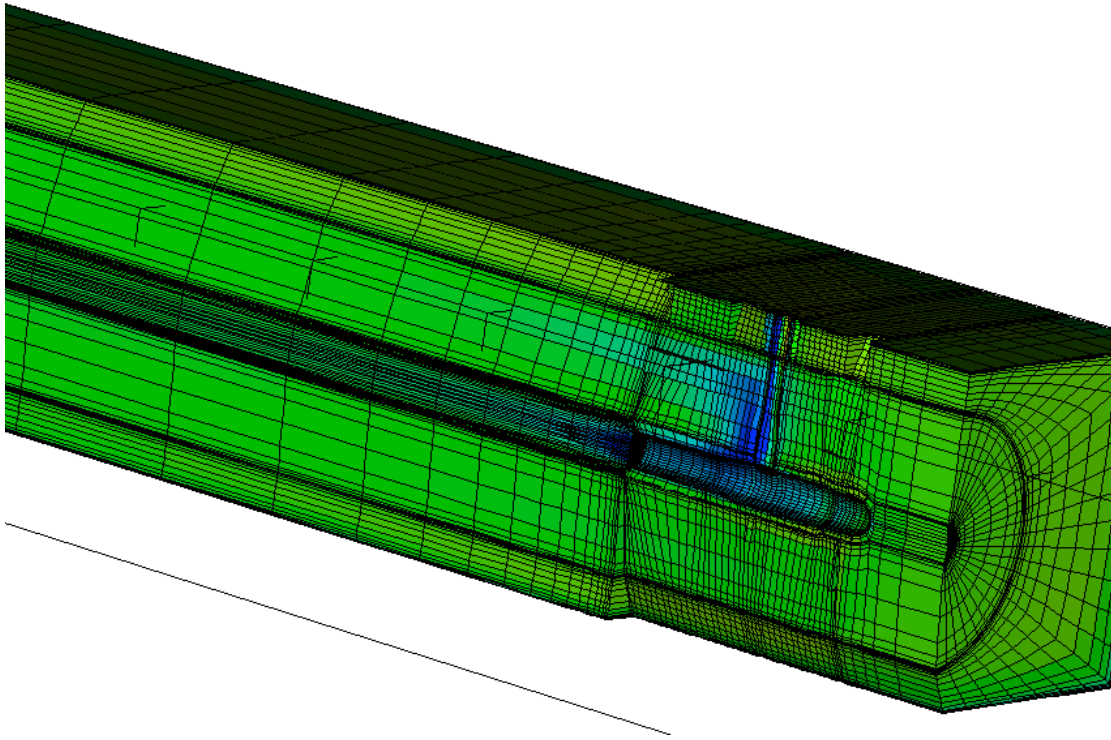


FIGURE 2. Velocity magnitude mosaic plot showing a section through the model single turbine tested in the EDF flume

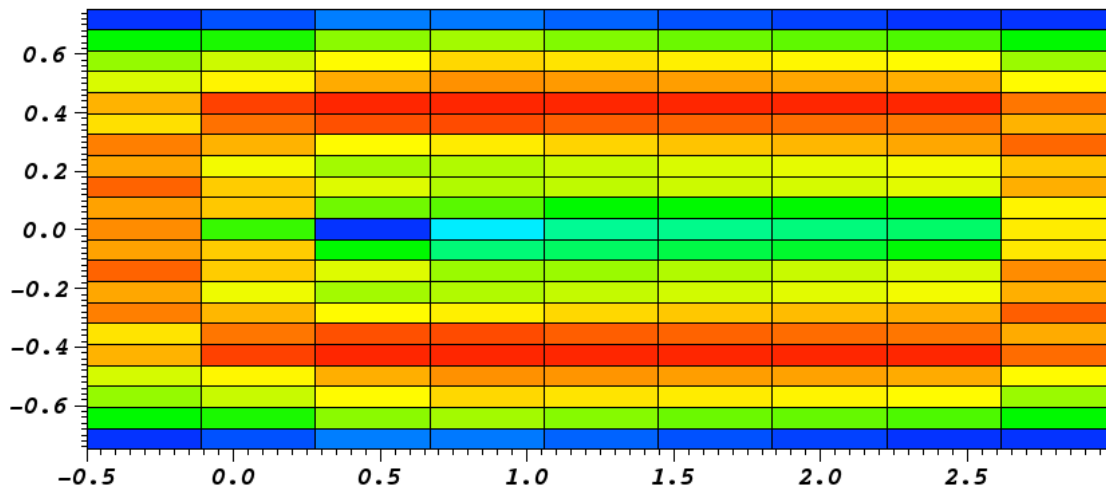


FIGURE 3. Velocity magnitude mosaic plot showing depth averaged analysis for the single turbine tested in the EDF, uses 9 stream wise bins and 21 cross flow bins. The centre of the turbine face is located at (0.0, 0.0)

CHAPTER 3

Results

With all of the cases presented in this report, there are two steps in setting up an actuator disk simulation. Firstly a computational grid must be generated which sufficiently resolves the regions of the flow domain containing the actuator disk(s), and, secondly the user modules `usinv.f90`, and `ustsns.f90` must be modified to specify the source terms associated with each disk (see appendices C and D). In all cases the mesh was generated using ANSYS's `ICEMCFD` meshing software with unstructured hexahedral grids. Each of the actuator disk regions is gridded as a thin cylindrical area of mesh and in all cases the nacelle of the turbine is exactly represented as a solid void within the computational domain. In each case a multi-block approach was used to generate the grid with an appropriate blocking strategy being selected. This strategy differed only slightly for the single and multiple turbine models, in that in the areas where the turbines exist the meshing density was increased to adequately resolve each turbine. One other important difference between the single and multiple turbine cases is that in the single case the nacelle support was modelled, whereas in the multi-turbine models only the nacelles are represented. The generated grids were exported in `.cgns` format for import into `Code_Saturne`.

1. Single turbine flume test

To demonstrate the actuator-disk model described in chapter 1 comparisons have been made with test conducted on a model scale turbine installed in the EDF flume in Chat-tou. In these computations the nacelle and its support have been modelled explicitly as solid boundaries within the grid while the rotor has been modelled as an actuator disk. Simulations have been performed at tip speed ratios of $\gamma = 4.0$ and $\gamma = 4.5$ based on the undisturbed free stream flow.

1.1. Computational set-up. Figure 1 shows the meshing strategy employed in `ICEM` in the neighbourhood of the turbine. A cylindrical O-grid which extends throughout the entire computational domain has been used to discretise the rotor plane, this O-grid has 15 cells in the radial direction and 60 cells in the circumferential direction. Mesh stretching has been used to refine the grid at the edge of the rotor so the shear between the free stream flow and the fluid which has passed through the actuator disk is sufficiently resolved. Both the nacelle and its support have been included in the computation. In meshing the nacelle a 6×6 H-grid region has been used at the centre of the O-grid, though this does not form part of the actuator disk. The computational domain extends from 30 diameters downstream of the turbine to 10 diameters upstream.

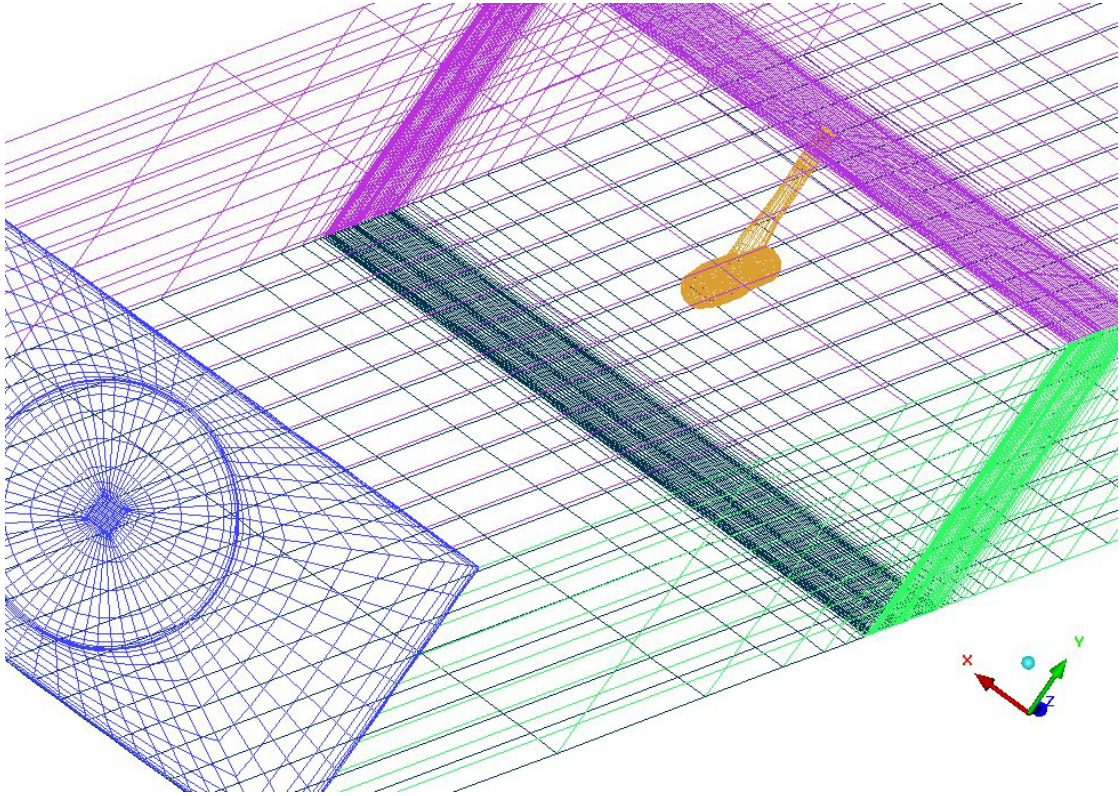


FIGURE 1. Detail from the ICEM mesh generator showing the cross-sectional grid (blue), the solid volumes for the nacelle and it's support (yellow) and the refined mesh region in the neighbourhood of the actuator disk.

The rotor has a diameter of 0.6m and the centre of the turbine rotor plane is defined as the origin for the computation. The flume is 1.5m wide and 0.8m deep with the rotor located on the centre line at midwater.

It is important to note that the support pylon has been modelled using its correct physical dimensions and this leads to an over prediction of C_P in $k - \omega$ turbulence models. The support pylon was included in this case to allow comparison both with the experimental studies performed by EDF in the Chattou file and with simulations performed by the University of Oxford – the issue of tower scaling was raised by the Oxford at the technical meeting in July, but a decision not to re-grid and re-compute was taken as the source of the variation could be explained.

The mesh shown in figure 1 gives details of the nacelle and tower environment as light brown mesh surface cells covering these parts, while the actuator disk cells illuminated in figure 3 indicate how thin the disk region is in relation to the solid nacelle and tower areas. The recommendation by iHarrison et al. [2010] is to keep the actuator disc thickness to 0.01 times its diameter. Figure 3 shows how thin the actuator disk (identified by the red bounding box) is in relation to the rest of the computational domain.

TABLE 1. Blade geometry for the three bladed horizontal axis tidal turbine tested in the EDF flume.

Radial ordinate	Twist angle	Chord length	Thickness type	Section
0.040	32.0	0.0203	100%	Circle
0.060	31.0	0.0204	15%	4415
0.065	30.1	0.0261	15%	4415
0.070	29.2	0.0318	15%	4415
0.075	28.3	0.0375	15%	4415
0.080	27.5	0.0433	15%	4415
0.084	26.6	0.0490	15%	4415
0.089	25.8	0.0548	15%	4415
0.094	25.0	0.0605	15%	4415
0.099	24.2	0.0663	15%	4415
0.104	23.4	0.0721	15%	4415
0.109	22.6	0.0779	15%	4415
0.114	21.8	0.0837	15%	4415
0.119	21.1	0.0895	15%	4415
0.124	20.4	0.0953	15%	4415
0.129	19.7	0.0939	15%	4415
0.133	19.0	0.0921	15%	4415
0.138	18.3	0.0904	15%	4415
0.143	17.6	0.0886	15%	4415
0.148	17.0	0.0868	15%	4415
0.153	16.4	0.0851	15%	4415
0.158	15.8	0.0833	15%	4415
0.163	15.2	0.0816	15%	4415
0.168	14.6	0.0798	15%	4415
0.173	14.0	0.0781	15%	4415
0.178	13.5	0.0763	15%	4415
0.182	13.0	0.0746	15%	4415
0.187	12.4	0.0728	15%	4415
0.192	12.0	0.0711	15%	4415
0.197	11.5	0.0693	15%	4415
0.202	11.0	0.0676	15%	4415
0.207	10.6	0.0658	15%	4415
0.212	10.1	0.0641	15%	4415
0.217	9.7	0.0623	15%	4415
0.222	9.3	0.0606	15%	4415
0.227	8.9	0.0589	15%	4415
0.231	8.6	0.0571	15%	4415
0.236	8.2	0.0554	15%	4415
0.241	7.9	0.0537	15%	4415
0.246	7.6	0.0519	15%	4415
0.251	7.2	0.0502	15%	4415
0.256	7.0	0.0484	15%	4415
0.261	6.7	0.0467	15%	4415
0.266	6.4	0.0450	15%	4415
0.271	6.2	0.0433	15%	4415
0.276	6.0	0.0415	15%	4415
0.280	5.8	0.0398	15%	4415
0.285	5.6	0.0381	15%	4415
0.290	5.4	0.0363	15%	4415
0.295	5.2	0.0346	15%	4415

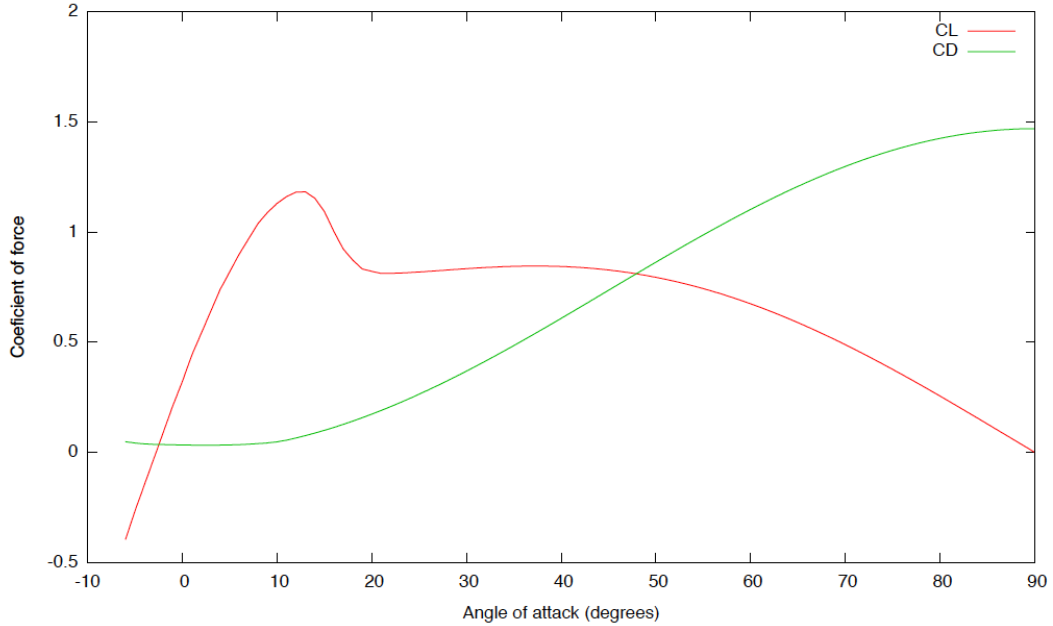


FIGURE 2. Coefficients of aerodynamic lift, C_L , and drag, C_D , for a NACA 4415 airfoil.

The blade geometry used in these tests is shown in Table 1. The required tables of coefficients of lift, C_L , and drag, C_D , against angle of attack, α , for the NACA4415 airfoil were obtained from the University of Oxford and can be found in the file `4415.txt`, the lift and drag coefficients for the airfoil are plotted in Figure 2. `usinv.f90` and `ustsns.f90` were modified to create a single actuator disk located on the face of the rotor. The source code for the user routines, together with the files `blade.txt`, `circle.txt` and `4415.txt` are included on the accompanying CD in the `Single` directory.

For both tip-speed ratios, the left, lower and right walls of the computational domain were specified as walls (and the zero tangential flow condition imposed), while the top of the computational domain was set as a symmetry condition (zero normal flow) to mimic a free surface with minimal deformation. The upstream boundary condition (located 11 diameters upstream of the rotor face) has a uniform velocity with 9.5% turbulence intensity. The `Code_Saturne` computations were run using the transient solver with a reference time step of 0.006 seconds, an adaptive time step was used with a maximum Courant number of 1:0. Convergence was accelerated by using local time-stepping and the solution was run for 3000 iterations. Full details of the setup are to be found in the `Code_Saturne` setup file, `D5_CASE.xml` which is to be found on the accompanying CD, also in the `Single` directory.

Figure 3 shows the velocity magnitude on the surface of the nacelle, the front face of the actuator disk and the downstream walls of the domain and also on a section through the centre plane of the domain, while figure 4 shows the velocity magnitude distribution on the vertical slice through the centreline of the flume.

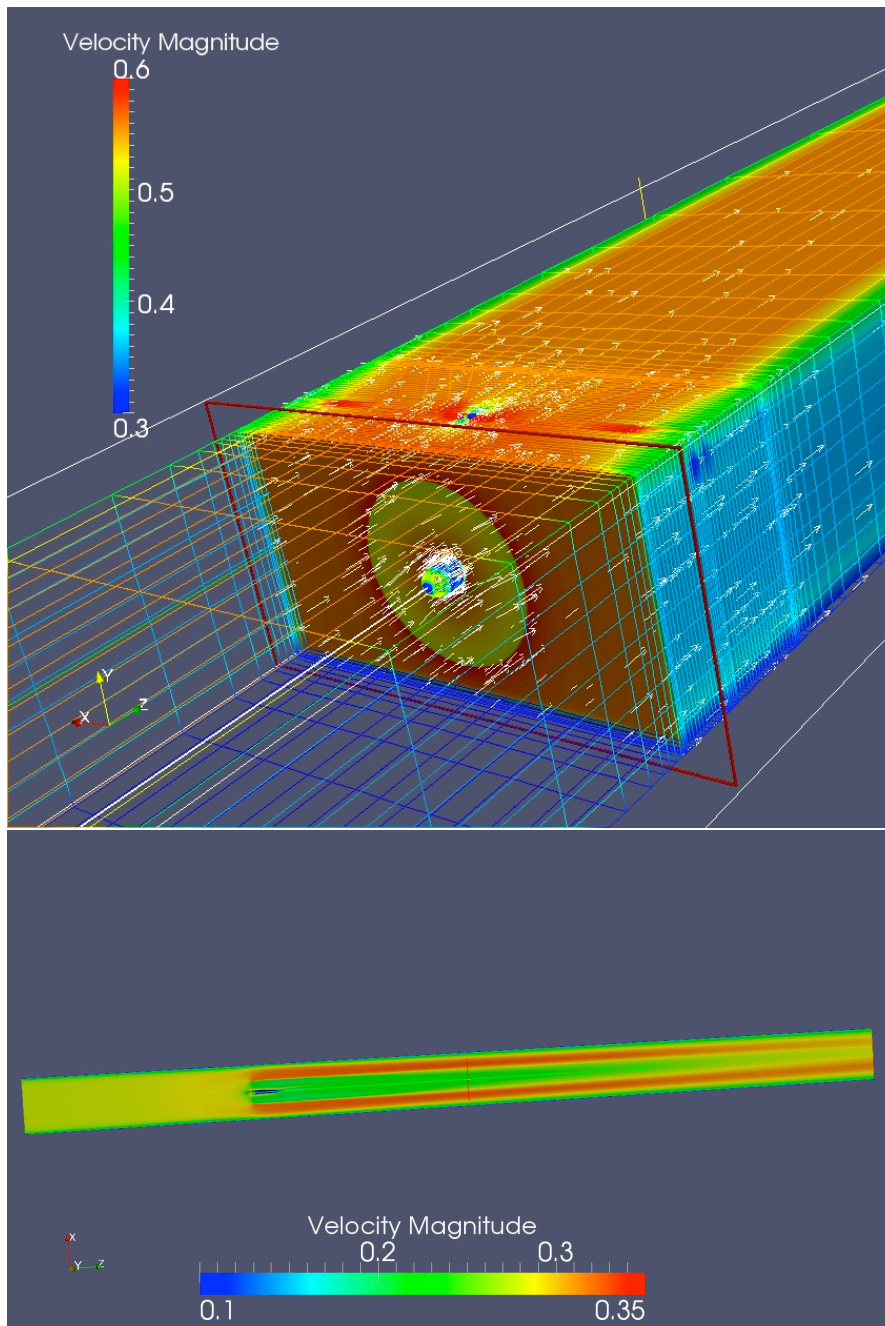


FIGURE 3. Velocity magnitude for flow passed a single horizontal axis tidal turbine in the centre of a flume. The top plot shows the mesh on the surface of the domain coloured by velocity together with pseudo-colour plots of the velocity on the nacelle and the rotor plane (incited in red). The lower plot shows the velocity distribution through the horizontal mid water plane.

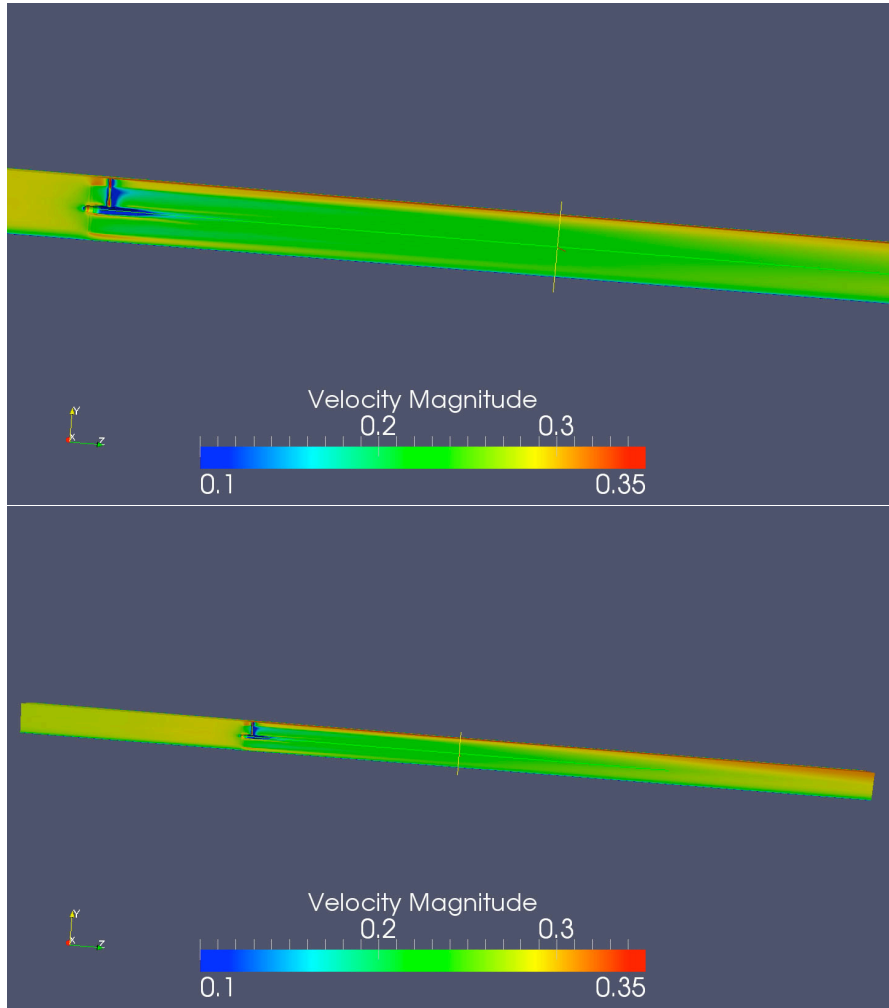


FIGURE 4. Velocity magnitude for flow passed a single horizontal axis tidal turbine in the centre of a flume. Both plots show pseudo-colour plots of the velocity magnitude on the vertical centre plane of the flume, with the top plot showing an enlargement of the turbine nacelle and the near wake region.

1.2. Comparison with experimental data. The single tidal turbine test case conducted at EDF’s test facility in Chatou, Paris under work package WG4 WP1 D4, was also simulated by the University of Oxford and has been chosen as a validation case for the actuator disk model. From the results seen in figure 5 the actuator disk model involved with `Code_Saturne` compares well for the uniform flow situation, even though slight discrepancies occurred, these were due to the shortcomings of the $k-\omega$ SST model in predicting drag on bluff bodies. The use of $k-\omega$ SST, leads to an over prediction of C_P and C_T particularly at higher tip-speed ratios. The University of Oxford reported in the sub-project technical meeting in Chatou (July 2012) that this can be corrected

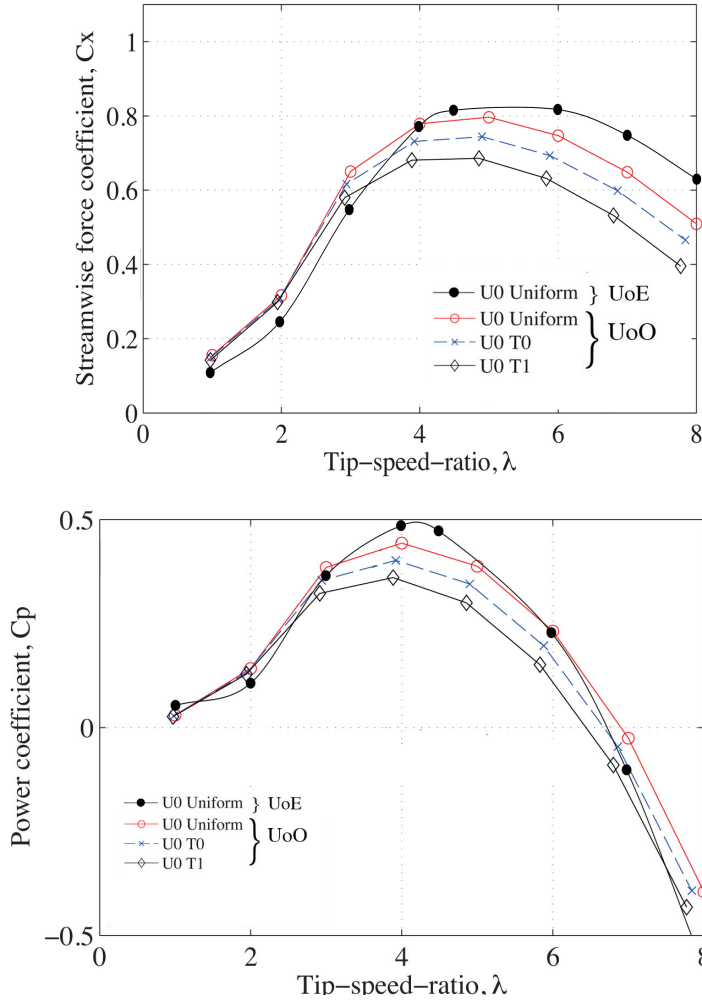


FIGURE 5. Comparison of computed thrust, C_T , and power, C_P , coefficients from the present actuator disk model and computations performed by the University of Oxford using the commercial CFD code Fluent.

by reducing the diameter of the supporting pylon. Since this change would require remeshing the computational domain, which would be very time consuming, this has not been done at the present time. The authors also note that the implantation of the $k - \omega$ SST turbulence model for rough surfaces in `Code_Saturne` is known to be defective [Nguyen, 2011]¹. As a result, in the computations for staggered and sequential arrays of horizontal axis tidal turbines presented in the following sections of this chapter, the $k - \epsilon$ turbulence model has been employed.

Figures 6 and 7 compare results from the present simulations (using a rigid lid, RANS simulations with a smooth flume floor and the $k - \omega$ turbulence model), the experiments

¹<http://code-saturne.org/forum/viewtopic.php?f=9&t=842&p=4703&hilit=rough+wall#p4703>

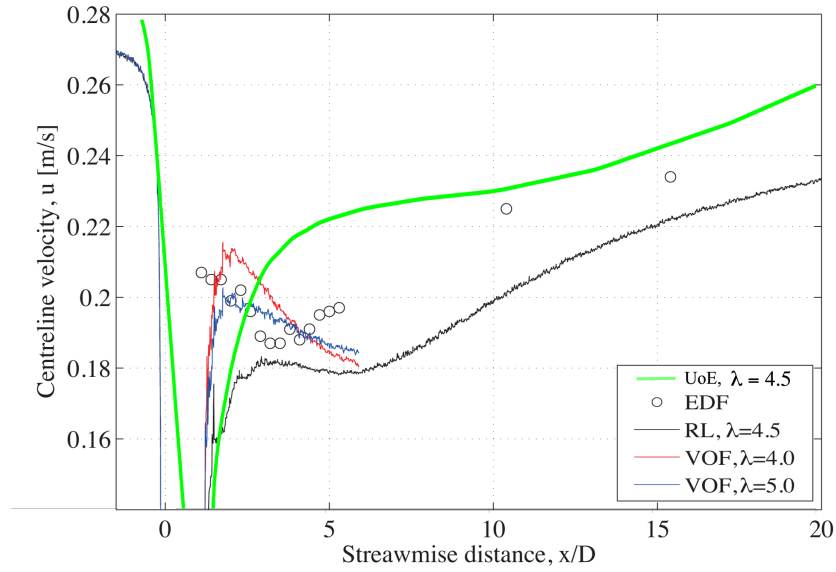


FIGURE 6. Velocity distribution on the centreline of the flume containing a single horizontal axis tidal turbine. Showing the present model at a tip speed ratio of $\gamma = 4.5$ (green line), experimental measurements from EDF (circles), and results from the University of Oxford's CFD models for a rigid lid calculation (RL) and free surface calculations using the Volume of Fluid (VOF) model.

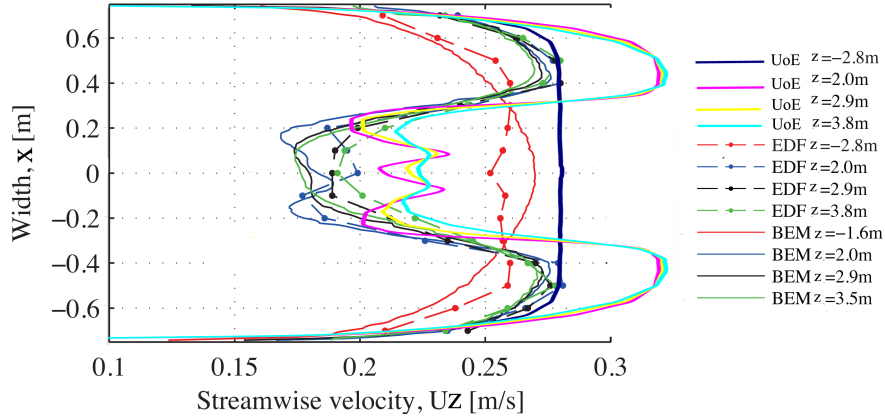


FIGURE 7. Velocity distribution across the width of a flume containing a single horizontal axis tidal turbine. Showing the present model at a tip speed ratio of $\gamma = 4.5$, experimental measurements from EDF, and results from the University of Oxford's RANS Blade Element Momentum (BEM) calculations.

conducted in the Chattou flume by EDF and simulations performed by the University of Oxford using both a rigid lid and free surface. In both the Oxford simulations and the EDF experiments the walls and floor of the flume are rough surfaces leading to the development of a thicker boundary layer and reducing the mean velocity and leading to the more parabolic upstream velocity profile than is observed in the smooth walled calculations using the present method (see the $z = -2.8$ profiles in figure 7). The higher mean velocity is also leads to an over prediction of the centreline velocity (Figure 6), though the error between the computational measurements and the experiments is comparable with the under prediction error in the Oxford simulations. In the cross stream profiles downstream of the turbine (Figure 7) similar the wake behind the rotor and the nacelle are clearly observed as the accelerated flow passing the turbine.

Although there are discrepancies between the present results and those from EDF and Oxford they are explained by the presence of smooth walls in the simulation. It was necessary to use smooth walls in these calculations as the rough wall model in `Code_Saturne` is know not to work with the $k - \omega$ turbulence model. This comparison demonstrates, however, that the actuator disk model is reproducing the wake of the turbine correctly. The comparisons also highlight the importance rough walls in the simulation and as a consequence the array simulations performed in the following section will utilise the $k - \epsilon$ turbulence model, which does work with rough walls in `Code_Saturne`.

1.3. Depth averaged results. The three dimensional Navier-Stokes results (Fig 2) have been discretised using 10 bins in the stream wise direction, covering $z = -1.0\text{m}$ to $z = 3.0\text{m}$ and 21 bins in the cross flow direction covering the full width of the computational region. The rotor is located at $z = 0.0\text{m}$. Increasing the number of bins in the stream wise direction leads to the occurrence of missing values in the discretised data as the computational grid is stretched down stream from the turbine. Where tabular data is presented the flow direction is indicated and the mean values for the bins containing the turbine are underlined.

The depth averaged results for both tip-speed ratios ($\gamma = 4.0$ and $\gamma = 4.5$) show a velocity drop at the centre of the turbine and strong generation of turbulence, in both cases this is particularly strong for the bin immediately behind the rotor, which contains the support pylon. In the results for the higher tip-speed ratio the collapse of the near wake region and the acceleration of the flow bypassing the rotor as it is constrained by the flume walls can clearly be identified.

1.3.1. *Tip speed ratio $\gamma = 4.0$.* Figure 8 shows mosaic plots of the binned depth averaged velocity magnitude, turbulent kinetic energy and turbulent viscosity. The bin containing the turbine hub is at $(0,0,0.0)$ and it is easily identifiable in the velocity plot showing the expected velocity deficit associated with the flow passing the turbine face. Tables 2 to 4 present the binned mean values with the bin containing the turbine nacelle underlined.

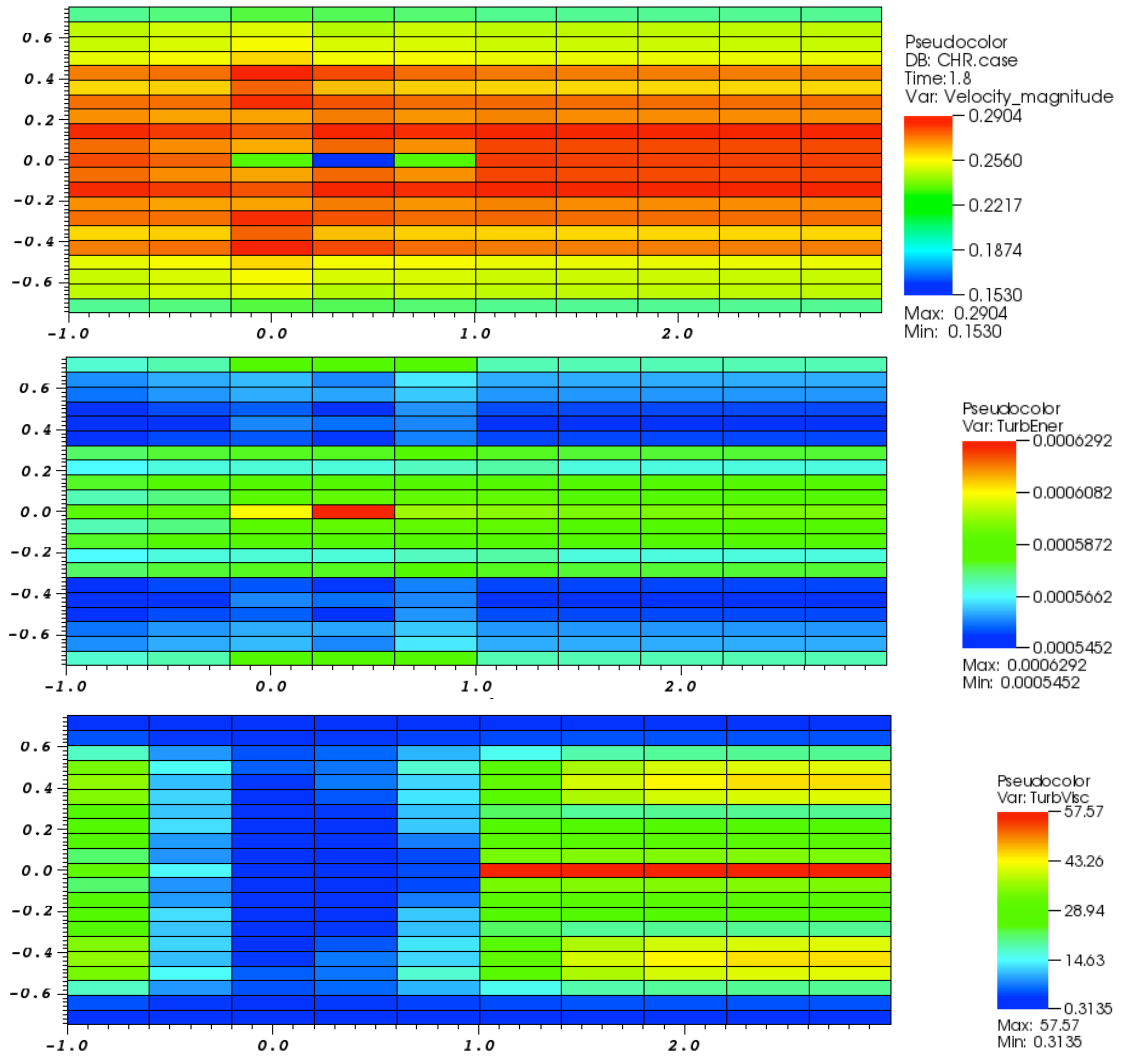


FIGURE 8. Single turbine in the EDF flume at a tip speed ratio of $\gamma = 4.0$: Mosaic plots showing binned depth averaged velocity magnitude, turbulent kinetic energy and turbulent viscosity.

TABLE 2. Single turbine in the EDF flume at a tip speed ratio of $\gamma = 4.0$: Depth averaged velocity magnitude. The value for the cell containing the turbine has been underlined

stream wise direction \rightarrow									
0.2415	0.2423	0.2441	0.2435	0.2425	0.2415	0.2415	0.2415	0.2415	0.2415
0.2573	0.2582	0.2591	0.2570	0.2582	0.2575	0.2574	0.2574	0.2574	0.2574
0.2580	0.2589	0.2603	0.2589	0.2588	0.2581	0.2581	0.2580	0.2580	0.2580
0.2595	0.2604	0.2625	0.2602	0.2603	0.2596	0.2596	0.2596	0.2595	0.2595
0.2668	0.2677	0.2717	0.2693	0.2677	0.2670	0.2669	0.2669	0.2669	0.2669
0.2625	0.2630	0.2682	0.2639	0.2632	0.2627	0.2627	0.2626	0.2626	0.2626
0.2677	0.2673	0.2710	0.2688	0.2678	0.2679	0.2678	0.2678	0.2678	0.2678
0.2659	0.2652	0.2651	0.2669	0.2657	0.2667	0.2661	0.2661	0.2661	0.2661
0.2711	0.2699	0.2688	0.2727	0.2707	0.2713	0.2714	0.2714	0.2714	0.2714
0.2677	0.2661	0.2648	0.2680	0.2660	0.2696	0.2692	0.2692	0.2692	0.2692
0.2695	0.2681	<u>0.2475</u>	0.2252	0.2459	0.2700	0.2699	0.2699	0.2699	0.2699
0.2677	0.2661	0.2649	0.2680	0.2660	0.2696	0.2692	0.2692	0.2692	0.2692
0.2711	0.2699	0.2690	0.2727	0.2707	0.2713	0.2714	0.2714	0.2714	0.2714
0.2659	0.2652	0.2652	0.2669	0.2657	0.2667	0.2661	0.2661	0.2661	0.2661
0.2677	0.2673	0.2710	0.2688	0.2678	0.2679	0.2678	0.2678	0.2678	0.2678
0.2625	0.2630	0.2682	0.2639	0.2632	0.2627	0.2627	0.2626	0.2626	0.2626
0.2668	0.2677	0.2717	0.2693	0.2677	0.2670	0.2669	0.2669	0.2669	0.2669
0.2595	0.2604	0.2625	0.2602	0.2603	0.2596	0.2596	0.2596	0.2595	0.2595
0.2580	0.2589	0.2603	0.2589	0.2588	0.2581	0.2581	0.2580	0.2580	0.2580
0.2573	0.2582	0.2591	0.2570	0.2582	0.2575	0.2574	0.2574	0.2574	0.2574
0.2415	0.2423	0.2441	0.2435	0.2425	0.2415	0.2415	0.2415	0.2415	0.2415

TABLE 3. Single turbine in the EDF flume at a tip speed ratio of $\gamma = 4.0$: Depth averaged turbulent kinetic energy. The value for the cell containing the turbine has been underlined

stream wise direction \rightarrow									
1.07e-03	1.11e-03	1.20e-03	1.28e-03	1.31e-03	1.31e-03	1.31e-03	1.30e-03	1.30e-03	1.22e-03
4.60e-04	5.36e-04	5.80e-04	6.40e-04	6.61e-04	6.77e-04	6.90e-04	7.02e-04	7.18e-04	7.41e-04
4.56e-04	5.21e-04	5.71e-04	6.28e-04	6.39e-04	6.56e-04	6.67e-04	6.78e-04	6.92e-04	7.23e-04
4.43e-04	5.05e-04	5.48e-04	5.97e-04	6.15e-04	6.30e-04	6.39e-04	6.47e-04	6.55e-04	6.69e-04
3.86e-04	4.56e-04	4.84e-04	5.25e-04	5.54e-04	5.73e-04	5.82e-04	5.88e-04	5.95e-04	5.89e-04
4.35e-04	4.94e-04	5.40e-04	6.05e-04	6.41e-04	6.72e-04	6.82e-04	6.85e-04	6.83e-04	6.09e-04
4.02e-04	4.64e-04	5.34e-04	7.52e-04	9.10e-04	9.60e-04	9.38e-04	9.04e-04	8.55e-04	6.00e-04
4.23e-04	4.83e-04	5.49e-04	7.05e-04	8.34e-04	8.81e-04	8.77e-04	8.48e-04	8.05e-04	5.92e-04
3.95e-04	4.65e-04	5.24e-04	6.75e-04	7.82e-04	7.85e-04	7.74e-04	7.39e-04	6.97e-04	5.47e-04
4.51e-04	5.08e-04	1.42e-03	1.50e-03	8.04e-04	5.79e-04	5.29e-04	4.92e-04	4.68e-04	5.40e-04
4.64e-04	5.15e-04	<u>2.45e-03</u>	2.65e-03	1.13e-03	6.19e-04	4.80e-04	4.20e-04	3.94e-04	5.47e-04
4.51e-04	5.08e-04	1.43e-03	1.37e-03	8.70e-04	6.20e-04	5.25e-04	4.81e-04	4.63e-04	5.56e-04
3.95e-04	4.64e-04	5.27e-04	6.93e-04	7.95e-04	7.90e-04	7.81e-04	7.54e-04	7.22e-04	5.81e-04
4.23e-04	4.83e-04	5.51e-04	7.21e-04	8.53e-04	9.21e-04	9.28e-04	9.04e-04	8.63e-04	6.38e-04
4.02e-04	4.63e-04	5.36e-04	7.66e-04	9.29e-04	9.96e-04	9.91e-04	9.69e-04	9.28e-04	6.50e-04
4.35e-04	4.93e-04	5.40e-04	6.06e-04	6.45e-04	6.80e-04	6.93e-04	7.00e-04	7.03e-04	6.38e-04
3.86e-04	4.56e-04	4.83e-04	5.25e-04	5.54e-04	5.74e-04	5.84e-04	5.91e-04	5.99e-04	6.05e-04
4.43e-04	5.05e-04	5.47e-04	5.96e-04	6.15e-04	6.31e-04	6.40e-04	6.48e-04	6.57e-04	6.79e-04
4.56e-04	5.21e-04	5.71e-04	6.27e-04	6.39e-04	6.56e-04	6.68e-04	6.79e-04	6.93e-04	7.28e-04
4.60e-04	5.36e-04	5.79e-04	6.39e-04	6.62e-04	6.76e-04	6.90e-04	7.03e-04	7.19e-04	7.42e-04
1.07e-03	1.10e-03	1.20e-03	1.28e-03	1.31e-03	1.31e-03	1.31e-03	1.31e-03	1.30e-03	1.22e-03

TABLE 4. Single turbine in the EDF flume at a tip speed ratio of $\gamma = 4.0$: Depth averaged turbulent viscosity. The value for the cell containing the turbine has been underlined

stream wise direction \rightarrow									
0.0800	0.0926	0.0974	0.1026	0.1048	0.1085	0.1109	0.1132	0.1158	0.1226
0.2312	0.2666	0.2804	0.3317	0.3729	0.3438	0.3391	0.3400	0.3432	0.3632
1.0007	0.9890	0.6176	0.7113	1.2369	1.2465	1.0796	1.0130	0.9693	0.8780
4.1645	3.0616	0.8809	1.3242	2.3596	2.4868	1.9668	1.6709	1.5059	1.9190
7.1444	3.7846	0.9353	1.8713	2.5800	2.6037	2.0130	1.6739	1.4674	1.7670
8.5392	3.6338	0.7018	1.4160	1.6840	1.2235	1.0296	0.9411	0.8876	1.7962
8.5473	3.2124	0.3296	0.4649	0.5492	0.5293	0.5367	0.5515	0.5755	1.3382
9.2228	3.0399	0.3374	0.4975	0.4581	0.4986	0.5282	0.5573	0.5965	1.6308
9.1551	2.9429	0.3159	0.3829	0.4003	0.4733	0.5029	0.5314	0.5661	1.8045
10.227	3.1585	0.1829	0.1504	0.1591	0.2200	0.2749	0.3143	0.3718	2.3280
13.138	3.7962	<u>0.1244</u>	0.0727	0.1052	0.1644	0.2038	0.2345	0.2921	3.3508
10.243	3.1912	0.1844	0.1364	0.1468	0.2035	0.2446	0.2799	0.3426	2.4512
9.1270	2.9405	0.3147	0.3805	0.3562	0.3946	0.4399	0.4819	0.5356	2.0462
9.2076	3.0106	0.3371	0.5064	0.4579	0.5020	0.5394	0.5738	0.6188	1.8574
8.5259	3.2224	0.3318	0.4717	0.5476	0.5414	0.5590	0.5806	0.6136	1.5480
8.5674	3.6727	0.7039	1.4263	1.6828	1.2257	1.0449	0.9582	0.9079	2.0116
7.2038	3.8613	0.9481	1.8863	2.6076	2.5959	2.0178	1.6980	1.4969	1.9867
4.1400	3.0575	0.8907	1.3267	2.3407	2.4569	1.9476	1.6686	1.5110	1.9994
0.9996	0.9873	0.6213	0.7102	1.2133	1.2358	1.0823	1.0156	0.9711	0.9123
0.2311	0.2660	0.2805	0.3314	0.3724	0.3439	0.3394	0.3403	0.3436	0.3663
0.0800	0.0926	0.0974	0.1026	0.1048	0.1086	0.1110	0.1132	0.1158	0.1227

1.3.2. *Tip speed ratio* $\gamma = 4.5$. Figure 9 shows mosaic plots of the binned depth averaged velocity magnitude, turbulent kinetic energy and turbulent viscosity. The bin containing the turbine hub is at (0,0,0.0) and it is easily identifiable in the velocity plot showing the expected velocity deficit associated with the flow passing the turbine face. Tables 5 to 7 present the binned mean values with the bin containing the turbine nacelle underlined.

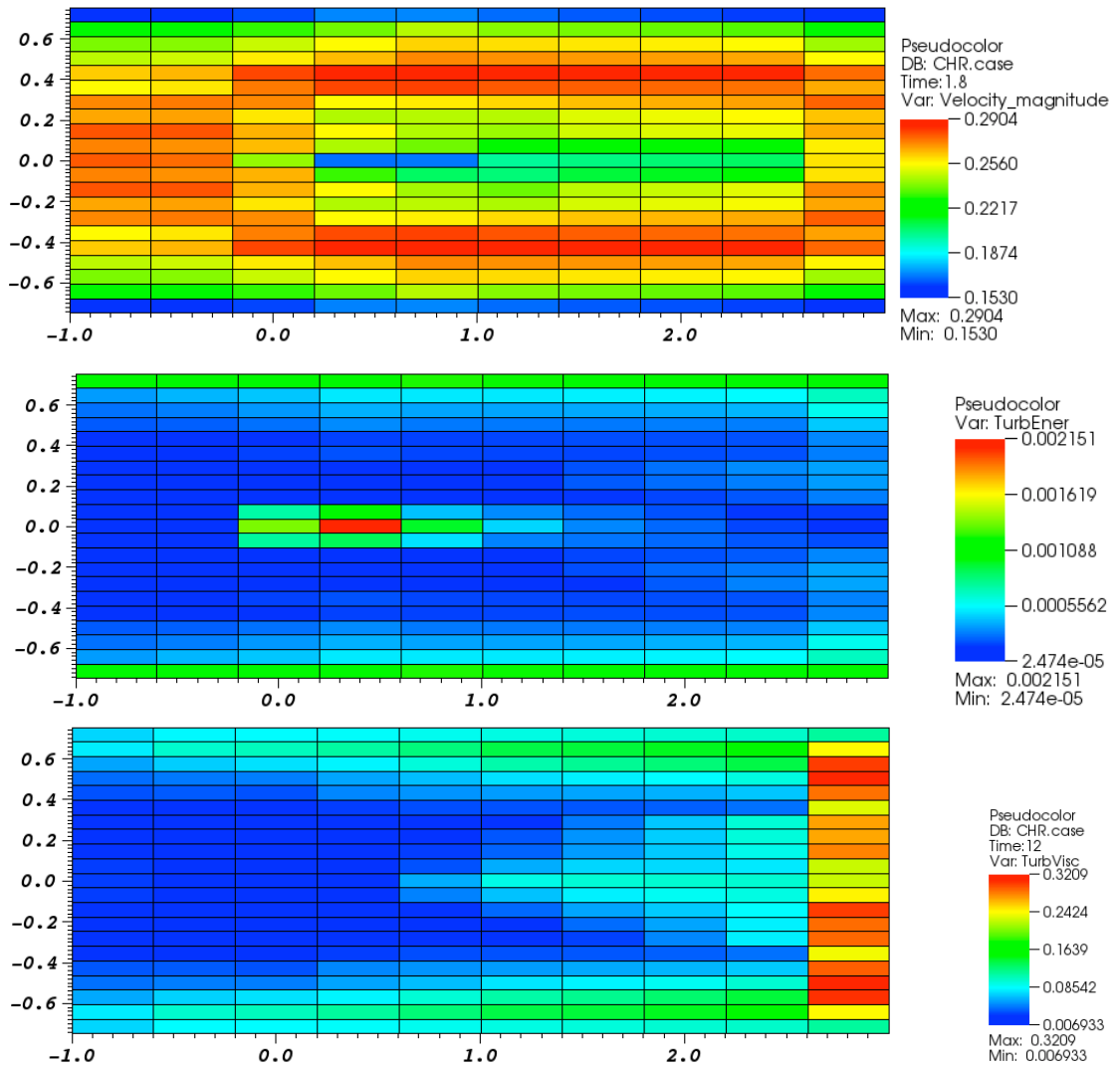


FIGURE 9. Single turbine in the EDF flume at a tip speed ratio of $\gamma = 4.5$: Mosaic plots showing binned depth averaged velocity magnitude, turbulent kinetic energy and turbulent viscosity.

TABLE 5. Single turbine in the EDF flume at a tip speed ratio of $\gamma = 4.5$: Depth averaged velocity magnitude. The value for the cell containing the turbine has been underlined

stream wise direction \rightarrow									
0.1560	0.1500	0.1613	0.1683	0.1684	0.1642	0.1615	0.1594	0.1570	0.1466
0.2268	0.2251	0.2330	0.2384	0.2501	0.2460	0.2433	0.2410	0.2382	0.2199
0.2401	0.2440	0.2523	0.2592	0.2656	0.2653	0.2646	0.2639	0.2627	0.2490
0.2473	0.2522	0.2616	0.2678	0.2755	0.2756	0.2755	0.2754	0.2752	0.2674
0.2634	0.2678	0.2831	0.2928	0.2945	0.2940	0.2939	0.2939	0.2939	0.2889
0.2573	0.2610	0.2754	0.2840	0.2872	0.2869	0.2871	0.2872	0.2873	0.2827
0.2731	0.2758	0.2689	0.2440	0.2433	0.2463	0.2530	0.2579	0.2634	0.2798
0.2689	0.2703	0.2575	0.2378	0.2358	0.2333	0.2408	0.2436	0.2473	0.2624
0.2795	0.2796	0.2655	0.2513	0.2393	0.2347	0.2420	0.2432	0.2444	0.2586
0.2734	0.2710	0.2685	0.2475	0.2508	0.2439	0.2360	0.2338	0.2331	0.2442
0.2805	0.2762	<u>0.2526</u>	0.1798	0.1853	0.2166	0.2216	0.2243	0.2266	0.2426
0.2734	0.2710	0.2704	0.2360	0.2191	0.2293	0.2357	0.2361	0.2355	0.2464
0.2796	0.2797	0.2662	0.2523	0.2398	0.2326	0.2427	0.2470	0.2512	0.2655
0.2690	0.2703	0.2579	0.2379	0.2355	0.2316	0.2375	0.2400	0.2444	0.2676
0.2731	0.2758	0.2693	0.2440	0.2429	0.2443	0.2494	0.2533	0.2573	0.2810
0.2574	0.2610	0.2755	0.2840	0.2872	0.2869	0.2870	0.2871	0.2871	0.2844
0.2635	0.2678	0.2831	0.2928	0.2945	0.2941	0.2940	0.2939	0.2939	0.2901
0.2474	0.2522	0.2616	0.2677	0.2755	0.2756	0.2755	0.2754	0.2752	0.2680
0.2402	0.2439	0.2523	0.2592	0.2655	0.2653	0.2646	0.2638	0.2626	0.2494
0.2268	0.2251	0.2330	0.2383	0.2501	0.2459	0.2433	0.2409	0.2380	0.2203
0.1560	0.1501	0.1613	0.1682	0.1684	0.1643	0.1616	0.1594	0.1569	0.1468

TABLE 6. Single turbine in the EDF flume at a tip speed ratio of $\gamma = 4.5$: Depth averaged turbulent kinetic energy. The value for the cell containing the turbine has been underlined

stream wise direction \rightarrow									
1.03e-03	1.05e-03	1.13e-03	1.20e-03	1.22e-03	1.21e-03	1.21e-03	1.20e-03	1.19e-03	1.13e-03
3.62e-04	4.09e-04	4.47e-04	5.12e-04	5.10e-04	5.12e-04	5.24e-04	5.38e-04	5.58e-04	6.87e-04
2.82e-04	3.01e-04	3.53e-04	4.06e-04	3.77e-04	3.81e-04	3.89e-04	3.98e-04	4.13e-04	5.88e-04
2.25e-04	2.35e-04	2.78e-04	3.24e-04	2.92e-04	2.93e-04	2.96e-04	3.00e-04	3.06e-04	4.51e-04
1.40e-04	1.57e-04	1.58e-04	1.85e-04	1.90e-04	1.98e-04	2.01e-04	2.05e-04	2.09e-04	3.19e-04
1.51e-04	1.56e-04	1.85e-04	2.13e-04	1.95e-04	1.95e-04	1.98e-04	2.02e-04	2.09e-04	3.04e-04
5.89e-05	6.10e-05	7.03e-05	7.94e-05	8.45e-05	1.36e-04	2.11e-04	2.75e-04	3.32e-04	3.71e-04
7.72e-05	8.02e-05	9.42e-05	1.14e-04	1.37e-04	1.69e-04	2.27e-04	2.61e-04	3.00e-04	3.59e-04
3.57e-05	4.85e-05	3.82e-05	6.73e-05	1.05e-04	1.29e-04	1.74e-04	1.96e-04	2.24e-04	2.99e-04
5.91e-05	6.47e-05	7.38e-05	1.01e-04	4.37e-04	3.28e-04	2.65e-04	2.09e-04	1.74e-04	1.81e-04
2.47e-05	2.69e-05	<u>1.36e-03</u>	2.15e-03	9.62e-04	4.81e-04	3.24e-04	2.54e-04	1.97e-04	1.50e-04
5.91e-05	6.46e-05	7.54e-05	8.81e-05	4.97e-04	3.11e-04	2.83e-04	2.55e-04	2.18e-04	2.01e-04
3.57e-05	4.86e-05	3.78e-05	6.02e-05	9.97e-05	1.43e-04	1.93e-04	2.09e-04	2.26e-04	3.23e-04
7.72e-05	8.01e-05	9.40e-05	1.09e-04	1.17e-04	1.39e-04	2.05e-04	2.51e-04	2.93e-04	3.78e-04
5.90e-05	6.08e-05	7.04e-05	7.88e-05	7.94e-05	1.01e-04	1.57e-04	2.26e-04	3.13e-04	3.80e-04
1.51e-04	1.56e-04	1.85e-04	2.13e-04	1.95e-04	1.95e-04	1.98e-04	2.01e-04	2.10e-04	3.14e-04
1.40e-04	1.57e-04	1.58e-04	1.85e-04	1.90e-04	1.98e-04	2.02e-04	2.05e-04	2.09e-04	3.23e-04
2.25e-04	2.35e-04	2.78e-04	3.24e-04	2.92e-04	2.93e-04	2.96e-04	3.01e-04	3.07e-04	4.54e-04
2.81e-04	3.00e-04	3.53e-04	4.05e-04	3.77e-04	3.81e-04	3.89e-04	3.99e-04	4.15e-04	5.89e-04
3.62e-04	4.08e-04	4.47e-04	5.11e-04	5.10e-04	5.13e-04	5.25e-04	5.39e-04	5.60e-04	6.88e-04
1.03e-03	1.05e-03	1.13e-03	1.20e-03	1.22e-03	1.22e-03	1.21e-03	1.20e-03	1.19e-03	1.14e-03

TABLE 7. Single turbine in the EDF flume at a tip speed ratio of $\gamma = 4.5$: Depth averaged turbulent viscosity. The value for the cell containing the turbine has been underlined

stream wise direction \rightarrow									
7.33e-02	8.42e-02	8.60e-02	8.76e-02	8.94e-02	9.32e-02	9.56e-02	9.78e-02	1.00e-01	1.14e-01
8.02e-02	9.97e-02	1.05e-01	1.14e-01	1.24e-01	1.37e-01	1.40e-01	1.46e-01	1.54e-01	2.45e-01
5.92e-02	7.19e-02	7.60e-02	8.22e-02	9.64e-02	1.11e-01	1.17e-01	1.25e-01	1.37e-01	3.02e-01
4.18e-02	4.69e-02	4.75e-02	5.92e-02	6.64e-02	7.63e-02	8.05e-02	8.60e-02	9.48e-02	3.13e-01
3.47e-02	3.65e-02	3.46e-02	5.09e-02	5.42e-02	5.64e-02	5.94e-02	6.29e-02	6.86e-02	2.86e-01
1.92e-02	1.94e-02	1.83e-02	2.92e-02	3.34e-02	3.45e-02	3.61e-02	3.86e-02	4.36e-02	2.33e-01
9.64e-03	9.07e-03	6.93e-03	1.00e-02	1.34e-02	2.63e-02	4.64e-02	6.86e-02	9.71e-02	2.71e-01
2.07e-02	1.71e-02	9.64e-03	1.49e-02	2.14e-02	3.53e-02	5.47e-02	7.17e-02	9.56e-02	2.71e-01
2.30e-02	2.65e-02	1.29e-02	2.14e-02	2.93e-02	3.93e-02	5.68e-02	7.01e-02	9.14e-02	2.80e-01
2.90e-02	2.59e-02	1.07e-02	2.38e-02	3.46e-02	6.10e-02	7.37e-02	7.48e-02	7.82e-02	2.27e-01
2.97e-02	2.45e-02	<u>8.74e-03</u>	2.72e-02	6.16e-02	9.23e-02	9.77e-02	9.82e-02	9.79e-02	2.26e-01
3.00e-02	2.62e-02	1.08e-02	2.75e-02	4.89e-02	6.75e-02	8.11e-02	8.83e-02	9.28e-02	2.47e-01
2.32e-02	2.65e-02	1.28e-02	1.92e-02	2.66e-02	4.11e-02	5.87e-02	7.01e-02	8.63e-02	3.02e-01
2.16e-02	1.74e-02	9.56e-03	1.34e-02	1.60e-02	2.43e-02	4.16e-02	5.87e-02	8.15e-02	2.87e-01
1.02e-02	9.15e-03	6.94e-03	9.91e-03	1.21e-02	1.74e-02	3.05e-02	5.01e-02	8.16e-02	2.89e-01
1.89e-02	1.95e-02	1.84e-02	2.93e-02	3.35e-02	3.46e-02	3.61e-02	3.84e-02	4.36e-02	2.39e-01
3.52e-02	3.72e-02	3.47e-02	5.10e-02	5.44e-02	5.67e-02	5.99e-02	6.38e-02	7.02e-02	2.92e-01
4.27e-02	4.74e-02	4.75e-02	5.93e-02	6.66e-02	7.69e-02	8.18e-02	8.81e-02	9.81e-02	3.21e-01
6.08e-02	7.26e-02	7.60e-02	8.22e-02	9.69e-02	1.11e-01	1.19e-01	1.27e-01	1.41e-01	3.05e-01
8.01e-02	9.92e-02	1.06e-01	1.14e-01	1.25e-01	1.38e-01	1.41e-01	1.47e-01	1.55e-01	2.44e-01
7.33e-02	8.42e-02	8.61e-02	8.76e-02	8.94e-02	9.33e-02	9.57e-02	9.78e-02	1.00e-01	1.14e-01

2. Array of turbines in series

To demonstrate the application of the model to arrays of turbines two cases have been considered. Both were modelled experimentally by the University of Manchester as test 19 (turbines in series) and test 20 (staggered turbines). In both cases two infinite-width rows of turbines have been simulated by imposing symmetry boundary conditions at the cross-flow (east and west) boundaries of the `Code_Saturne` simulation. This section presents results from Manchester test 19, while section 3 considers Manchester test 20.

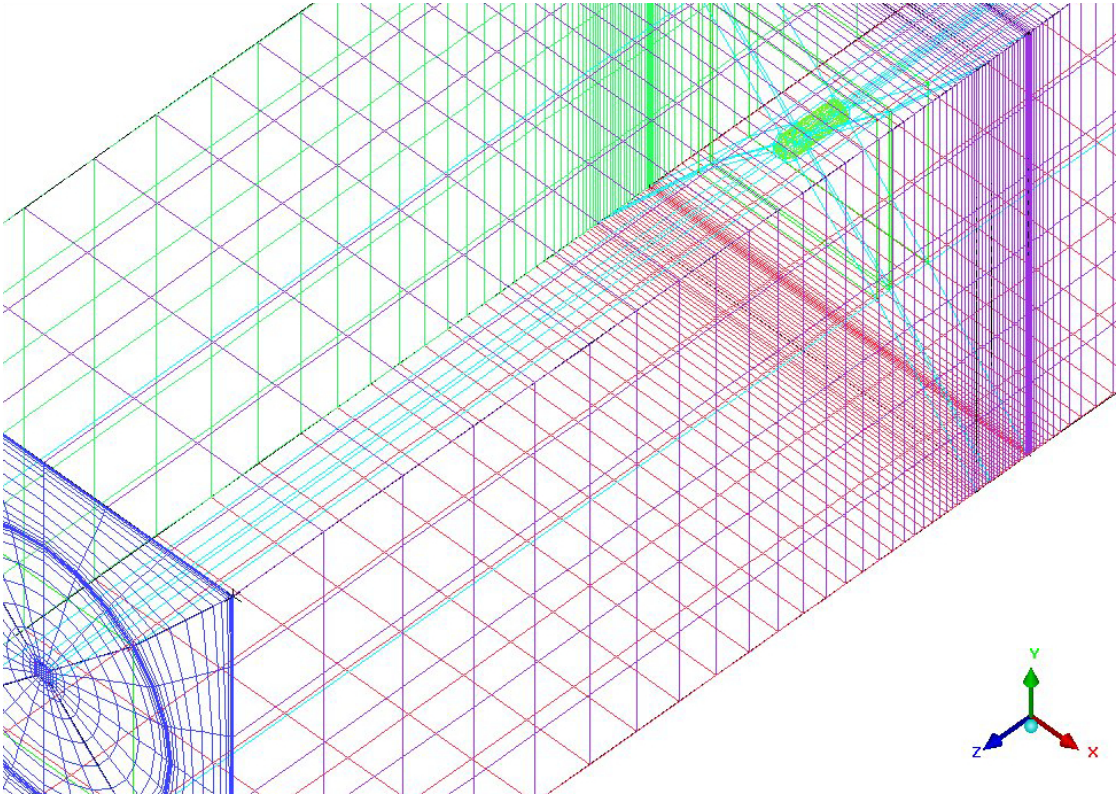


FIGURE 10. Detail from the ICEM mesh generator showing the cross-sectional grid (blue), the solid volumes for the nacelle (green) and the refined mesh region in the neighbourhood of the upstream actuator disk.

2.1. Computational set-up. The meshing strategy employed (again using ICEM) is similar to that used in the single turbine case. A cylindrical O-grid which extends throughout the entire computational domain has been used to discretise the rotor plane, this O-grid has 15 cells in the radial direction and 24 cells in the circumferential direction. Mesh stretching has been used to refine the grid at the edge of the rotor so the shear between the free stream flow and the fluid which has passed through the actuator disk is sufficiently resolved. In this case only the nacelles have been included in the computation and there are no support structures. In meshing the nacelle a 6×6 H-grid region has

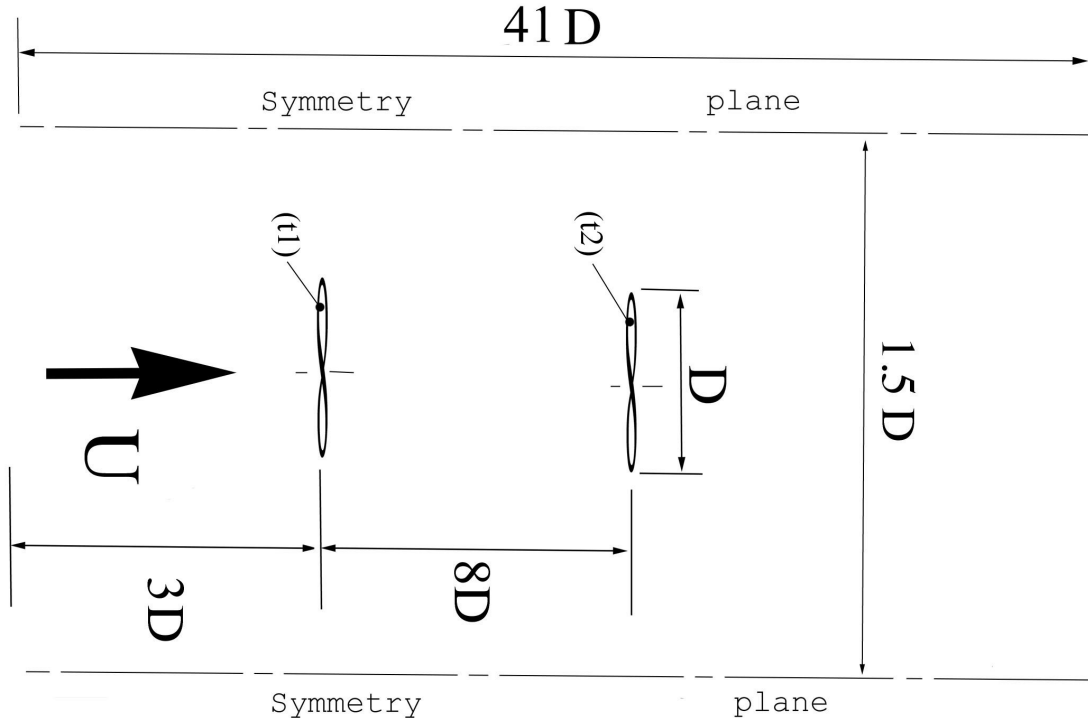


FIGURE 11. Arrangement of the turbines for the array test with two rows of turbines in series.

been used at the centre of the O-grid, though this does not form part of the actuator disk. The computational domain extends from 30 diameters downstream of the downstream turbine and 3 diameters upstream of the upstream turbine. Figure 11 shows a schematic of the problem set-up.

The blade geometry used in these tests is shown in Table 8. The required tables of for coefficients of lift, C_L , and drag, C_D , against angle of attack, α , for the GOE804 airfoil were obtained from the University of Manchester and can be found in the file `Goe804.txt`, the lift and drag coefficients for the airfoil are plotted in Figure ???. `usin.v.f90`, `ustsns.f90` were modified to create two actuator disks, located on for the faces of the upstream and downstream rotors. The source code for the user routines, together with the files `blade.txt`, `circle.txt` and `Geo804.txt` are included on the accompanying CD in the `Double` directory.

For all four tip-speed ratios ($\gamma = 3.5, 4.0, 5.5$, and 6.0) the left and right walls of the computational domain were specified as symmetry conditions (with the zero normal flow condition imposed) to simulate an infinite width array. The top of the computational domain was also set as a symmetry condition to mimic a free surface with minimal deformation, while the lower boundary was set as a no-slip wall, with a roughness of

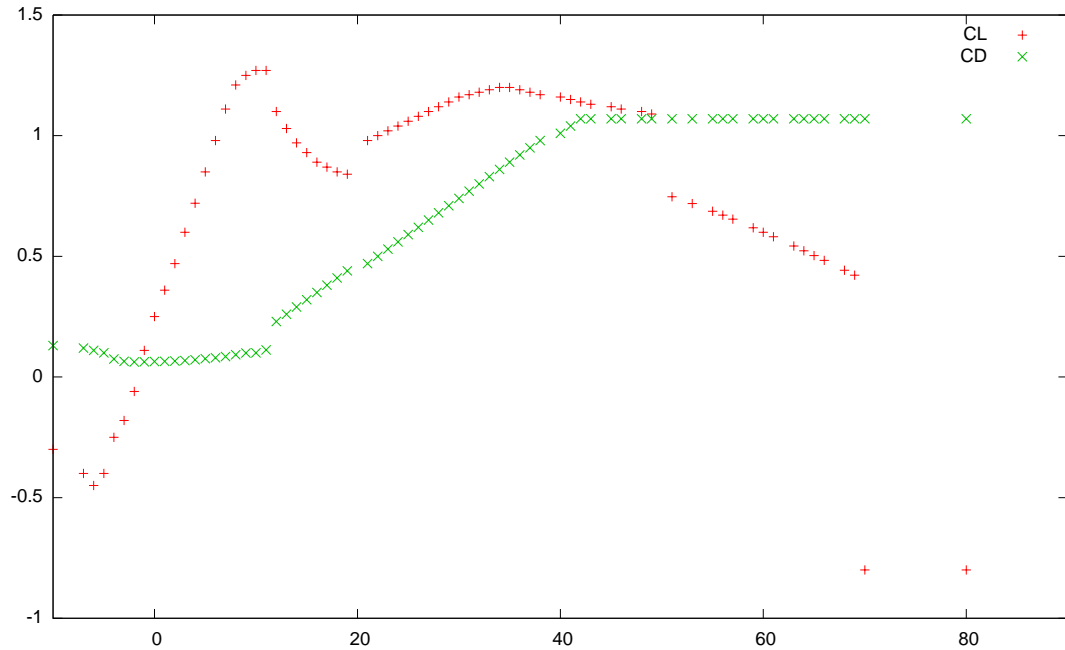


FIGURE 12. Coefficients of aerodynamic lift, C_L , and drag, C_D , for a GOE 804 airfoil.

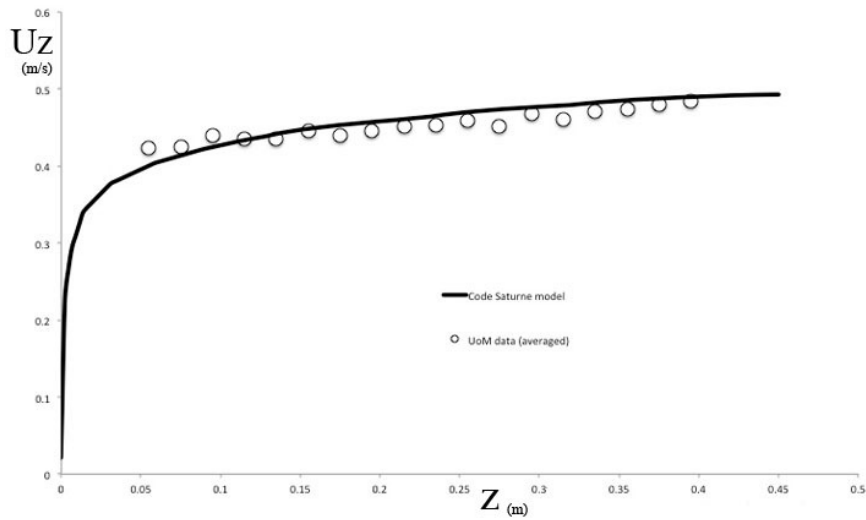


FIGURE 13. Predicted and measure mean velocity profiles at the location of the upstream rotor in the Manchester tests of an array of turbines in series, in an empty channel.

TABLE 8. Blade geometry for the three bladed horizontal axis tidal turbine tested in the Manchester array tests.

Radial ordinate	Twist angle	Chord length	Thickness type	Section
0.001	38.4	0.0150	100%	Circle
0.015	38.4	0.0150	100%	Circle
0.033	22.9	0.0200	4%	Goe804
0.045	16.0	0.0300	4%	Goe804
0.059	11.3	0.0275	4%	Goe804
0.073	9.0	0.0250	4%	Goe804
0.085	7.5	0.0223	4%	Goe804
0.099	5.8	0.0195	4%	Goe804
0.113	4.1	0.0175	4%	Goe804
0.125	3.1	0.0155	4%	Goe804
0.135	2.6	0.0130	4%	Goe804

$\epsilon = 6^{-6}$. The upstream boundary condition (located 3 diameters upstream of the rotor face) has a velocity profile designed to match that of the Manchester experiments with 10% turbulence intensity (Figure 13). The `Code_Saturne` computations were run using the transient solver with a reference time step of 0.001 seconds, an adaptive time step was used with a maximum Courant number of 1.0. Convergence was accelerated by using local time-stepping and the solution was run for 3000 iterations. In this case the $k - \epsilon$ turbulence model was used as it is able to cope with rough walls. Full details of the setup are to be found in the `Code_Saturne` setup file, `D5_CASE.xml` which is to be found on the accompanying CD, also in the `Double` directory. Figures 14 to 17 show various pseudo-colour plots of the axial velocity distribution from the $\gamma = 3.5$ simulations with both smooth and rough floors, it should be noted in these plots that because the z-ordinate vector is pointing downstream higher velocities appear in blue and lower velocities in red.

Before considering the depth averaged results, the axial velocity profiles are presented (Figure 18). These results show the drop in velocity as the flow passes the upstream turbine followed by a region of recovery and then a second drop before the wake recovers towards the free stream. It is interesting to note that the wake behind the first turbine recovers faster than the second, due to the presence of the downstream turbine. It is also important to note that the wake down stream of both turbines recovers more quickly than may normally be expected, this is due to enhanced mixing caused by the symmetry planes in the array model which mimic contra-rotating turbines on either side of the simulated turbines.

For this case (Manchester test 19) comparisons with experimental data have not been made as the required experimental measurements have not yet been received from the University of Manchester, though they have been promised. Once the data has been received comparisons will be made and discussed as part of deliverable D5b.

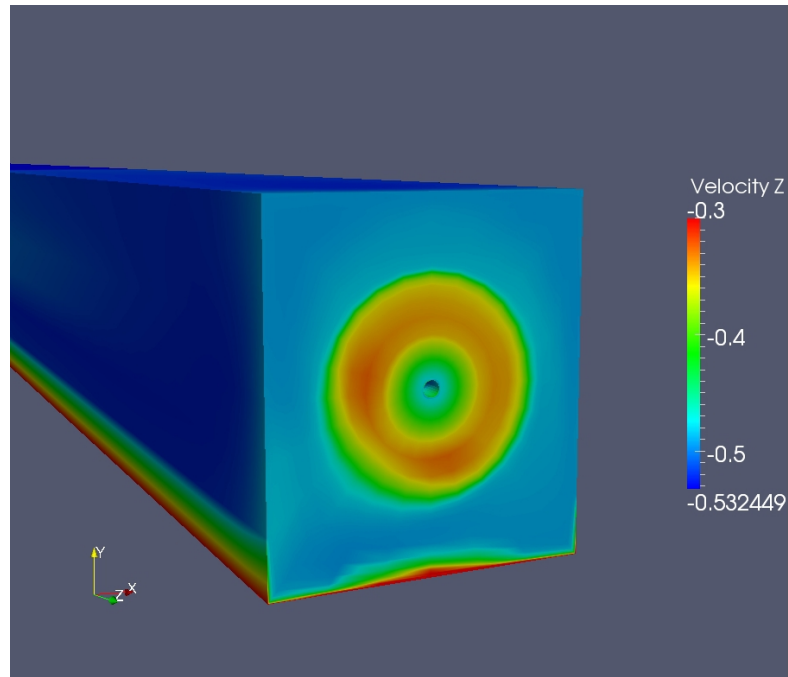


FIGURE 14. Two row array of horizontal axis tidal turbines in series: axial (Z) velocity distribution on the front actuator disc from a simulation with a smooth lower wall at a tip speed ratio of $\gamma = 3.5$, after 1642 iterations.

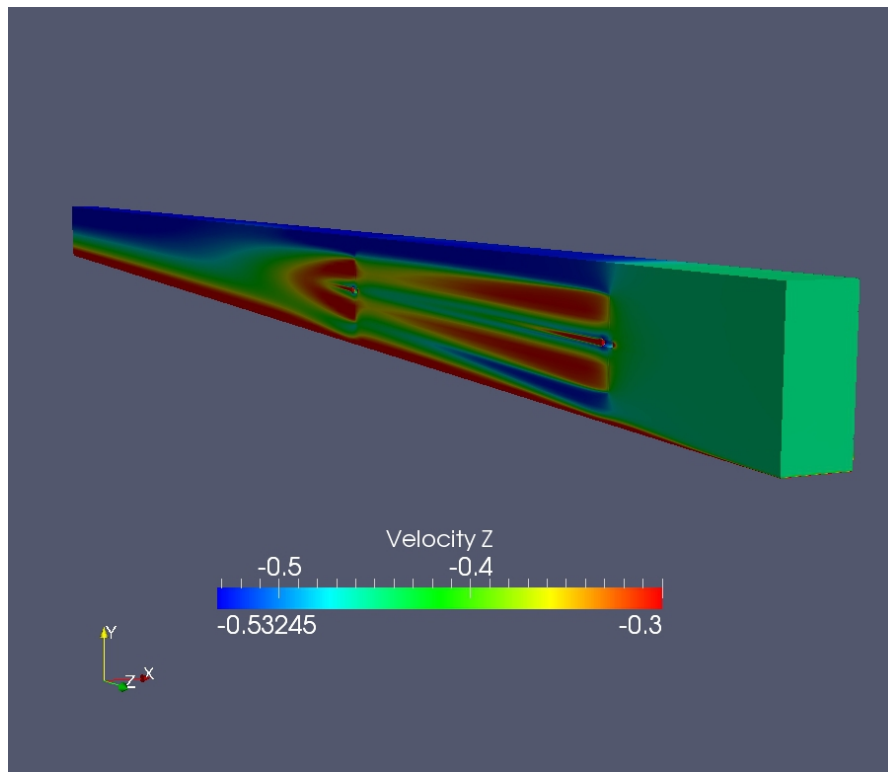


FIGURE 15. Two row array of horizontal axis tidal turbines in series: axial (Z) velocity distribution through the central, vertical, plane of the water column from a simulation with a smooth lower wall at a tip speed ratio of $\gamma = 3.5$, after 1642 iterations.

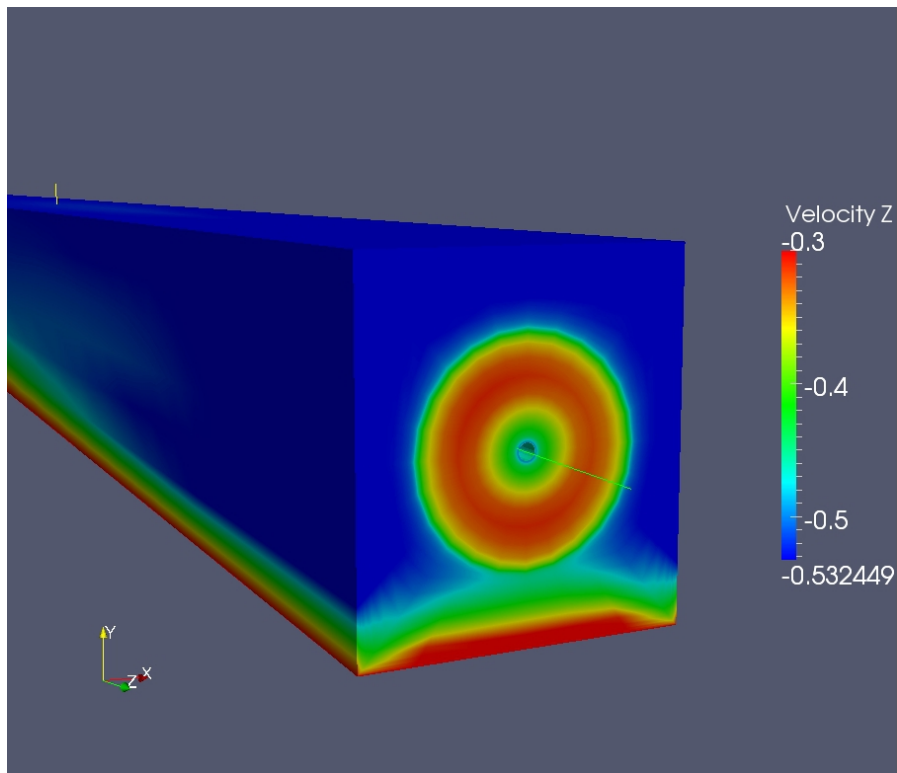


FIGURE 16. Two row array of horizontal axis tidal turbines in series: axial (Z) velocity distribution on the down stream actuator disc from a simulation with a smooth lower wall at a tip speed ratio of $\gamma = 3.5$, after 1642 iterations.

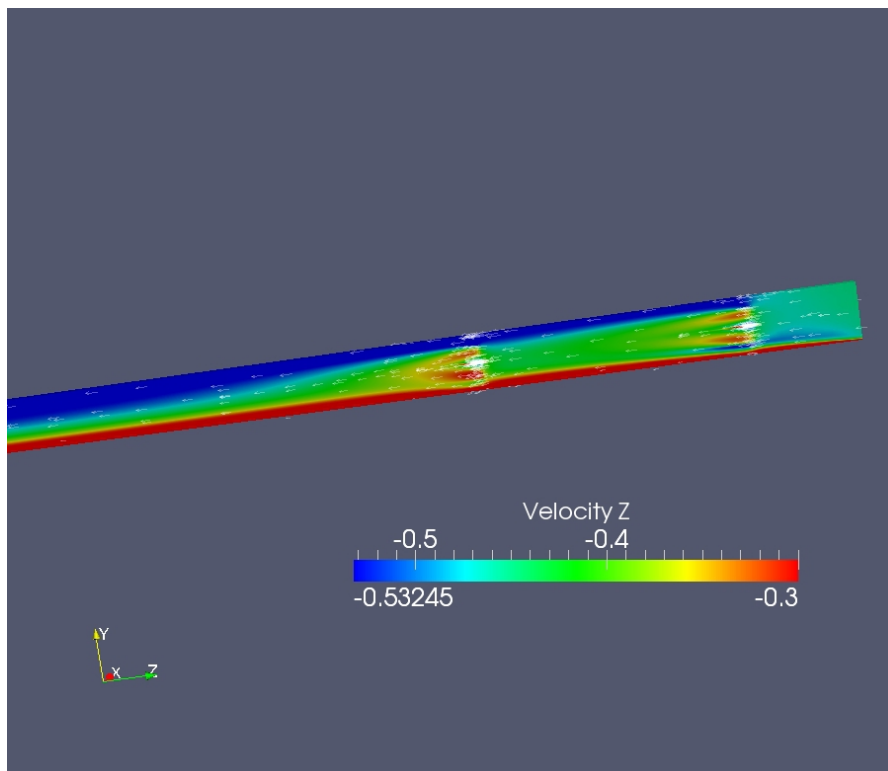


FIGURE 17. Two row array of horizontal axis tidal turbines in series: axial (Z) velocity distribution through the central, vertical, plane of the water column from a simulation with a rough lower wall at a tip speed ratio of $\gamma = 3.5$, after 3000 iterations.

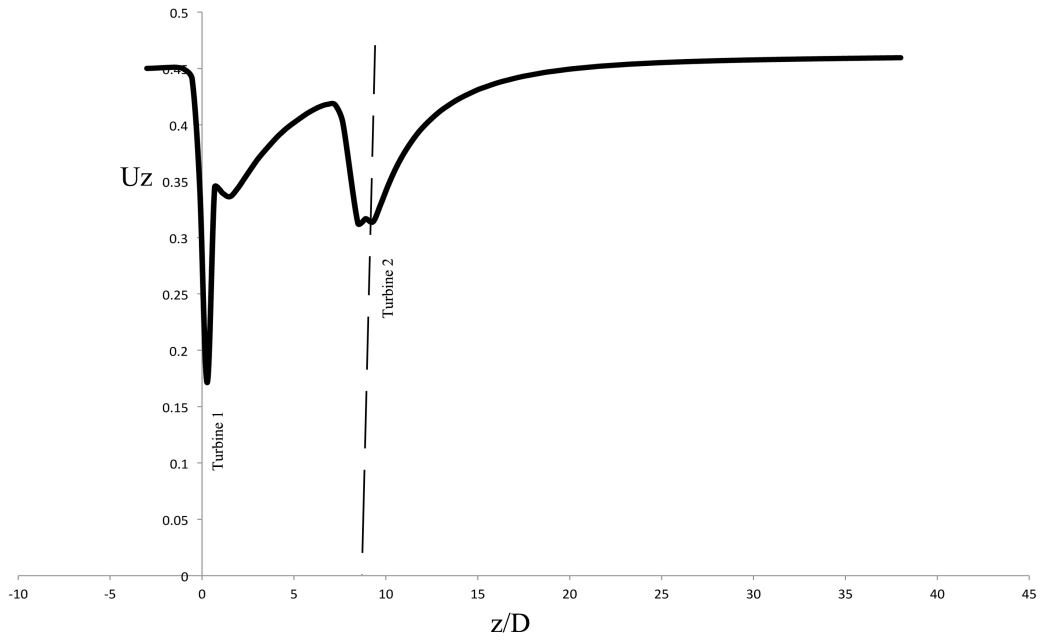


FIGURE 18. Axial velocity distribution from two turbines in series at a tip speed ratio of $\gamma = 4.5$.

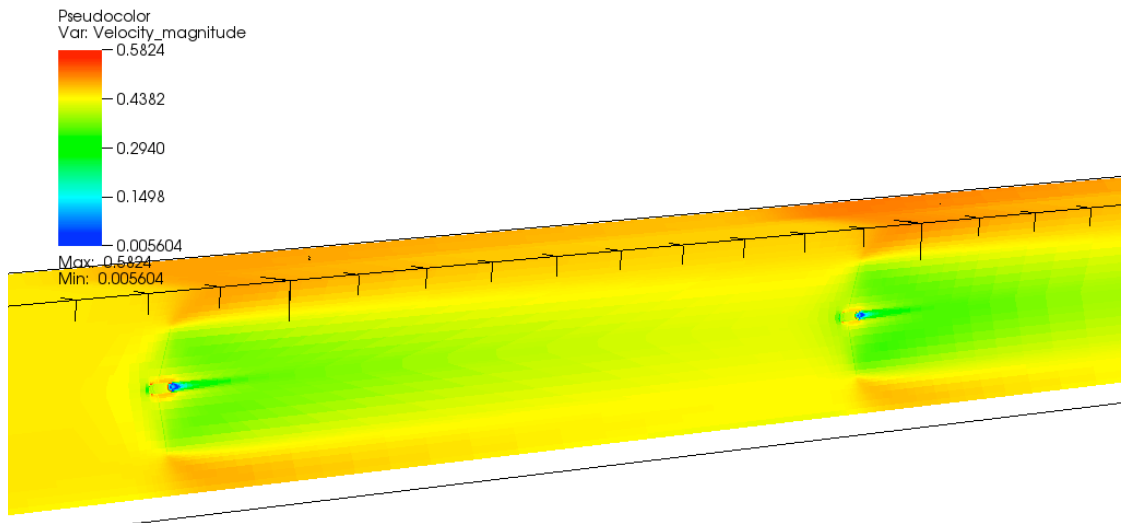


FIGURE 19. Pseudo-colour plot showing velocity magnitude for a section through the centre of the computational domain for a case with two turbines in series a tip speed ratio of $\gamma = 3.5$.

2.2. Depth averaged results. Figure 19 shows a pseudo-colour plot of the velocity magnitude from the three dimensional Reynolds averaged Navier-Stokes simulations, at a tip-speed ratio of $\gamma = 3.5$. For all the cases presented the computational domain in the neighbourhood of the two turbines has been binned using 19 bins in the stream wise direction from 11 diameters upstream of the downstream turbine ($z = -3.0m$) to 9 diameters downstream of the same turbine ($z = 2.5m$). 11 bins have been used in the cross flow direction. The origin of the computational domain is located at the centre of the front face of the downstream turbine and orientated so the flow direction is from right to left in the mosaic plots.

The depth averaged velocity plots for all four tip speed ratios, clearly show retardation on the centre line of the turbine, with the minimum velocities occurring just downstream of the turbine face, and acceleration of the flow towards the left and right symmetry planes, resulting in fluid jets bypassing the turbines., this jetting effect is more pronounced at higher tip speed ratios. This effect is due to the close, horizontal, packing of the turbines in the array. As in the previous case, as flow passes the nacelle most turbulence is generated. It should also be noted that an side-effect of the use of symmetry conditions to limit the width of the computational domain is that the fluid behaves as if the turbines in each row are contra-rotating.

2.2.1. *Tip speed ratio $\gamma = 3.5$.* Figure 20 shows mosaic plots of the binned depth averaged velocity magnitude, turbulent kinetic energy and turbulent viscosity. The bin containing the upstream hub is at (2.1,0.0) while the downstream hub is at (0.0,0.0) and it is easily identifiable in the velocity plot showing the expected velocity deficit associated with the flow passing the turbine face. Tables 9 to 11 present the binned mean values with the bin containing the turbine nacelle underlined.

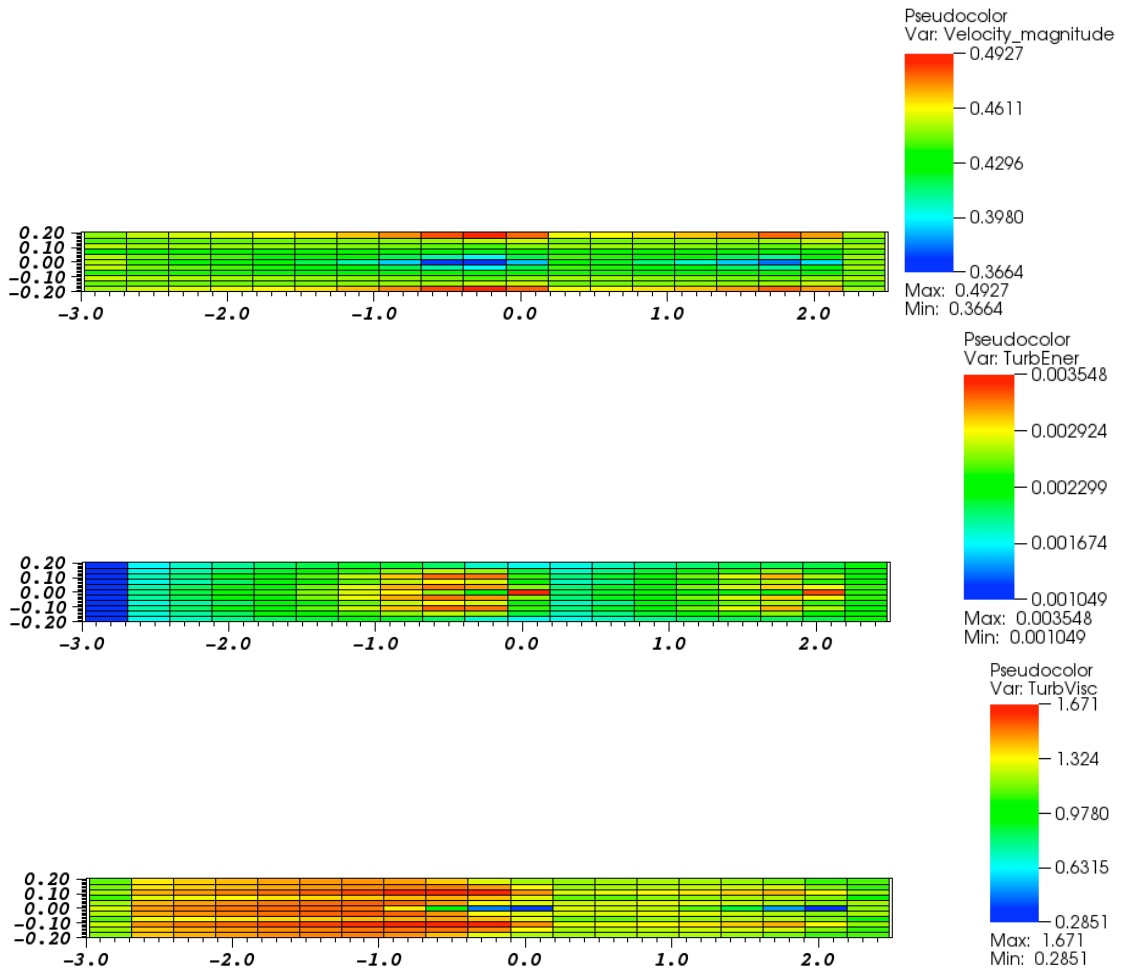


FIGURE 20. Two turbines in series tested in the Manchester basin at a tip speed ratio of $\gamma = 3.5$: Mosaic plots showing binned depth averaged velocity magnitude, turbulent kinetic energy and turbulent viscosity.

TABLE 9. Two turbines in series tested in the Manchester basin at a tip speed ratio of $\gamma = 3.5$: Depth averaged velocity magnitude. The value for the cells containing the turbines have been underlined

	downstream			stream wise direction ←									
1	<u>0.4481</u>	0.4541	0.4560	0.4583	0.4608	0.4637	0.4684	0.4750	0.4828	0.4924	0.4800	0.4594	0.4614
2	0.4402	0.4416	0.4421	0.4427	0.4434	0.4442	0.4455	0.4473	0.4493	0.4530	0.4543	0.4440	0.4447
3	0.4530	0.4505	0.4499	0.4492	0.4486	0.4478	0.4468	0.4453	0.4434	0.4404	0.4466	0.4495	0.4494
4	0.4354	0.4358	0.4357	0.4354	0.4350	0.4344	0.4333	0.4315	0.4290	0.4235	0.4274	0.4366	0.4369
5	0.4527	0.4451	0.4426	0.4397	0.4367	0.4330	0.4270	0.4184	0.4084	0.3985	0.4189	0.4396	0.4377
6	0.4509	0.4389	0.4351	0.4304	0.4250	0.4189	0.4083	0.3926	0.3750	0.3664	<u>0.3909</u>	0.4267	0.4231
7	0.4535	0.4459	0.4434	0.4405	0.4374	0.4338	0.4277	0.4192	0.4092	0.3992	0.4195	0.4398	0.4378
8	0.4375	0.4376	0.4374	0.4371	0.4365	0.4358	0.4346	0.4328	0.4302	0.4244	0.4282	0.4370	0.4372
9	0.4550	0.4521	0.4514	0.4507	0.4500	0.4492	0.4481	0.4465	0.4444	0.4413	0.4474	0.4498	0.4496
10	0.4429	0.4437	0.4440	0.4445	0.4450	0.4457	0.4468	0.4484	0.4503	0.4537	0.4550	0.4444	0.4449
11	0.4508	0.4557	0.4573	0.4594	0.4618	0.4645	0.4691	0.4754	0.4831	0.4927	0.4804	0.4597	0.4614

	stream wise direction ←					inlet
1	0.4646	0.4684	0.4732	0.4803	0.4731	0.4499
2	0.4458	0.4469	0.4481	0.4499	0.4541	0.4428
3	0.4478	0.4471	0.4451	0.4433	0.4482	0.4505
4	0.4359	0.4355	0.4330	0.4317	0.4323	0.4417
5	0.4323	0.4265	0.4168	0.4107	0.4252	0.4497
6	0.4144	0.4038	0.3918	0.3810	<u>0.3945</u>	0.4461
7	0.4324	0.4266	0.4168	0.4107	0.4251	0.4497
8	0.4361	0.4357	0.4331	0.4317	0.4322	0.4417
9	0.4480	0.4472	0.4452	0.4433	0.4482	0.4505
10	0.4459	0.4469	0.4481	0.4498	0.4541	0.4427
11	0.4646	0.4684	0.4731	0.4803	0.4731	0.4498

TABLE 10. Two turbines in series tested in the Manchester basin at a tip speed ratio of $\gamma = 3.5$: Depth averaged turbulent kinetic energy. The value for the cells containing the turbines have been underlined

	downstream			stream wise direction ←							
1	<u>1.05e-03</u>	1.69e-03	1.81e-03	1.92e-03	2.02e-03	2.09e-03	2.15e-03	2.14e-03	2.03e-03	1.80e-03	1.71e-03
2	1.05e-03	1.74e-03	1.88e-03	2.02e-03	2.16e-03	2.29e-03	2.47e-03	2.64e-03	2.77e-03	2.68e-03	2.12e-03
3	1.11e-03	1.85e-03	2.01e-03	2.18e-03	2.36e-03	2.53e-03	2.78e-03	3.06e-03	3.29e-03	3.26e-03	2.49e-03
4	1.08e-03	1.74e-03	1.88e-03	2.03e-03	2.19e-03	2.34e-03	2.54e-03	2.76e-03	2.91e-03	2.83e-03	2.25e-03
5	1.14e-03	1.88e-03	2.05e-03	2.23e-03	2.41e-03	2.60e-03	2.85e-03	3.11e-03	3.25e-03	3.17e-03	2.64e-03
6	1.14e-03	1.93e-03	2.10e-03	2.28e-03	2.47e-03	2.63e-03	2.83e-03	2.92e-03	2.66e-03	2.41e-03	3.55e-03
7	1.14e-03	1.90e-03	2.07e-03	2.25e-03	2.43e-03	2.62e-03	2.88e-03	3.13e-03	3.26e-03	3.18e-03	2.64e-03
8	1.09e-03	1.76e-03	1.90e-03	2.05e-03	2.21e-03	2.36e-03	2.57e-03	2.78e-03	2.93e-03	2.83e-03	2.25e-03
9	1.13e-03	1.89e-03	2.05e-03	2.22e-03	2.39e-03	2.57e-03	2.81e-03	3.08e-03	3.30e-03	3.26e-03	2.49e-03
10	1.08e-03	1.78e-03	1.92e-03	2.06e-03	2.19e-03	2.32e-03	2.49e-03	2.66e-03	2.77e-03	2.68e-03	2.13e-03
11	1.07e-03	1.73e-03	1.84e-03	1.95e-03	2.05e-03	2.12e-03	2.17e-03	2.16e-03	2.05e-03	1.81e-03	1.72e-03

	stream wise direction ←							inlet	
1	1.74e-03	1.84e-03	1.94e-03	2.01e-03	2.06e-03	2.07e-03	2.09e-03	2.35e-03	
2	1.82e-03	1.96e-03	2.13e-03	2.29e-03	2.47e-03	2.65e-03	2.38e-03	2.29e-03	
3	1.98e-03	2.15e-03	2.38e-03	2.60e-03	2.85e-03	3.10e-03	2.72e-03	2.44e-03	
4	1.82e-03	1.93e-03	2.17e-03	2.33e-03	2.55e-03	2.71e-03	2.47e-03	2.28e-03	
5	1.99e-03	2.16e-03	2.40e-03	2.61e-03	2.82e-03	3.04e-03	2.90e-03	2.48e-03	
6	<u>2.02e-03</u>	2.15e-03	2.33e-03	2.43e-03	2.42e-03	2.23e-03	<u>3.36e-03</u>	2.46e-03	
7	2.00e-03	2.17e-03	2.40e-03	2.62e-03	2.83e-03	3.04e-03	2.90e-03	2.48e-03	
8	1.83e-03	1.94e-03	2.18e-03	2.34e-03	2.56e-03	2.72e-03	2.47e-03	2.28e-03	
9	2.00e-03	2.16e-03	2.39e-03	2.61e-03	2.86e-03	3.11e-03	2.73e-03	2.44e-03	
10	1.84e-03	1.97e-03	2.14e-03	2.30e-03	2.47e-03	2.66e-03	2.38e-03	2.29e-03	
11	1.75e-03	1.85e-03	1.94e-03	2.02e-03	2.07e-03	2.07e-03	2.09e-03	2.35e-03	

TABLE 11. Two turbines in series tested in the Manchester basin at a tip speed ratio of $\gamma = 3.5$: Depth averaged turbulent viscosity. The value for the cells containing the turbines have been underlined

	downstream			stream wise direction ←									
1	<u>1.1253</u>	<u>1.3566</u>	<u>1.3900</u>	1.4198	1.4439	1.4604	1.4677	1.4508	1.3973	1.2758	1.2080	1.1934	1.2059
2	1.1538	1.3634	1.3931	1.4200	1.4431	1.4619	1.4814	1.4953	1.4988	1.4650	1.3205	1.1982	1.2134
3	1.2077	1.4316	1.4637	1.4937	1.5209	1.5452	1.5766	1.6125	1.6479	1.6493	1.4671	1.2785	1.2961
4	1.0904	1.2814	1.3071	1.3308	1.3593	1.3779	1.3999	1.4199	1.4305	1.4059	1.2846	1.1253	1.1198
5	1.2053	1.4226	1.4528	1.4809	1.5031	1.5235	1.5397	1.5284	1.4609	1.3200	1.2843	1.2554	1.2670
6	1.2654	1.4609	1.4879	1.5116	1.5288	1.5347	1.5038	1.3511	0.9378	0.4597	<u>0.3875</u>	1.2714	1.2481
7	1.2210	1.4399	1.4696	1.4974	1.5188	1.5387	1.5539	1.5406	1.4689	1.3218	1.2858	1.2613	1.2725
8	1.1132	1.3054	1.3302	1.3530	1.3805	1.3981	1.4187	1.4367	1.4448	1.4158	1.2902	1.1327	1.1262
9	1.2488	1.4748	1.5051	1.5330	1.5579	1.5797	1.6075	1.6391	1.6709	1.6670	1.4785	1.2904	1.3064
10	1.1939	1.4041	1.4317	1.4563	1.4769	1.4931	1.5088	1.5184	1.5182	1.4795	1.3313	1.2083	1.2219
11	1.1700	1.4012	1.4320	1.4589	1.4795	1.4924	1.4952	1.4732	1.4155	1.2898	1.2202	1.2031	1.2134

	stream wise direction ←						inlet
1	1.2144	1.2129	1.1979	1.1531	1.0823	1.1004	
2	1.2300	1.2445	1.2576	1.2655	1.1637	1.0774	
3	1.3292	1.3553	1.3907	1.4260	1.3198	1.1908	
4	1.1755	1.1789	1.2080	1.2155	1.1526	1.0525	
5	1.2887	1.2861	1.2525	1.2179	1.1757	1.2078	
6	1.2298	1.1148	0.8803	0.5062	<u>0.2851</u>	1.1683	
7	1.2935	1.2904	1.2562	1.2208	1.1768	1.2078	
8	1.1817	1.1841	1.2124	1.2186	1.1539	1.0525	
9	1.3377	1.3622	1.3960	1.4297	1.3214	1.1908	
10	1.2369	1.2498	1.2615	1.2680	1.1648	1.0775	
11	1.2196	1.2164	1.1999	1.1541	1.0824	1.1004	

2.2.2. *Tip speed ratio $\gamma = 4.0$.* Figure 21 shows mosaic plots of the binned depth averaged velocity magnitude, turbulent kinetic energy and turbulent viscosity. The bin containing the upstream hub is at (2.1,0.0) while the downstream hub is at (0.0,0.0) and it is easily identifiable in the velocity plot showing the expected velocity deficit associated with the flow passing the turbine face. Tables 12 to 14 present the binned mean values with the bin containing the turbine nacelle underlined.

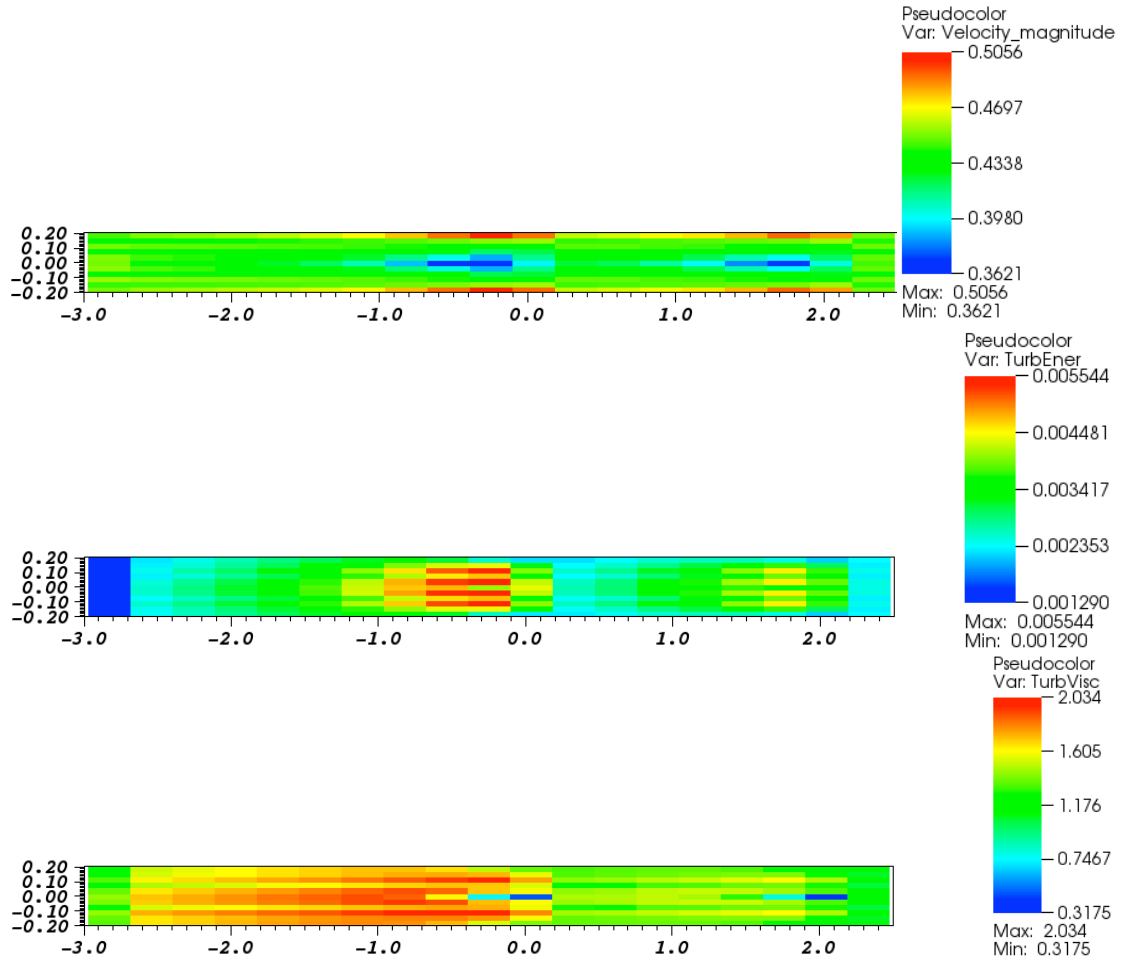


FIGURE 21. Two turbines in series tested in the Manchester basin at a tip speed ratio of $\gamma = 4.0$: Mosaic plots showing binned depth averaged velocity magnitude, turbulent kinetic energy and turbulent viscosity.

TABLE 12. Two turbines in series tested in the Manchester basin at a tip speed ratio of $\gamma = 4.0$: Depth averaged velocity magnitude. The value for the cells containing the turbines have been underlined

	downstream			stream wise direction ←									
1	<u>0.4457</u>	0.4524	0.4546	0.4572	0.4602	0.4638	0.4697	0.4784	0.4894	0.5049	0.4898	0.4611	0.4637
2	0.4391	0.4406	0.4411	0.4418	0.4426	0.4435	0.4452	0.4475	0.4501	0.4536	0.4556	0.4440	0.4449
3	0.4516	0.4494	0.4488	0.4480	0.4472	0.4462	0.4447	0.4426	0.4396	0.4330	0.4403	0.4483	0.4481
4	0.4356	0.4358	0.4357	0.4355	0.4349	0.4343	0.4330	0.4309	0.4276	0.4189	0.4222	0.4360	0.4366
5	0.4524	0.4453	0.4428	0.4397	0.4363	0.4322	0.4251	0.4144	0.4009	0.3862	0.4130	0.4376	0.4353
6	0.4514	0.4405	0.4365	0.4316	0.4259	0.4191	0.4073	0.3892	0.3670	0.3621	<u>0.3965</u>	0.4241	0.4202
7	0.4542	0.4470	0.4445	0.4414	0.4380	0.4339	0.4268	0.4162	0.4028	0.3879	0.4139	0.4381	0.4357
8	0.4398	0.4399	0.4396	0.4392	0.4384	0.4376	0.4361	0.4339	0.4305	0.4214	0.4240	0.4372	0.4375
9	0.4559	0.4530	0.4522	0.4513	0.4504	0.4494	0.4478	0.4455	0.4424	0.4353	0.4417	0.4493	0.4489
10	0.4447	0.4452	0.4455	0.4458	0.4464	0.4470	0.4484	0.4505	0.4528	0.4556	0.4572	0.4451	0.4457
11	0.4516	0.4558	0.4574	0.4597	0.4625	0.4656	0.4713	0.4796	0.4902	0.5056	0.4907	0.4618	0.4641

	stream wise direction ←					inlet
1	0.4681	0.4735	0.4802	0.4910	0.4834	0.4507
2	0.4463	0.4478	0.4493	0.4512	0.4563	0.4429
3	0.4460	0.4449	0.4419	0.4382	0.4421	0.4502
4	0.4348	0.4345	0.4310	0.4287	0.4269	0.4416
5	0.4286	0.4212	0.4087	0.3995	0.4191	0.4490
6	0.4099	0.3972	0.3826	0.3722	<u>0.4020</u>	0.4456
7	0.4290	0.4215	0.4089	0.3997	0.4191	0.4490
8	0.4355	0.4350	0.4314	0.4289	0.4268	0.4416
9	0.4466	0.4453	0.4423	0.4384	0.4421	0.4502
10	0.4468	0.4481	0.4495	0.4512	0.4563	0.4429
11	0.4684	0.4736	0.4802	0.4910	0.4835	0.4507

TABLE 13. Two turbines in series tested in the Manchester basin at a tip speed ratio of $\gamma = 4.0$: Depth averaged turbulent kinetic energy. The value for the cells containing the turbines have been underlined

	downstream			stream wise direction ←								
1	<u>1.29e-03</u>	2.26e-03	2.46e-03	2.67e-03	2.86e-03	3.03e-03	3.20e-03	3.26e-03	3.11e-03	2.55e-03	2.23e-03	
2	1.29e-03	2.30e-03	2.53e-03	2.77e-03	3.01e-03	3.26e-03	3.59e-03	3.98e-03	4.30e-03	4.39e-03	3.22e-03	
3	1.37e-03	2.45e-03	2.71e-03	2.98e-03	3.28e-03	3.58e-03	4.04e-03	4.61e-03	5.17e-03	5.52e-03	4.01e-03	
4	1.32e-03	2.30e-03	2.53e-03	2.77e-03	3.04e-03	3.31e-03	3.70e-03	4.17e-03	4.57e-03	4.74e-03	3.66e-03	
5	1.42e-03	2.51e-03	2.78e-03	3.08e-03	3.39e-03	3.72e-03	4.21e-03	4.81e-03	5.29e-03	5.51e-03	4.24e-03	
6	1.42e-03	2.58e-03	2.86e-03	3.16e-03	3.48e-03	3.81e-03	4.27e-03	4.72e-03	4.79e-03	4.07e-03	4.37e-03	
7	1.44e-03	2.57e-03	2.84e-03	3.14e-03	3.45e-03	3.78e-03	4.28e-03	4.88e-03	5.36e-03	5.54e-03	4.24e-03	
8	1.36e-03	2.37e-03	2.61e-03	2.85e-03	3.13e-03	3.40e-03	3.79e-03	4.25e-03	4.64e-03	4.77e-03	3.67e-03	
9	1.43e-03	2.58e-03	2.84e-03	3.12e-03	3.42e-03	3.72e-03	4.16e-03	4.71e-03	5.24e-03	5.54e-03	4.03e-03	
10	1.36e-03	2.43e-03	2.66e-03	2.90e-03	3.14e-03	3.38e-03	3.70e-03	4.06e-03	4.35e-03	4.41e-03	3.24e-03	
11	1.37e-03	2.40e-03	2.61e-03	2.81e-03	3.00e-03	3.16e-03	3.31e-03	3.36e-03	3.18e-03	2.61e-03	2.28e-03	

	stream wise direction ←								inlet
1	2.24e-03	2.38e-03	2.52e-03	2.61e-03	2.63e-03	2.49e-03	2.16e-03	2.36e-03	
2	2.35e-03	2.57e-03	2.83e-03	3.10e-03	3.39e-03	3.73e-03	3.01e-03	2.29e-03	
3	2.57e-03	2.83e-03	3.20e-03	3.57e-03	4.02e-03	4.55e-03	3.74e-03	2.45e-03	
4	2.36e-03	2.54e-03	2.92e-03	3.19e-03	3.58e-03	3.90e-03	3.35e-03	2.29e-03	
5	2.62e-03	2.89e-03	3.28e-03	3.67e-03	4.10e-03	4.55e-03	3.89e-03	2.48e-03	
6	<u>2.67e-03</u>	2.90e-03	3.25e-03	3.54e-03	3.70e-03	3.48e-03	<u>3.65e-03</u>	2.46e-03	
7	2.64e-03	2.91e-03	3.30e-03	3.69e-03	4.12e-03	4.56e-03	3.89e-03	2.48e-03	
8	2.39e-03	2.57e-03	2.95e-03	3.22e-03	3.60e-03	3.92e-03	3.35e-03	2.29e-03	
9	2.62e-03	2.87e-03	3.23e-03	3.60e-03	4.04e-03	4.56e-03	3.74e-03	2.45e-03	
10	2.39e-03	2.60e-03	2.85e-03	3.12e-03	3.40e-03	3.74e-03	3.01e-03	2.29e-03	
11	2.27e-03	2.41e-03	2.54e-03	2.63e-03	2.64e-03	2.49e-03	2.16e-03	2.36e-03	

TABLE 14. Two turbines in series tested in the Manchester basin at a tip speed ratio of $\gamma = 4.0$: Depth averaged turbulent viscosity. The value for the cells containing the turbines have been underlined

	downstream			stream wise direction ←									
1	<u>1.2358</u>	<u>1.5220</u>	<u>1.5697</u>	<u>1.6147</u>	<u>1.6542</u>	<u>1.6852</u>	<u>1.7111</u>	<u>1.7103</u>	<u>1.6598</u>	<u>1.4974</u>	<u>1.3647</u>	<u>1.3286</u>	<u>1.3461</u>
2	<u>1.2722</u>	<u>1.5365</u>	<u>1.5784</u>	<u>1.6180</u>	<u>1.6535</u>	<u>1.6835</u>	<u>1.7162</u>	<u>1.7406</u>	<u>1.7494</u>	<u>1.7325</u>	<u>1.5588</u>	<u>1.3332</u>	<u>1.3520</u>
3	<u>1.3419</u>	<u>1.6253</u>	<u>1.6703</u>	<u>1.7135</u>	<u>1.7534</u>	<u>1.7892</u>	<u>1.8340</u>	<u>1.8812</u>	<u>1.9274</u>	<u>1.9708</u>	<u>1.7654</u>	<u>1.4275</u>	<u>1.4481</u>
4	<u>1.2226</u>	<u>1.4720</u>	<u>1.5089</u>	<u>1.5440</u>	<u>1.5852</u>	<u>1.6145</u>	<u>1.6505</u>	<u>1.6851</u>	<u>1.7074</u>	<u>1.7030</u>	<u>1.5486</u>	<u>1.2633</u>	<u>1.2573</u>
5	<u>1.3666</u>	<u>1.6520</u>	<u>1.6958</u>	<u>1.7390</u>	<u>1.7774</u>	<u>1.8156</u>	<u>1.8620</u>	<u>1.8943</u>	<u>1.8633</u>	<u>1.6996</u>	<u>1.5876</u>	<u>1.4280</u>	<u>1.4498</u>
6	<u>1.4365</u>	<u>1.7065</u>	<u>1.7497</u>	<u>1.7928</u>	<u>1.8339</u>	<u>1.8697</u>	<u>1.9011</u>	<u>1.8686</u>	<u>1.5935</u>	<u>0.7393</u>	<u>0.4702</u>	<u>1.4758</u>	<u>1.4719</u>
7	<u>1.4028</u>	<u>1.6967</u>	<u>1.7403</u>	<u>1.7831</u>	<u>1.8202</u>	<u>1.8579</u>	<u>1.9036</u>	<u>1.9349</u>	<u>1.9014</u>	<u>1.7230</u>	<u>1.6032</u>	<u>1.4439</u>	<u>1.4645</u>
8	<u>1.2754</u>	<u>1.5360</u>	<u>1.5718</u>	<u>1.6056</u>	<u>1.6455</u>	<u>1.6731</u>	<u>1.7068</u>	<u>1.7383</u>	<u>1.7564</u>	<u>1.7424</u>	<u>1.5748</u>	<u>1.2832</u>	<u>1.2748</u>
9	<u>1.4368</u>	<u>1.7414</u>	<u>1.7844</u>	<u>1.8247</u>	<u>1.8609</u>	<u>1.8923</u>	<u>1.9301</u>	<u>1.9682</u>	<u>2.0050</u>	<u>2.0344</u>	<u>1.8082</u>	<u>1.4608</u>	<u>1.4767</u>
10	<u>1.3658</u>	<u>1.6483</u>	<u>1.6876</u>	<u>1.7235</u>	<u>1.7546</u>	<u>1.7796</u>	<u>1.8045</u>	<u>1.8191</u>	<u>1.8174</u>	<u>1.7846</u>	<u>1.5940</u>	<u>1.3609</u>	<u>1.3750</u>
11	<u>1.3402</u>	<u>1.6464</u>	<u>1.6899</u>	<u>1.7298</u>	<u>1.7631</u>	<u>1.7874</u>	<u>1.8034</u>	<u>1.7900</u>	<u>1.7261</u>	<u>1.5448</u>	<u>1.4025</u>	<u>1.3581</u>	<u>1.3692</u>
				stream wise direction ←					inlet				
				1	1.3588	1.3573	1.3350	1.2624	1.1062	1.1011			
				2	1.3716	1.3868	1.3978	1.4039	1.2712	1.0790			
				3	1.4870	1.5160	1.5556	1.6012	1.4746	1.1930			
				4	1.3274	1.3330	1.3708	1.3797	1.2814	1.0543			
				5	1.4917	1.5129	1.5045	1.4556	1.3353	1.2098			
				6	1.5044	1.4591	1.2917	0.7898	<u>0.3175</u>	1.1692			
				7	1.5045	1.5238	1.5132	1.4614	1.3366	1.2098			
				8	1.3437	1.3466	1.3818	1.3870	1.2830	1.0543			
				9	1.5104	1.5344	1.5694	1.6100	1.4763	1.1930			
				10	1.3898	1.4006	1.4076	1.4093	1.2723	1.0790			
				11	1.3749	1.3676	1.3405	1.2642	1.1064	1.1011			

2.2.3. *Tip speed ratio $\gamma = 5.5$.* Figure 22 shows mosaic plots of the binned depth averaged velocity magnitude, turbulent kinetic energy and turbulent viscosity. The bin containing the upstream hub is at (2.1,0.0) while the downstream hub is at (0.0,0.0) and it is easily identifiable in the velocity plot showing the expected velocity deficit associated with the flow passing the turbine face. Tables 15 to 17 present the binned mean values with the bin containing the turbine nacelle underlined.

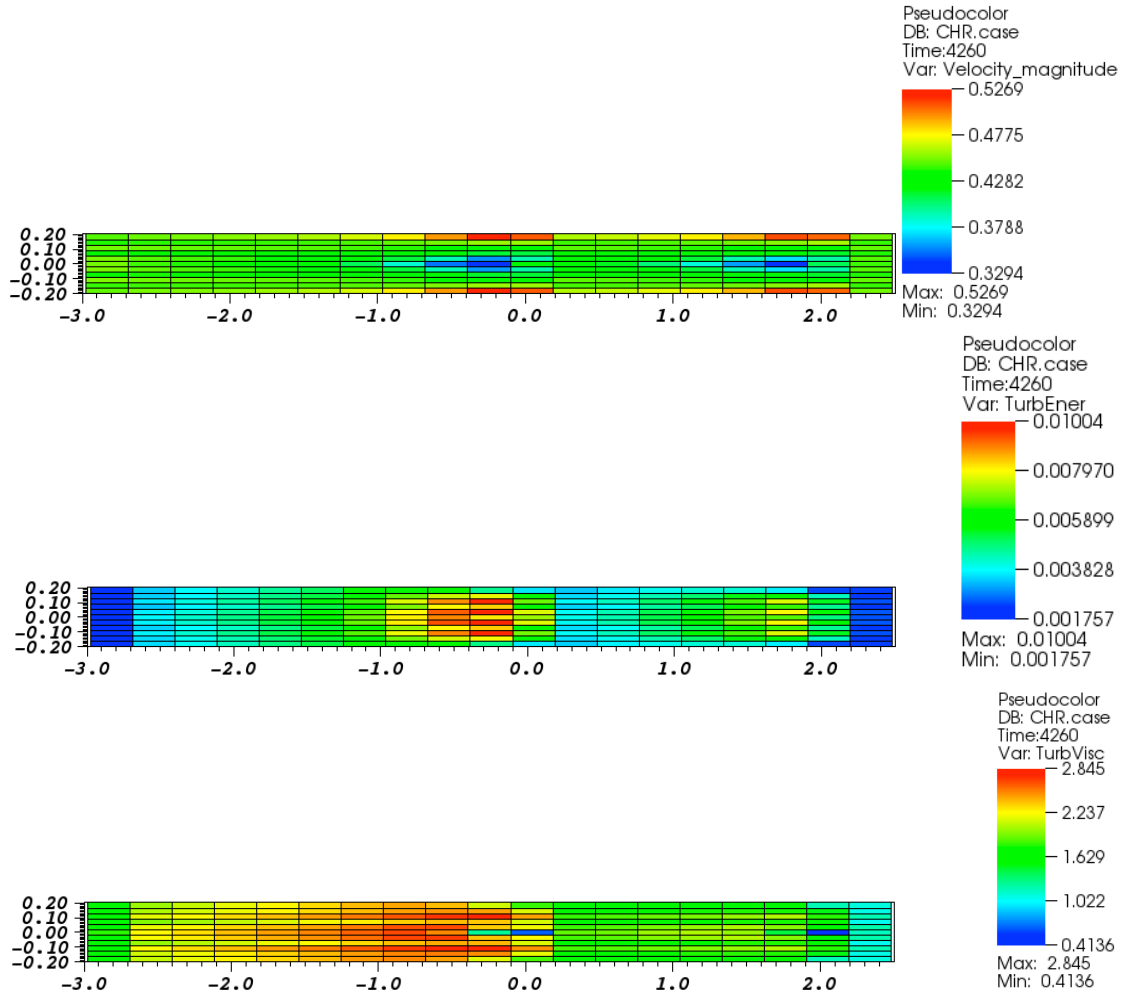


FIGURE 22. Two turbines in series tested in the Manchester basin at a tip speed ratio of $\gamma = 5.5$: Mosaic plots showing binned depth averaged velocity magnitude, turbulent kinetic energy and turbulent viscosity.

TABLE 15. Two turbines in series tested in the Manchester basin at a tip speed ratio of $\gamma = 5.5$: Depth averaged velocity magnitude. The value for the cells containing the turbines have been underlined

	downstream			stream wise direction ←									
1	<u>0.4468</u>	<u>0.4513</u>	<u>0.4531</u>	0.4554	0.4585	0.4622	0.4692	0.4806	0.4971	0.5267	0.5094	0.4627	0.4660
2	0.4410	0.4417	0.4420	0.4424	0.4429	0.4436	0.4452	0.4482	0.4527	0.4584	0.4587	0.4440	0.4449
3	0.4527	0.4507	0.4501	0.4492	0.4482	0.4470	0.4449	0.4419	0.4377	0.4260	0.4301	0.4475	0.4470
4	0.4377	0.4379	0.4377	0.4374	0.4369	0.4361	0.4346	0.4321	0.4279	0.4144	0.4133	0.4361	0.4365
5	0.4531	0.4480	0.4458	0.4429	0.4395	0.4351	0.4267	0.4129	0.3923	0.3594	0.3941	0.4363	0.4332
6	0.4522	0.4443	0.4409	0.4364	0.4307	0.4236	0.4101	0.3875	0.3529	0.3315	<u>0.4260</u>	0.4225	0.4177
7	0.4538	0.4488	0.4466	0.4438	0.4403	0.4360	0.4277	0.4139	0.3934	0.3605	0.3947	0.4367	0.4336
8	0.4396	0.4399	0.4397	0.4393	0.4388	0.4380	0.4364	0.4337	0.4296	0.4161	0.4145	0.4371	0.4374
9	0.4546	0.4524	0.4517	0.4508	0.4497	0.4485	0.4465	0.4434	0.4393	0.4274	0.4310	0.4482	0.4476
10	0.4435	0.4439	0.4441	0.4443	0.4448	0.4454	0.4469	0.4497	0.4542	0.4597	0.4597	0.4449	0.4456
11	0.4495	0.4530	0.4544	0.4565	0.4594	0.4629	0.4698	0.4810	0.4974	0.5269	0.5098	0.4632	0.4664

	stream wise direction ←					inlet
1	0.4723	0.4805	0.4917	0.5117	0.5071	0.4528
2	0.4466	0.4488	0.4517	0.4556	0.4606	0.4435
3	0.4440	0.4420	0.4376	0.4313	0.4302	0.4498
4	0.4337	0.4330	0.4279	0.4244	0.4159	0.4413
5	0.4244	0.4136	0.3938	0.3733	0.3954	0.4475
6	0.4042	0.3859	0.3610	0.3294	<u>0.4102</u>	0.4442
7	0.4247	0.4138	0.3941	0.3735	0.3955	0.4475
8	0.4343	0.4335	0.4282	0.4246	0.4160	0.4413
9	0.4445	0.4425	0.4380	0.4315	0.4302	0.4498
10	0.4471	0.4492	0.4520	0.4557	0.4606	0.4435
11	0.4727	0.4808	0.4918	0.5118	0.5071	0.4528

TABLE 16. Two turbines in series tested in the Manchester basin at a tip speed ratio of $\gamma = 5.5$: Depth averaged turbulent kinetic energy. The value for the cells containing the turbines have been underlined

	downstream			stream wise direction ←								
1	<u>1.76e-03</u>	3.41e-03	3.81e-03	4.23e-03	4.66e-03	5.07e-03	5.58e-03	5.96e-03	5.88e-03	4.68e-03	3.62e-03	
2	<u>1.77e-03</u>	3.44e-03	3.85e-03	4.29e-03	4.76e-03	5.24e-03	5.95e-03	6.79e-03	7.53e-03	7.83e-03	5.57e-03	
3	<u>1.88e-03</u>	3.65e-03	4.09e-03	4.58e-03	5.11e-03	5.67e-03	6.55e-03	7.70e-03	8.90e-03	9.71e-03	6.87e-03	
4	<u>1.78e-03</u>	3.39e-03	3.79e-03	4.22e-03	4.72e-03	5.22e-03	6.00e-03	7.01e-03	7.97e-03	8.34e-03	6.07e-03	
5	<u>1.93e-03</u>	3.70e-03	4.15e-03	4.65e-03	5.20e-03	5.79e-03	6.75e-03	8.03e-03	9.29e-03	9.98e-03	7.71e-03	
6	<u>1.93e-03</u>	3.77e-03	4.23e-03	4.75e-03	5.31e-03	5.92e-03	6.88e-03	8.08e-03	8.93e-03	8.16e-03	7.20e-03	
7	<u>1.95e-03</u>	3.75e-03	4.20e-03	4.71e-03	5.25e-03	5.85e-03	6.82e-03	8.11e-03	9.37e-03	1.00e-02	7.72e-03	
8	<u>1.80e-03</u>	3.46e-03	3.86e-03	4.30e-03	4.80e-03	5.31e-03	6.10e-03	7.11e-03	8.06e-03	8.40e-03	6.10e-03	
9	<u>1.92e-03</u>	3.76e-03	4.21e-03	4.71e-03	5.25e-03	5.81e-03	6.69e-03	7.83e-03	9.00e-03	9.78e-03	6.92e-03	
10	<u>1.81e-03</u>	3.56e-03	3.97e-03	4.42e-03	4.90e-03	5.38e-03	6.09e-03	6.91e-03	7.62e-03	7.88e-03	5.63e-03	
11	<u>1.81e-03</u>	3.54e-03	3.95e-03	4.38e-03	4.81e-03	5.22e-03	5.73e-03	6.10e-03	5.99e-03	4.77e-03	3.69e-03	

	stream wise direction ←								inlet
1	3.41e-03	3.70e-03	3.98e-03	4.16e-03	4.16e-03	3.71e-03	2.43e-03	2.37e-03	
2	3.54e-03	3.94e-03	4.43e-03	4.95e-03	5.51e-03	6.17e-03	4.33e-03	2.31e-03	
3	3.86e-03	4.34e-03	5.01e-03	5.74e-03	6.62e-03	7.68e-03	5.46e-03	2.48e-03	
4	3.53e-03	3.88e-03	4.57e-03	5.15e-03	5.92e-03	6.53e-03	4.70e-03	2.31e-03	
5	3.91e-03	4.43e-03	5.17e-03	6.01e-03	6.99e-03	7.91e-03	6.09e-03	2.51e-03	
6	<u>4.01e-03</u>	4.47e-03	5.21e-03	5.98e-03	6.65e-03	6.73e-03	<u>4.85e-03</u>	2.48e-03	
7	3.94e-03	4.45e-03	5.19e-03	6.03e-03	7.01e-03	7.92e-03	6.08e-03	2.51e-03	
8	3.56e-03	3.91e-03	4.60e-03	5.18e-03	5.95e-03	6.54e-03	4.69e-03	2.31e-03	
9	3.91e-03	4.38e-03	5.05e-03	5.77e-03	6.64e-03	7.68e-03	5.45e-03	2.48e-03	
10	3.58e-03	3.97e-03	4.46e-03	4.97e-03	5.52e-03	6.17e-03	4.33e-03	2.31e-03	
11	3.45e-03	3.73e-03	4.01e-03	4.17e-03	4.17e-03	3.71e-03	2.43e-03	2.37e-03	

TABLE 17. Two turbines in series tested in the Manchester basin at a tip speed ratio of $\gamma = 5.5$: Depth averaged turbulent viscosity. The value for the cells containing the turbines have been underlined

	downstream		stream wise direction ←										
1	1.5387	2.0169	2.0991	2.1807	2.2578	<u>2.3263</u>	2.4028	2.4477	2.4036	2.1253	1.8118	1.6778	1.7041
2	1.5975	2.0503	2.1241	2.1965	2.2650	2.3268	2.4009	2.4636	2.4903	2.4626	2.1535	1.6930	1.7222
3	1.6974	2.1730	2.2500	2.3261	2.3988	2.4661	2.5523	2.6404	2.7147	2.7944	2.4638	1.8177	1.8503
4	1.5341	1.9586	2.0230	2.0855	2.1564	2.2112	2.2816	2.3529	2.4007	2.3786	2.1342	1.6047	1.6007
5	1.7219	2.1904	2.2621	2.3332	2.3982	2.4649	2.5557	2.6484	2.6695	2.3652	2.2081	1.8197	1.8614
6	1.7931	2.2507	2.3209	2.3909	2.4601	2.5266	2.6131	2.6736	2.5153	1.2656	<u>0.6569</u>	1.8929	1.9135
7	1.7421	2.2211	2.2934	2.3648	2.4291	2.4957	2.5859	2.6778	2.6982	2.3881	2.2233	1.8322	1.8730
8	1.5634	2.0034	2.0683	2.1307	2.2012	2.2551	2.3238	2.3931	2.4386	2.4101	2.1564	1.6205	1.6145
9	1.7489	2.2536	2.3319	2.4081	2.4799	2.5453	2.6272	2.7086	2.7756	2.8453	2.5018	1.8456	1.8743
10	1.6478	2.1288	2.2035	2.2756	2.3425	2.4019	2.4708	2.5263	2.5449	2.5056	2.1859	1.7166	1.7419
11	1.5939	2.1028	2.1855	2.2664	2.3419	2.4078	2.4791	2.5159	2.4630	2.1705	1.8470	1.7040	1.7255

	stream wise direction ←					inlet
1	1.7228	1.7176	1.6761	1.5356	1.1852	1.1040
2	1.7525	1.7736	1.7846	1.7807	1.5098	1.0850
3	1.9093	1.9517	2.0061	2.0661	1.7924	1.2010
4	1.7044	1.7187	1.7779	1.7775	1.5280	1.0610
5	1.9428	2.0086	2.0544	1.9644	1.6499	1.2172
6	2.0124	2.0537	1.9936	1.4488	<u>0.4136</u>	1.1729
7	1.9529	2.0172	2.0614	1.9689	1.6501	1.2172
8	1.7173	1.7296	1.7867	1.7831	1.5285	1.0610
9	1.9288	1.9668	2.0171	2.0727	1.7930	1.2010
10	1.7679	1.7853	1.7927	1.7849	1.5101	1.0850
11	1.7387	1.7282	1.6820	1.5377	1.1853	1.1040

2.2.4. *Tip speed ratio $\gamma = 6.0$.* Figure 23 shows mosaic plots of the binned depth averaged velocity magnitude, turbulent kinetic energy and turbulent viscosity. The bin containing the upstream hub is at (2.1,0.0) while the downstream hub is at (0.0,0.0) and it is easily identifiable in the velocity plot showing the expected velocity deficit associated with the flow passing the turbine face. Tables 18 to 20 present the binned mean values with the bin containing the turbine nacelle underlined.

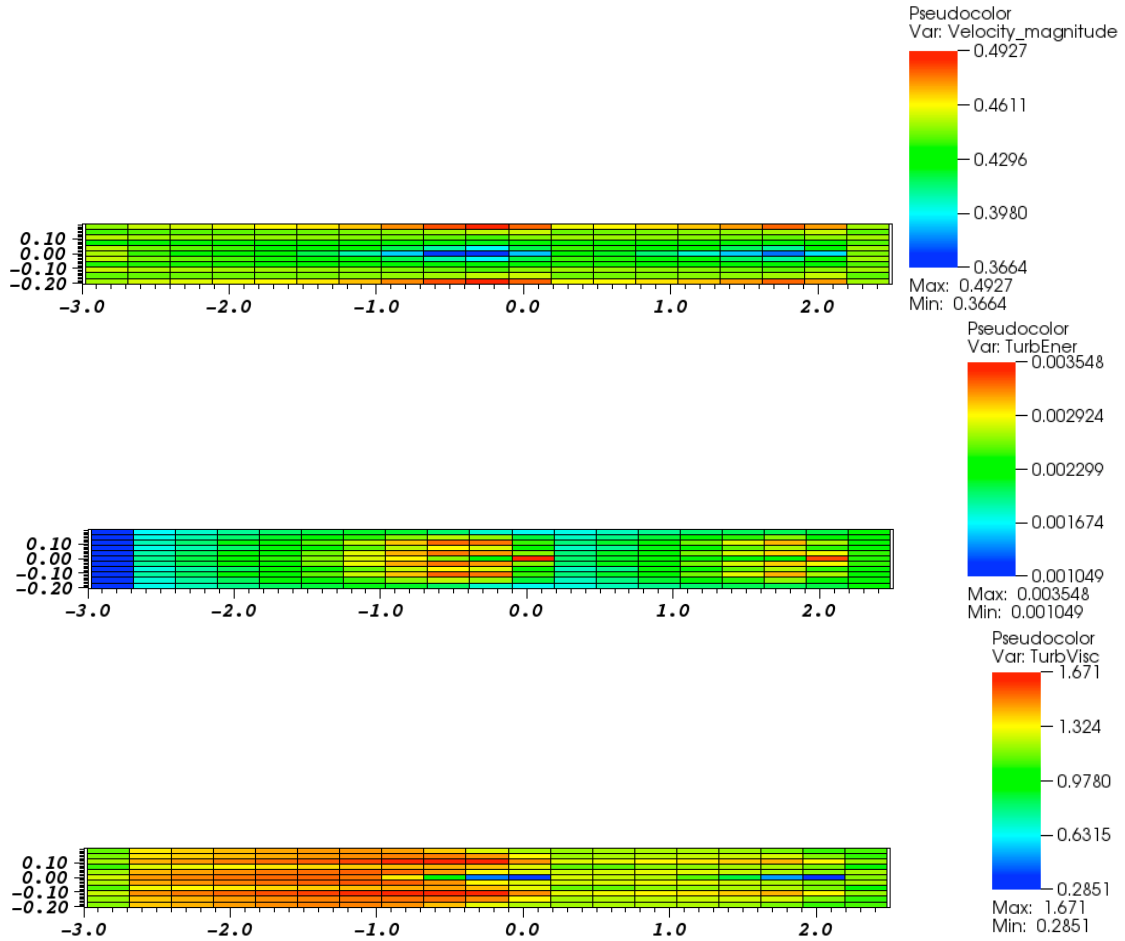


FIGURE 23. Two turbines in series tested in the Manchester basin at a tip speed ratio of $\gamma = 6.0$: Mosaic plots showing binned depth averaged velocity magnitude, turbulent kinetic energy and turbulent viscosity.

TABLE 18. Two turbines in series tested in the Manchester basin at a tip speed ratio of $\gamma = 6.0$: Depth averaged velocity magnitude. The value for the cells containing the turbines have been underlined

	downstream			stream wise direction ←									
1	<u>0.4481</u>	0.4541	0.4560	0.4583	0.4608	0.4637	0.4684	0.4750	0.4828	0.4924	0.4800	0.4594	0.4614
2	0.4402	0.4416	0.4421	0.4427	0.4434	0.4442	0.4455	0.4473	0.4493	0.4530	0.4543	0.4440	0.4447
3	0.4530	0.4505	0.4499	0.4492	0.4486	0.4478	0.4468	0.4453	0.4434	0.4404	0.4466	0.4495	0.4494
4	0.4354	0.4358	0.4357	0.4354	0.4350	0.4344	0.4333	0.4315	0.4290	0.4235	0.4274	0.4366	0.4369
5	0.4527	0.4451	0.4426	0.4397	0.4367	0.4330	0.4270	0.4184	0.4084	0.3985	0.4189	0.4396	0.4377
6	0.4509	0.4389	0.4351	0.4304	0.4250	0.4189	0.4083	0.3926	0.3750	0.3664	<u>0.3909</u>	0.4267	0.4231
7	0.4535	0.4459	0.4434	0.4405	0.4374	0.4338	0.4277	0.4192	0.4092	0.3992	0.4195	0.4398	0.4378
8	0.4375	0.4376	0.4374	0.4371	0.4365	0.4358	0.4346	0.4328	0.4302	0.4244	0.4282	0.4370	0.4372
9	0.4550	0.4521	0.4514	0.4507	0.4500	0.4492	0.4481	0.4465	0.4444	0.4413	0.4474	0.4498	0.4496
10	0.4429	0.4437	0.4440	0.4445	0.4450	0.4457	0.4468	0.4484	0.4503	0.4537	0.4550	0.4444	0.4449
11	0.4508	0.4557	0.4573	0.4594	0.4618	0.4645	0.4691	0.4754	0.4831	0.4927	0.4804	0.4597	0.4614

	stream wise direction ←					inlet
1	0.4646	0.4684	0.4732	0.4803	0.4731	0.4499
2	0.4458	0.4469	0.4481	0.4499	0.4541	0.4428
3	0.4478	0.4471	0.4451	0.4433	0.4482	0.4505
4	0.4359	0.4355	0.4330	0.4317	0.4323	0.4417
5	0.4323	0.4265	0.4168	0.4107	0.4252	0.4497
6	0.4144	0.4038	0.3918	0.3810	<u>0.3945</u>	0.4461
7	0.4324	0.4266	0.4168	0.4107	0.4251	0.4497
8	0.4361	0.4357	0.4331	0.4317	0.4322	0.4417
9	0.4480	0.4472	0.4452	0.4433	0.4482	0.4505
10	0.4459	0.4469	0.4481	0.4498	0.4541	0.4427
11	0.4646	0.4684	0.4731	0.4803	0.4731	0.4498

TABLE 19. Two turbines in series tested in the Manchester basin at a tip speed ratio of $\gamma = 6.0$: Depth averaged turbulent kinetic energy. The value for the cells containing the turbines have been underlined

	downstream			stream wise direction ←								
1	<u>1.05e-03</u>	1.69e-03	1.81e-03	1.92e-03	2.02e-03	2.09e-03	2.15e-03	2.14e-03	2.03e-03	1.80e-03	1.71e-03	
2	1.05e-03	1.74e-03	1.88e-03	2.02e-03	2.16e-03	2.29e-03	2.47e-03	2.64e-03	2.77e-03	2.68e-03	2.12e-03	
3	1.11e-03	1.85e-03	2.01e-03	2.18e-03	2.36e-03	2.53e-03	2.78e-03	3.06e-03	3.29e-03	3.26e-03	2.49e-03	
4	1.08e-03	1.74e-03	1.88e-03	2.03e-03	2.19e-03	2.34e-03	2.54e-03	2.76e-03	2.91e-03	2.83e-03	2.25e-03	
5	1.14e-03	1.88e-03	2.05e-03	2.23e-03	2.41e-03	2.60e-03	2.85e-03	3.11e-03	3.25e-03	3.17e-03	2.64e-03	
6	1.14e-03	1.93e-03	2.10e-03	2.28e-03	2.47e-03	2.63e-03	2.83e-03	2.92e-03	2.66e-03	2.41e-03	3.55e-03	
7	1.14e-03	1.90e-03	2.07e-03	2.25e-03	2.43e-03	2.62e-03	2.88e-03	3.13e-03	3.26e-03	3.18e-03	2.64e-03	
8	1.09e-03	1.76e-03	1.90e-03	2.05e-03	2.21e-03	2.36e-03	2.57e-03	2.78e-03	2.93e-03	2.83e-03	2.25e-03	
9	1.13e-03	1.89e-03	2.05e-03	2.22e-03	2.39e-03	2.57e-03	2.81e-03	3.08e-03	3.30e-03	3.26e-03	2.49e-03	
10	1.08e-03	1.78e-03	1.92e-03	2.06e-03	2.19e-03	2.32e-03	2.49e-03	2.66e-03	2.77e-03	2.68e-03	2.13e-03	
11	1.07e-03	1.73e-03	1.84e-03	1.95e-03	2.05e-03	2.12e-03	2.17e-03	2.16e-03	2.05e-03	1.81e-03	1.72e-03	

	stream wise direction ←								inlet
1	1.74e-03	1.84e-03	1.94e-03	2.01e-03	2.06e-03	2.07e-03	2.09e-03	2.35e-03	
2	1.82e-03	1.96e-03	2.13e-03	2.29e-03	2.47e-03	2.65e-03	2.38e-03	2.29e-03	
3	1.98e-03	2.15e-03	2.38e-03	2.60e-03	2.85e-03	3.10e-03	2.72e-03	2.44e-03	
4	1.82e-03	1.93e-03	2.17e-03	2.33e-03	2.55e-03	2.71e-03	2.47e-03	2.28e-03	
5	1.99e-03	2.16e-03	2.40e-03	2.61e-03	2.82e-03	3.04e-03	2.90e-03	2.48e-03	
6	<u>2.02e-03</u>	2.15e-03	2.33e-03	2.43e-03	2.42e-03	2.23e-03	<u>3.36e-03</u>	2.46e-03	
7	2.00e-03	2.17e-03	2.40e-03	2.62e-03	2.83e-03	3.04e-03	2.90e-03	2.48e-03	
8	1.83e-03	1.94e-03	2.18e-03	2.34e-03	2.56e-03	2.72e-03	2.47e-03	2.28e-03	
9	2.00e-03	2.16e-03	2.39e-03	2.61e-03	2.86e-03	3.11e-03	2.73e-03	2.44e-03	
10	1.84e-03	1.97e-03	2.14e-03	2.30e-03	2.47e-03	2.66e-03	2.38e-03	2.29e-03	
11	1.75e-03	1.85e-03	1.94e-03	2.02e-03	2.07e-03	2.07e-03	2.09e-03	2.35e-03	

TABLE 20. Two turbines in series tested in the Manchester basin at a tip speed ratio of $\gamma = 6.0$: Depth averaged turbulent viscosity. The value for the cells containing the turbines have been underlined

	downstream			stream wise direction ←									
1	<u>1.1253</u>	<u>1.3566</u>	<u>1.3900</u>	1.4198	1.4439	1.4604	1.4677	1.4508	1.3973	1.2758	1.2080	1.1934	1.2059
2	1.1538	1.3634	1.3931	1.4200	1.4431	1.4619	1.4814	1.4953	1.4988	1.4650	1.3205	1.1982	1.2134
3	1.2077	1.4316	1.4637	1.4937	1.5209	1.5452	1.5766	1.6125	1.6479	1.6493	1.4671	1.2785	1.2961
4	1.0904	1.2814	1.3071	1.3308	1.3593	1.3779	1.3999	1.4199	1.4305	1.4059	1.2846	1.1253	1.1198
5	1.2053	1.4226	1.4528	1.4809	1.5031	1.5235	1.5397	1.5284	1.4609	1.3200	1.2843	1.2554	1.2670
6	1.2654	1.4609	1.4879	1.5116	1.5288	1.5347	1.5038	1.3511	0.9378	0.4597	<u>0.3875</u>	1.2714	1.2481
7	1.2210	1.4399	1.4696	1.4974	1.5188	1.5387	1.5539	1.5406	1.4689	1.3218	1.2858	1.2613	1.2725
8	1.1132	1.3054	1.3302	1.3530	1.3805	1.3981	1.4187	1.4367	1.4448	1.4158	1.2902	1.1327	1.1262
9	1.2488	1.4748	1.5051	1.5330	1.5579	1.5797	1.6075	1.6391	1.6709	1.6670	1.4785	1.2904	1.3064
10	1.1939	1.4041	1.4317	1.4563	1.4769	1.4931	1.5088	1.5184	1.5182	1.4795	1.3313	1.2083	1.2219
11	1.1700	1.4012	1.4320	1.4589	1.4795	1.4924	1.4952	1.4732	1.4155	1.2898	1.2202	1.2031	1.2134

	stream wise direction ←					inlet	
1	1.2144	1.2129	1.1979	1.1531	1.0823	1.1004	
2	1.2300	1.2445	1.2576	1.2655	1.1637	1.0774	
3	1.3292	1.3553	1.3907	1.4260	1.3198	1.1908	
4	1.1755	1.1789	1.2080	1.2155	1.1526	1.0525	
5	1.2887	1.2861	1.2525	1.2179	1.1757	1.2078	
6	1.2298	1.1148	0.8803	0.5062	<u>0.2851</u>	1.1683	
7	1.2935	1.2904	1.2562	1.2208	1.1768	1.2078	
8	1.1817	1.1841	1.2124	1.2186	1.1539	1.0525	
9	1.3377	1.3622	1.3960	1.4297	1.3214	1.1908	
10	1.2369	1.2498	1.2615	1.2680	1.1648	1.0775	
11	1.2196	1.2164	1.1999	1.1541	1.0824	1.1004	

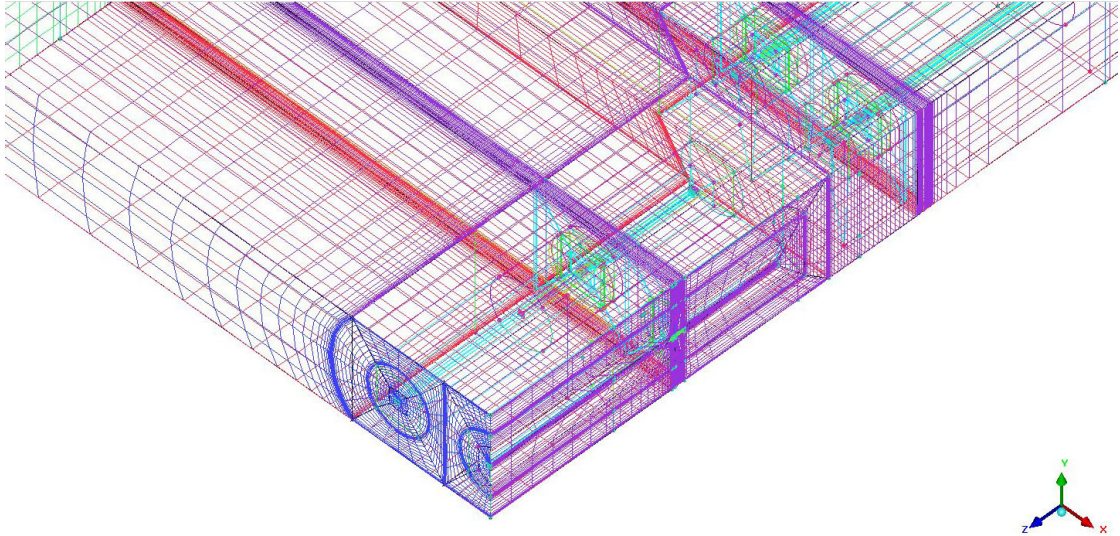


FIGURE 24. Detail from the ICEM mesh generator showing the cross-sectional grid (dark blue) and the mesh regions for the neighbourhood of the actuator disks (light blue), the stream-wise refinement zones for the two rows of turbines can also be seen as can the mesh stretching towards the downstream and westward boundaries.

3. Staggered array of turbines

To demonstrate the application of the model to arrays of turbines two cases have been considered. Both were modelled experimentally by the University of Manchester as test 19 (turbines in series) and test 20 (staggered turbines). In this, the second, case a small array of turbines has been simulated by imposing a symmetry boundary conditions at the east boundary of the `Code_Saturne` simulation, while extending the domain westwards away from the array to allow the flow passing the array to develop. This section presents results from Manchester test 20, while section 2 considers Manchester test 19, which comprised an infinitely wide array of turbines in series.

3.1. Computational set-up. The meshing strategy employed (again using ICEM) treats each turbine in a similar to that used in the previous cases, but requires a more complex blocking arrangement to account for the staggered turbines, see Figure 24. Each individual turbine is meshed using cylindrical O-grid to discretise its rotor plane, as before, this O-grid has 15 cells in the radial direction and 24 cells in the circumferential direction. Mesh stretching has been used to refine the grid at the edge of the rotor so the shear between the free stream flow and the fluid which has passed through the actuator disk is sufficiently resolved. Once again, only the nacelles have been included in the computation and there are no support structures. In meshing the nacelle a 6×6 H-grid region has been used at the centre of the O-grid, though this does not form part of the actuator disk. The computational domain extends from 30 diameters downstream of the downstream turbine and 3 diameters upstream of the upstream turbine. Figure 25

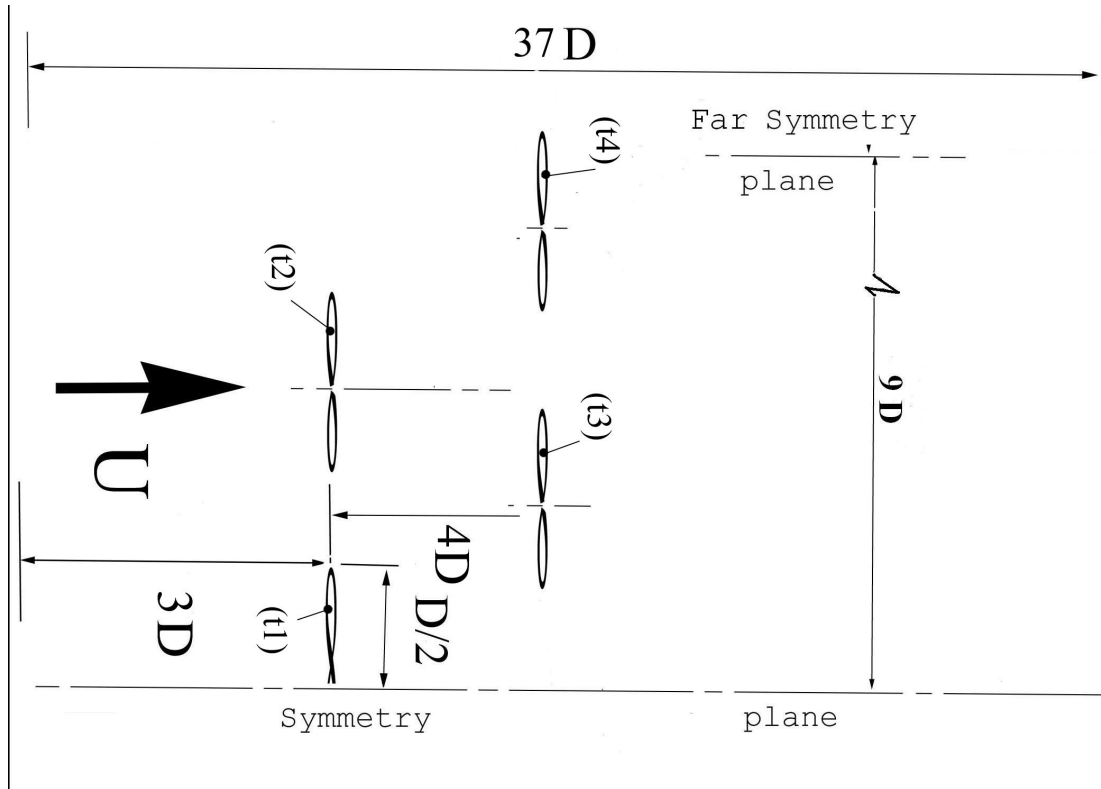


FIGURE 25. Schematic diagram of the arrangement of the turbines and boundary conditions for the staggered array of turbines.

shows a schematic of the problem set-up. Because a symmetry condition is imposed on the centreline only half of the centre upstream rotor is discretised, although the rotating near wake behind the turbine does not have mirror symmetry this approximation has been made to reduce the computational overhead associated with the computation by halving the mesh size.

The blade geometry used in these tests is shown in Table 8, in the previous section. The required tables of for coefficients of lift, C_L , and drag, C_D , against angle of attack, γ , for the GOE804 airfoil were obtained from the University of Manchester and can be found in the file `Goe804.txt`, the lift and drag coefficients for the airfoil are plotted in Figure 12. `usinv.f90` and `ustsns.f90` were modified to create an actuator disk located on the face of each rotor. The source code for the user routines, together with the files `blade.txt`, `circle.txt` and `Geo804.txt` are included on the accompanying CD in the `Staggered` directory.

For all four tip-speed ratios ($\gamma = 3.5, 4.0, 4.5,$ and 5.5) the left and right walls of the computational domain were specified as symmetry conditions (with the zero normal flow condition imposed) to simulate a small array of turbines in the centre of an infinitely wide farm. The top of the computational domain was also set as a symmetry condition to mimic a free surface with minimal deformation, while the lower boundary was set

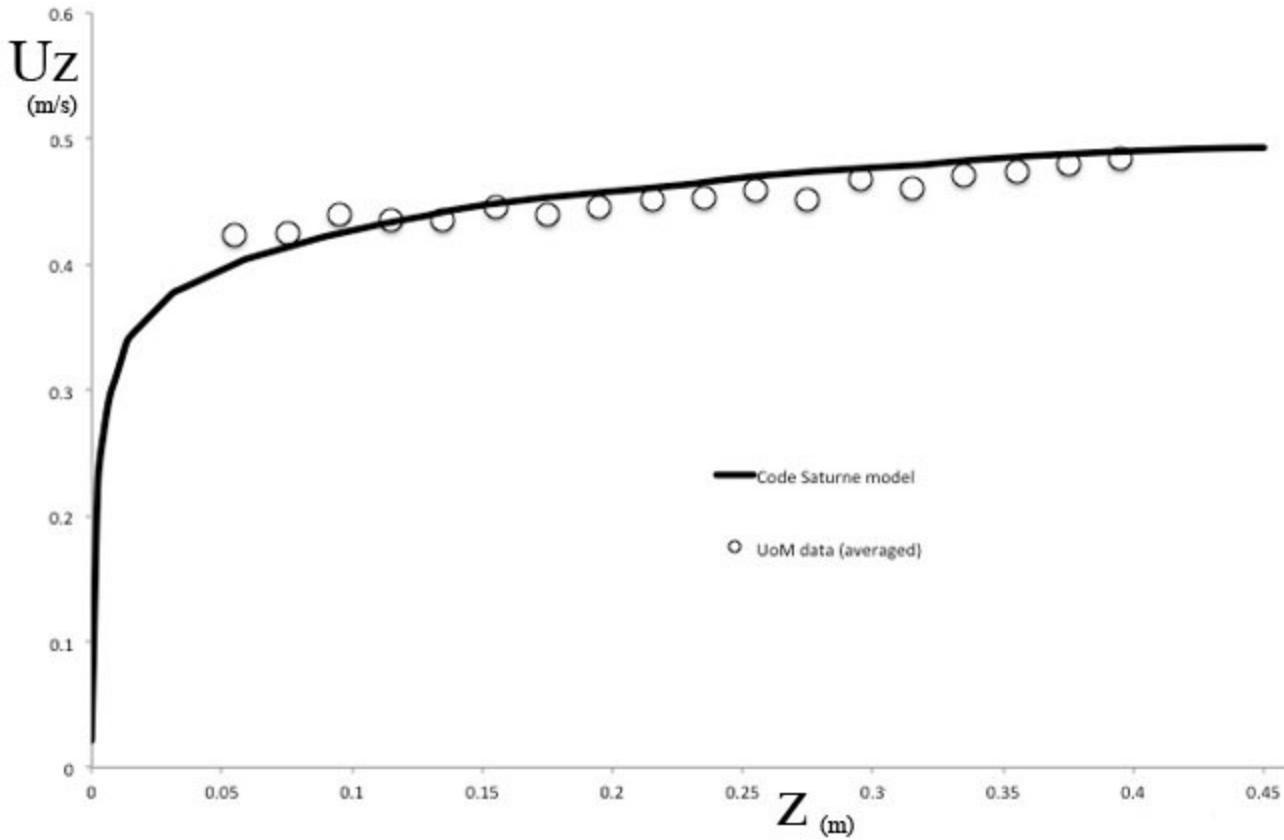


FIGURE 26. Predicted and measure mean velocity profiles at the location of the upstream, centre, rotor in the Manchester tests of an array of turbines in a staggered arrangement, in an empty channel.

as a no-slip wall, with a roughness of $\epsilon = 6 \times 10^{-6}$. The upstream boundary condition (located 3 diameters upstream of the rotor face) has a velocity profile designed to match that of the Manchester experiments with 10% turbulence intensity (Figure ??). The `Code_Saturne` computations were run using the transient solver with a reference time step of 0.006 seconds, an adaptive time step was used with a maximum Courant number of 1.0. Convergence was accelerated by using local time-stepping and the solution was run for 3000 iterations. In this case, as for the array in series, the $k-\epsilon$ turbulence model was used as it is able to cope with rough walls. Full details of the setup are to be found in the `Code_Saturne` setup file, `D5_CASE.xml` which is to be found on the accompanying CD, also in the `Staggered` directory.

Figure 30 shows iso-surfaces of velocity magnitude in the lower half of the water column from the simulations at a tip speed ratio of $\gamma = 4.0$. The interaction of the wake from the first row of turbines with the second can clearly be seen as can the development and subsequent merger of the wakes from the two downstream turbines.

TABLE 21. Coefficients of thrust and power for the turbines in the staggered array case at a tip speed ratio of $\gamma = 4.5$.

Turbine position	Turbine No.	C_T	C_P
upstream row, centre	1	0.856	0.392
upstream row, outer	2	0.840	0.380
downstream row, inner	3	0.778	0.316
downstream row, outer	4	0.824	0.356

3.2. Comparison with experimental data. Figure 27 shows C_T as a function of local tip-speed ratio for the turbines in the staggered array, compared with the experimental measurements from the Manchester tests. The black symbols refer to the experimental results and the coloured circles to the simulation, it is not clear why the tip speed ratio of the downstream turbines is lower than for the upstream in the Manchester tests as the rotor speed is not recorded, in the simulations the tip speed ratio is held constant ($\gamma = 4.5$) for all rotors, the agreement between the simulation and the experiments for the upstream turbines is excellent. Table 21 shows the thrust and drag coefficient from the simulation. Stream-wise velocity distributions through the centres of the turbines are shown in figure 28. The velocity approaching the outer turbine in the downstream row accelerates as it passes the front turbine row, and the flow on the centreline of the array (on the symmetry plane) is accelerated downstream of the second row as it is squeezed by the wakes of the downstream turbines. It should be noted that the application of a symmetry boundary condition on the centre of the array enhances mixing in the down stream turbine wakes as the wake sees a contra-rotating turbine on the other side of the symmetry plane. At the tip speed ratio of $\gamma = 4.5$ the assumption of symmetry does not seem to have a significant effect on the centre wake but this is not necessarily true at higher ratios.

Figure 29 compares the cross stream velocity deficit distribution two diameters downstream from the first row of turbines (five diameters downstream of the inlet). This location coincides with the minimum velocity in the wake of the upstream turbines (Figure 28). The deficit velocity distribution shows the expected trend but the magnitude is about half that measured in the experiment. One possible cause of this is the definition of the reference velocity used to calculate the velocity deficit, in the simulation results the velocity in the flow passing the turbine array has been used (to ensure $U_{defnor} = 0$ at the edge of the array, but this velocity is higher than the free stream velocity in front of the array. It may be possible that the imposition of a symmetry plane at the centre of the array further exacerbates this. A more complete comparison awaits a more detailed discussion with the Manchester team and more detailed experimental data. In general, the it seems reasonable to conclude that the methodology is giving a reasonable simulation of the turbine array. D5b will include a more complete analysis (once data from Manchester is available) and tests which do not include a symmetry plane at the centre of the array.

3.3. Depth averaged results. Figure 30 shows iso-surfaces of velocity magnitude in the lower half of the water column from the Reynolds averaged Navier-Stokes simulations of a staggered arrangement of two rows of turbines at a tip speed ratio of $\gamma = 4.0$. For all the cases presented the computational domain in the neighbourhood of the two turbines has been binned using 25 bins in the stream wise direction from 11 diameters upstream of the downstream turbine ($z = -3.0\text{m}$) to 8 diameters downstream of the same turbine ($z = 2.0\text{m}$). 13 bins have been used in the cross flow direction, with the domain restricted to six turbine diameters away from the centre turbine. The origin of the computational domain is located at the centre of the front face of the downstream turbine and orientated so the flow direction is from right to left in the mosaic plots. Because the upper boundary of the discretised region is a symmetry plane only half the upstream rotor is represented.

In three of the four cases, $\gamma = 3.5, 4.0,$ and 4.5 , the development of an accelerated plume of fluid passing the turbine array can be seen. This farm wake persists down stream to beyond the end of the computational domain, and it is likely that it's full development can only be seen in basin scale models. Furthermore, the depth averaged results show that the wakes of the front row of turbines are completely truncated by passing the second row. Some degree of flow acceleration can also be observed between the turbines in the second row, but this effect is quickly lost as the turbine wakes merge. Velocity shear associated with these jets leads to the generation of high levels of turbulence in the inter-turbine region and this leads to faster merger of the wakes due to enhanced mixing. Although the flow passing the array is accelerated eddy dissipation means the turbulence intensity in the flow quickly reduces.

The only anomaly in this behaviour is the highest tip speed ratio, where the effects of the centre-line turbine seem to dominate. One possible explanation for this is that the assumption of mirror symmetry through the centre plane of this turbine is incorrect, and the apparent interaction of two contra-rotating flows in this region is dominating the flow solution. The only way of testing this would be to perform a, computationally demanding, simulation of the entire array.

3.3.1. Tip speed ratio $\gamma = 3.5$. Figure 31 shows mosaic plots of the binned depth averaged velocity magnitude, turbulent kinetic energy and turbulent viscosity. The bin containing the upstream hubs are at $(2.1, 0.0)$ while the downstream hubs are at $(0.0, 0.0)$ and it is easily identifiable in the velocity plot showing the expected velocity deficit associated with the flow passing the turbine face. It should be noted that the centre upstream hub lies on the symmetry plane and so only half the rotor plane is used in the simulation. Tables 22 to 24 present the binned mean values with the bin containing the turbine nacelle underlined.

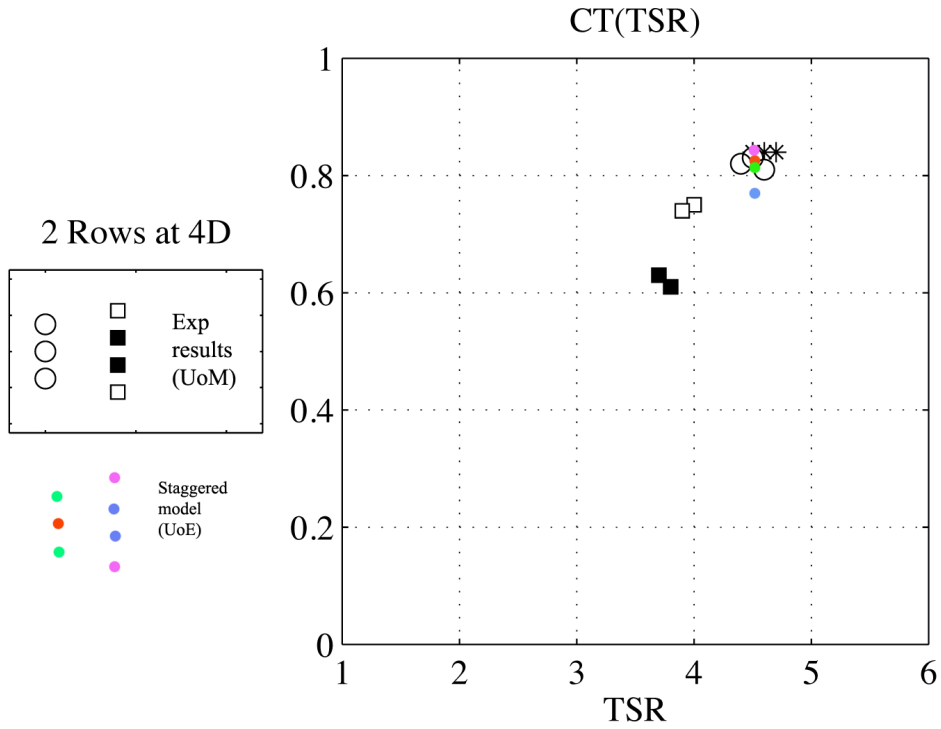


FIGURE 27. Tip speed ratio vs thrust coefficient for the turbines in a staggered array for both the Manchester experiments and the present simulations.

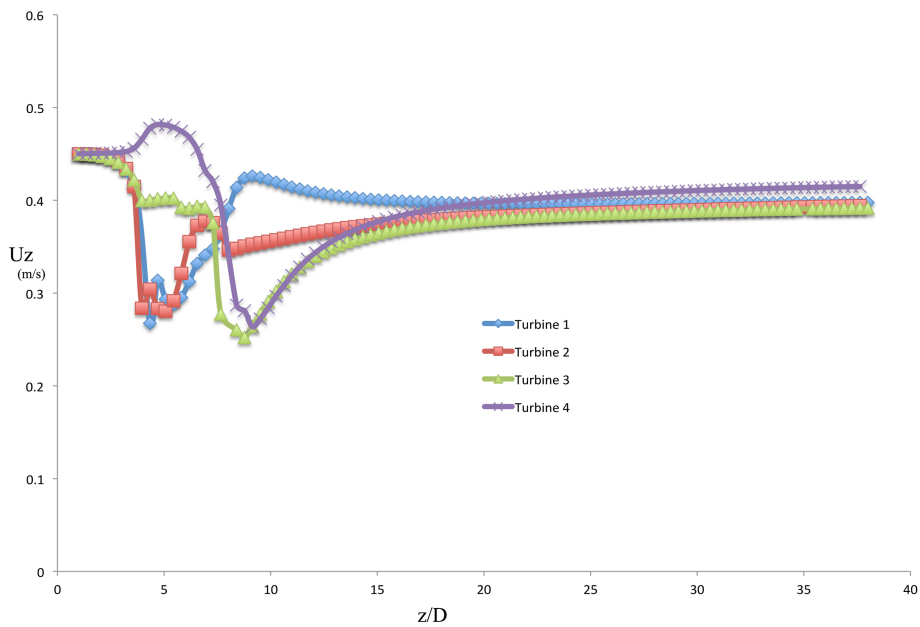


FIGURE 28. Streamwise velocity distributions through the centres of four of the turbines in the staggered array simulation. Turbine 1 is upstream on the symmetry plane, turbine 2 is also upstream, turbines 3 and 4 are downstream with turbine 3 nearest the symmetry plane and turbine 4 on the outside of the array.

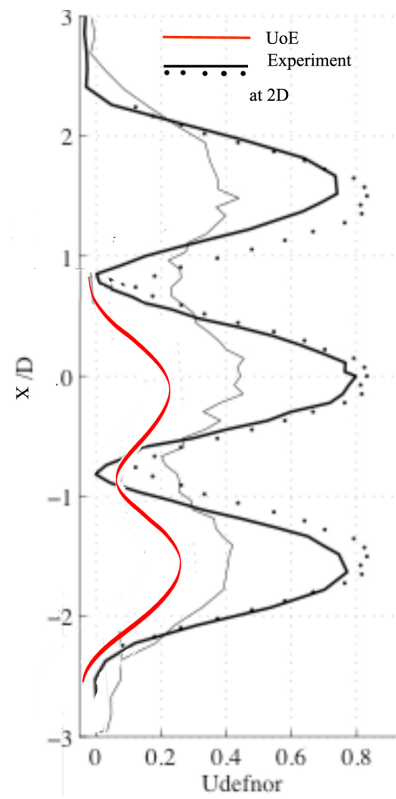


FIGURE 29. Crossflow velocity deficit distribution two diameters downstream from the front turbine row, simulated results are shown in red with experimental measurements from Manchester shown in black.

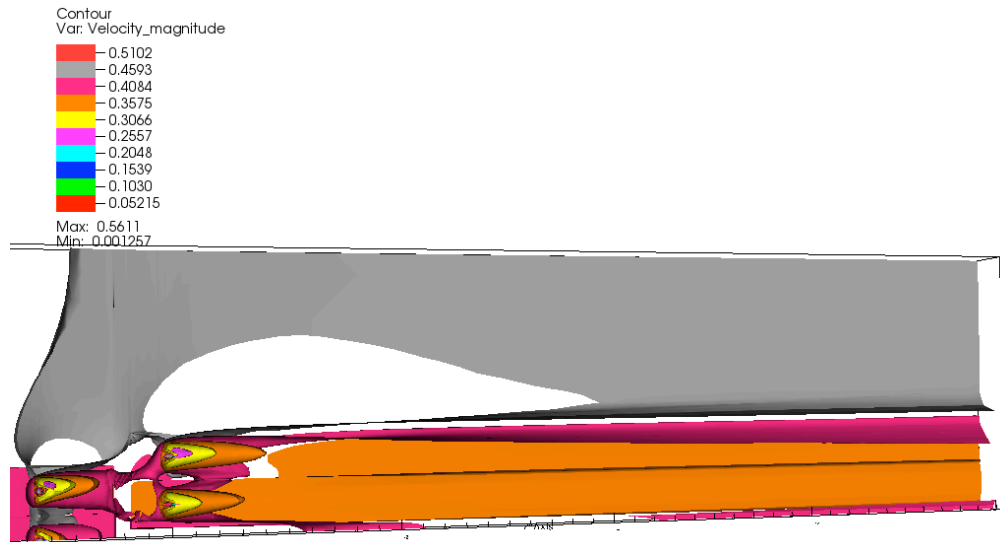


FIGURE 30. Iso-surfaces of velocity magnitude in the lower half of the water column from the Reynolds averaged Navier-Stokes simulations of a staggered arrangement of two rows of turbines at a tip speed ratio of $\gamma = 4.0$.

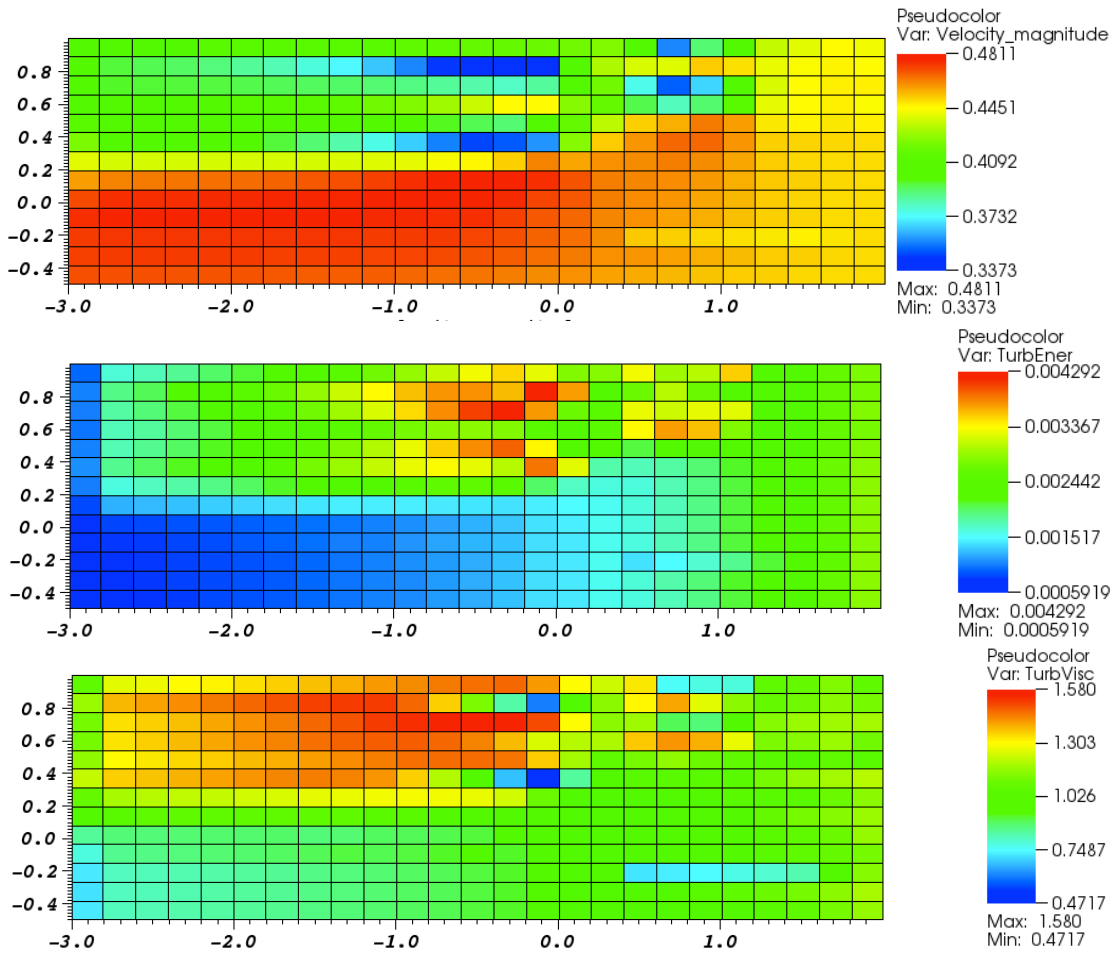


FIGURE 31. Staggered array of turbines tested in the Manchester basin at a tip speed ratio of $\gamma = 3.5$: Mosaic plots showing binned depth averaged velocity magnitude, turbulent kinetic energy and turbulent viscosity.

TABLE 22. Staggered array of turbines tested in the Manchester basin at a tip speed ratio of $\gamma = 3.5$: Depth averaged velocity magnitude. The value for the cells containing the turbines have been underlined

	stream wise direction ←												
downstream													
1	<u>0.4077</u>	0.4100	0.4103	0.4106	0.4109	0.4113	0.4118	0.4123	0.4129	0.4138	0.4148	0.4160	0.4172
2	0.4044	<u>0.3951</u>	<u>0.3933</u>	0.3912	0.3888	0.3858	0.3823	0.3780	0.3726	0.3658	0.3570	0.3463	0.3374
3	0.3994	0.3960	0.3955	0.3949	0.3943	0.3936	0.3928	0.3919	0.3909	0.3896	0.3881	0.3860	0.3836
4	0.4079	0.4084	0.4089	0.4095	0.4103	0.4114	0.4128	0.4146	0.4169	0.4200	0.4241	0.4296	0.4363
5	0.4146	0.4094	0.4089	0.4082	0.4074	0.4066	0.4056	0.4044	0.4030	0.4013	0.3991	0.3963	0.3931
6	0.4229	0.4105	0.4083	0.4058	0.4028	0.3993	0.3950	0.3900	0.3838	0.3762	0.3668	0.3560	0.3483
7	0.4403	0.4388	0.4388	0.4387	0.4386	0.4385	0.4385	0.4387	0.4390	0.4400	0.4412	0.4435	0.4466
8	0.4591	0.4630	0.4637	0.4645	0.4653	0.4662	0.4674	0.4688	0.4704	0.4726	0.4750	0.4777	0.4799
9	0.4714	0.4750	0.4754	0.4757	0.4761	0.4764	0.4768	0.4768	0.4771	0.4778	0.4780	0.4780	0.4777
10	0.4757	0.4773	0.4774	0.4774	0.4774	0.4774	0.4774	0.4774	0.4773	0.4763	0.4761	0.4758	0.4750
11	0.4735	0.4743	0.4743	0.4742	0.4742	0.4742	0.4741	0.4741	0.4739	0.4737	0.4735	0.4729	0.4719
12	0.4725	0.4730	0.4730	0.4729	0.4729	0.4728	0.4726	0.4725	0.4723	0.4720	0.4716	0.4708	0.4697
13	0.4701	0.4700	0.4699	0.4698	0.4696	0.4694	0.4691	0.4687	0.4682	0.4676	0.4669	0.4658	0.4647
	stream wise direction ←												inlet
1	0.4178	0.4189	0.4208	0.4241	0.4052	<u>0.3573</u>	0.3895	0.4015	0.4352	0.4405	0.4448	0.4433	
2	0.3373	<u>0.3424</u>	0.4057	0.4321	0.4394	0.4400	0.4527	0.4495	0.4415	0.4442	0.4469	0.4458	
3	0.3801	0.3856	0.4054	0.4201	0.3760	<u>0.3515</u>	0.3680	0.4063	0.4392	0.4458	0.4477	0.4475	
4	0.4450	0.4462	0.4245	0.4179	0.3935	0.3815	0.3905	0.4146	0.4412	0.4451	0.4475	0.4445	
5	0.3895	0.3979	0.4181	0.4341	0.4519	0.4568	0.4641	0.4587	0.4483	0.4472	0.4481	0.4478	
6	0.3512	<u>0.3591</u>	0.4248	0.4529	0.4599	0.4667	0.4667	0.4600	0.4518	0.4508	0.4504	0.4501	
7	0.4518	0.4626	0.4579	0.4604	0.4620	0.4634	0.4619	0.4579	0.4527	0.4506	0.4500	0.4499	
8	0.4811	0.4760	0.4694	0.4636	0.4620	0.4612	0.4593	0.4565	0.4533	0.4515	0.4505	0.4500	
9	0.4765	0.4720	0.4687	0.4632	0.4612	0.4598	0.4579	0.4556	0.4527	0.4510	0.4502	0.4499	
10	0.4725	0.4688	0.4665	0.4623	0.4604	0.4585	0.4566	0.4547	0.4524	0.4509	0.4501	0.4497	
11	0.4703	0.4671	0.4653	0.4620	0.4534	0.4521	0.4507	0.4496	0.4483	0.4478	0.4489	0.4498	
12	0.4681	0.4654	0.4639	0.4608	0.4600	0.4584	0.4564	0.4547	0.4527	0.4514	0.4506	0.4501	
13	0.4634	0.4616	0.4606	0.4585	0.4572	0.4554	0.4538	0.4526	0.4514	0.4506	0.4501	0.4499	

TABLE 23. Staggered array of turbines tested in the Manchester basin at a tip speed ratio of $\gamma = 3.5$: Depth averaged turbulent kinetic energy. The value for the cells containing the turbines have been underlined

	stream wise direction ←												
downstream													
1	9.90e-04	1.65e-03	1.75e-03	1.85e-03	1.97e-03	2.09e-03	2.23e-03	2.38e-03	2.54e-03	2.72e-03	2.92e-03	3.12e-03	3.32e-03
2	1.09e-03	1.89e-03	2.02e-03	2.16e-03	2.31e-03	2.49e-03	2.69e-03	2.90e-03	3.14e-03	3.38e-03	3.60e-03	3.75e-03	3.76e-03
3	1.06e-03	1.81e-03	1.93e-03	2.05e-03	2.20e-03	2.36e-03	2.54e-03	2.74e-03	2.96e-03	3.21e-03	3.49e-03	3.78e-03	4.07e-03
4	1.03e-03	1.73e-03	1.83e-03	1.94e-03	2.06e-03	2.18e-03	2.30e-03	2.43e-03	2.56e-03	2.68e-03	2.79e-03	2.86e-03	2.88e-03
5	1.07e-03	1.76e-03	1.87e-03	1.98e-03	2.11e-03	2.26e-03	2.42e-03	2.61e-03	2.81e-03	3.04e-03	3.29e-03	3.55e-03	3.78e-03
6	1.14e-03	1.87e-03	1.99e-03	2.11e-03	2.25e-03	2.41e-03	2.58e-03	2.76e-03	2.95e-03	3.13e-03	3.28e-03	3.34e-03	3.27e-03
7	1.06e-03	1.63e-03	1.71e-03	1.80e-03	1.89e-03	1.99e-03	2.10e-03	2.21e-03	2.33e-03	2.44e-03	2.54e-03	2.61e-03	2.64e-03
8	8.94e-04	1.25e-03	1.28e-03	1.31e-03	1.35e-03	1.38e-03	1.41e-03	1.44e-03	1.46e-03	1.46e-03	1.46e-03	1.45e-03	1.44e-03
9	6.90e-04	8.69e-04	8.90e-04	9.13e-04	9.38e-04	9.64e-04	9.93e-04	1.01e-03	1.05e-03	1.09e-03	1.14e-03	1.19e-03	1.25e-03
10	6.12e-04	8.24e-04	8.50e-04	8.79e-04	9.09e-04	9.43e-04	9.79e-04	1.02e-03	1.06e-03	1.09e-03	1.15e-03	1.20e-03	1.26e-03
11	5.95e-04	8.00e-04	8.26e-04	8.54e-04	8.84e-04	9.17e-04	9.53e-04	9.91e-04	1.03e-03	1.08e-03	1.13e-03	1.18e-03	1.24e-03
12	5.93e-04	7.99e-04	8.25e-04	8.54e-04	8.84e-04	9.17e-04	9.52e-04	9.90e-04	1.03e-03	1.08e-03	1.13e-03	1.18e-03	1.24e-03
13	5.92e-04	7.97e-04	8.23e-04	8.51e-04	8.81e-04	9.14e-04	9.49e-04	9.88e-04	1.03e-03	1.07e-03	1.12e-03	1.18e-03	1.24e-03
	stream wise direction ←												inlet
1	3.50e-03	3.26e-03	2.80e-03	2.85e-03	3.32e-03	<u>2.97e-03</u>	3.05e-03	3.55e-03	2.25e-03	2.43e-03	2.67e-03	2.79e-03	
2	3.62e-03	<u>4.28e-03</u>	3.71e-03	2.49e-03	2.70e-03	3.07e-03	2.70e-03	2.33e-03	2.23e-03	2.41e-03	2.65e-03	2.79e-03	
3	4.29e-03	3.74e-03	2.71e-03	2.53e-03	3.27e-03	<u>3.15e-03</u>	3.25e-03	3.24e-03	2.27e-03	2.46e-03	2.68e-03	2.83e-03	
4	2.80e-03	2.53e-03	2.43e-03	2.55e-03	3.39e-03	3.73e-03	3.60e-03	2.81e-03	2.26e-03	2.43e-03	2.68e-03	2.78e-03	
5	3.93e-03	3.40e-03	2.41e-03	2.22e-03	2.06e-03	2.24e-03	2.13e-03	2.14e-03	2.25e-03	2.41e-03	2.65e-03	2.82e-03	
6	3.06e-03	<u>3.87e-03</u>	3.24e-03	1.79e-03	1.74e-03	1.82e-03	1.95e-03	2.10e-03	2.31e-03	2.50e-03	2.69e-03	2.88e-03	
7	2.55e-03	1.98e-03	1.70e-03	1.62e-03	1.65e-03	1.75e-03	1.90e-03	2.08e-03	2.25e-03	2.44e-03	2.65e-03	2.86e-03	
8	1.43e-03	1.47e-03	1.50e-03	1.56e-03	1.64e-03	1.74e-03	1.89e-03	2.07e-03	2.29e-03	2.47e-03	2.67e-03	2.87e-03	
9	1.32e-03	1.42e-03	1.46e-03	1.56e-03	1.63e-03	1.74e-03	1.89e-03	2.07e-03	2.26e-03	2.45e-03	2.65e-03	2.87e-03	
10	1.31e-03	1.40e-03	1.45e-03	1.56e-03	1.63e-03	1.74e-03	1.89e-03	2.07e-03	2.26e-03	2.45e-03	2.64e-03	2.85e-03	
11	1.31e-03	1.40e-03	1.45e-03	1.56e-03	1.42e-03	1.52e-03	1.67e-03	1.86e-03	2.08e-03	2.31e-03	2.63e-03	2.87e-03	
12	1.31e-03	1.40e-03	1.45e-03	1.56e-03	1.65e-03	1.78e-03	1.93e-03	2.11e-03	2.29e-03	2.48e-03	2.67e-03	2.87e-03	
13	1.31e-03	1.40e-03	1.45e-03	1.56e-03	1.63e-03	1.74e-03	1.89e-03	2.07e-03	2.27e-03	2.46e-03	2.66e-03	2.87e-03	

TABLE 24. Staggered array of turbines tested in the Manchester basin at a tip speed ratio of $\gamma = 3.5$: Depth averaged turbulent viscosity. The value for the cells containing the turbines have been underlined

	stream wise direction ←												
downstream													
1	1.0724	1.2647	1.2820	1.2998	1.3180	<u>1.3365</u>	1.3552	1.3739	1.3927	1.4113	1.4295	1.4470	1.4619
2	1.1797	1.3820	1.4028	1.4247	1.4473	1.4702	1.4923	1.5111	1.5219	1.5149	1.4702	1.3508	1.1310
3	1.1204	1.3330	1.3540	1.3757	1.3981	1.4211	1.4446	1.4685	1.4923	1.5158	1.5382	1.5583	1.5732
4	1.1223	1.3328	1.3546	1.3767	1.3987	1.4200	1.4400	1.4578	1.4720	1.4805	1.4805	1.4679	1.4385
5	1.1626	1.3112	1.3271	1.3433	1.3599	1.3766	1.3935	1.4103	1.4269	1.4428	1.4568	1.4658	1.4665
6	1.2259	1.3557	1.3712	1.3873	1.4036	1.4194	1.4332	1.4422	1.4410	1.4183	1.3521	1.2056	0.9689
7	1.0916	1.1975	1.2092	1.2213	1.2334	1.2456	1.2576	1.2690	1.2792	1.2873	1.2918	1.2871	1.2760
8	0.9815	1.0670	1.0697	1.0726	1.0763	1.0790	1.0805	1.0801	1.0770	1.0648	1.0535	1.0383	1.0183
9	0.8478	0.8718	0.8741	0.8764	0.8786	0.8808	0.8832	0.8707	0.8743	0.8917	0.8983	0.9063	0.9155
10	0.7798	0.8534	0.8600	0.8670	0.8744	0.8823	0.8908	0.8997	0.9093	0.9017	0.9123	0.9235	0.9350
11	0.7282	0.8080	0.8156	0.8234	0.8316	0.8401	0.8489	0.8580	0.8676	0.8776	0.8880	0.8990	0.9101
12	0.7219	0.8073	0.8151	0.8232	0.8315	0.8401	0.8490	0.8583	0.8679	0.8779	0.8883	0.8993	0.9104
13	0.7280	0.8122	0.8199	0.8278	0.8359	0.8444	0.8531	0.8621	0.8716	0.8815	0.8918	0.9026	0.9136
	stream wise direction ←												
													inlet
1	1.4713	1.4117	1.3081	1.2394	1.3249	<u>0.7547</u>	0.7776	0.7842	1.0701	1.0988	1.1356	1.0820	
2	0.8347	<u>0.6118</u>	1.0256	1.1561	1.3138	1.4011	1.2677	1.1554	1.0965	1.1151	1.1552	1.1241	
3	1.5796	1.5048	1.2999	1.1597	1.1829	<u>0.8984</u>	0.8721	0.9437	1.1471	1.1750	1.1858	1.1922	
4	1.3783	1.2581	1.2120	1.2009	1.3655	1.4165	1.3898	1.2764	1.1303	1.1452	1.1782	1.1140	
5	1.4508	1.3591	1.1861	1.0840	1.1265	1.1641	1.1015	1.0757	1.0600	1.0361	1.0838	1.0649	
6	0.6874	<u>0.4717</u>	0.8402	0.9959	1.0475	1.0421	1.0508	1.0618	1.1177	1.1697	1.1925	1.2160	
7	1.2434	1.1060	1.0239	0.9740	0.9888	1.0003	1.0207	1.0425	1.0517	1.0688	1.1055	1.1514	
8	0.9954	0.9838	0.9876	0.9705	0.9869	0.9858	1.0065	1.0309	1.0930	1.1185	1.1456	1.1746	
9	0.9369	0.9514	0.9606	0.9668	0.9710	0.9862	1.0069	1.0296	1.0503	1.0734	1.1046	1.1675	
10	0.9225	0.9376	0.9455	0.9624	0.9713	0.9866	1.0073	1.0303	1.0516	1.0753	1.0940	1.1169	
11	0.9225	0.9379	0.9457	0.9696	0.7243	0.7342	0.7503	0.7706	0.7926	0.8226	0.9995	1.1512	
12	0.9228	0.9383	0.9461	0.9648	0.9970	1.0377	1.0595	1.0833	1.1053	1.1285	1.1570	1.1950	
13	0.9259	0.9413	0.9486	0.9654	0.9736	0.9892	1.0104	1.0343	1.0585	1.0850	1.1192	1.1691	

3.3.2. *Tip speed ratio $\gamma = 4.0$.* Figure 32 shows mosaic plots of the binned depth averaged velocity magnitude, turbulent kinetic energy and turbulent viscosity. The bin containing the upstream hubs are at (2.1,0.0) while the downstream hubs are at (0.0,0.0) and it is easily identifiable in the velocity plot showing the expected velocity deficit associated with the flow passing the turbine face. It should be noted that the centre upstream hub lies on the symmetry plane and so only half the rotor plane is used in the simulation. Tables 25 to 27 present the binned mean values with the bin containing the turbine nacelle underlined.

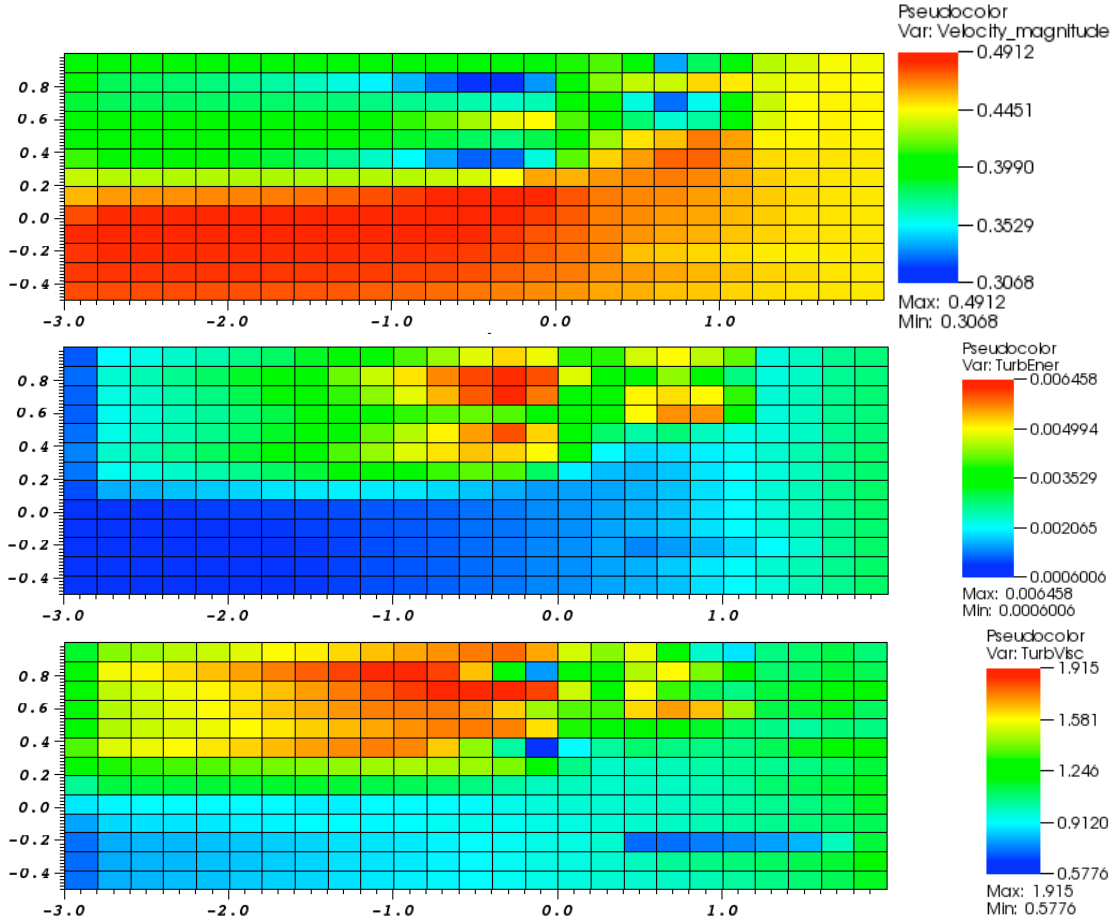


FIGURE 32. Staggered array of turbines tested in the Manchester basin at a tip speed ratio of $\gamma = 4.0$: Mosaic plots showing binned depth averaged velocity magnitude, turbulent kinetic energy and turbulent viscosity.

TABLE 25. Staggered array of turbines tested in the Manchester basin at a tip speed ratio of $\gamma = 4.0$: Depth averaged velocity magnitude. The value for the cells containing the turbines have been underlined

	stream wise direction ←												
downstream													
1	0.3942	0.3956	0.3960	0.3964	0.3969	0.3975	0.3983	0.3991	0.4001	0.4014	0.4028	0.4046	0.4062
2	0.3904	0.3814	0.3797	0.3777	0.3753	0.3724	0.3688	0.3643	0.3586	0.3510	0.3408	0.3274	0.3127
3	0.3863	0.3816	0.3810	0.3804	0.3797	0.3790	0.3781	0.3772	0.3760	0.3746	0.3728	0.3705	0.3677
4	0.3952	0.3940	0.3945	0.3952	0.3962	0.3974	0.3991	0.4012	0.4040	0.4078	0.4131	0.4203	0.4293
5	0.4033	0.3975	0.3970	0.3965	0.3959	0.3952	0.3944	0.3933	0.3920	0.3902	0.3880	0.3847	0.3807
6	0.4140	0.4010	0.3988	0.3962	0.3932	0.3895	0.3850	0.3795	0.3725	0.3637	0.3525	0.3385	0.3262
7	0.4349	0.4324	0.4322	0.4319	0.4315	0.4312	0.4310	0.4308	0.4308	0.4315	0.4324	0.4350	0.4385
8	0.4584	0.4633	0.4642	0.4651	0.4661	0.4672	0.4686	0.4704	0.4728	0.4762	0.4797	0.4842	0.4883
9	0.4771	0.4833	0.4839	0.4844	0.4849	0.4855	0.4860	0.4864	0.4869	0.4877	0.4880	0.4880	0.4877
10	0.4837	0.4867	0.4868	0.4869	0.4869	0.4869	0.4869	0.4868	0.4867	0.4856	0.4853	0.4849	0.4838
11	0.4817	0.4833	0.4833	0.4833	0.4832	0.4831	0.4830	0.4828	0.4826	0.4823	0.4820	0.4811	0.4798
12	0.4804	0.4815	0.4814	0.4814	0.4812	0.4811	0.4809	0.4807	0.4803	0.4799	0.4794	0.4782	0.4767
13	0.4770	0.4772	0.4771	0.4769	0.4766	0.4763	0.4759	0.4754	0.4747	0.4739	0.4728	0.4714	0.4698
	stream wise direction ←												inlet
1	0.4069	0.4069	0.4109	0.4158	0.3962	<u>0.3382</u>	0.3805	0.3997	0.4328	0.4391	0.4442	0.4432	
2	0.3068	<u>0.3351</u>	0.3939	0.4250	0.4348	0.4351	0.4527	0.4489	0.4398	0.4436	0.4469	0.4458	
3	0.3632	0.3664	0.3920	0.4102	0.3587	<u>0.3289</u>	0.3553	0.3998	0.4363	0.4450	0.4476	0.4475	
4	0.4416	0.4452	0.4167	0.4070	0.3769	0.3605	0.3696	0.4011	0.4390	0.4445	0.4474	0.4445	
5	0.3753	0.3827	0.4079	0.4281	0.4508	0.4572	0.4686	0.4622	0.4479	0.4469	0.4481	0.4478	
6	0.3273	<u>0.3582</u>	0.4183	0.4535	0.4628	0.4725	0.4729	0.4638	0.4522	0.4508	0.4504	0.4501	
7	0.4450	0.4616	0.4591	0.4639	0.4664	0.4685	0.4666	0.4612	0.4540	0.4511	0.4502	0.4499	
8	0.4912	0.4846	0.4756	0.4683	0.4664	0.4655	0.4630	0.4591	0.4545	0.4520	0.4506	0.4500	
9	0.4860	0.4797	0.4753	0.4678	0.4654	0.4635	0.4610	0.4578	0.4538	0.4515	0.4503	0.4499	
10	0.4805	0.4755	0.4724	0.4667	0.4642	0.4616	0.4591	0.4565	0.4533	0.4514	0.4503	0.4498	
11	0.4775	0.4733	0.4707	0.4662	0.4567	0.4548	0.4528	0.4511	0.4491	0.4482	0.4491	0.4498	
12	0.4746	0.4709	0.4689	0.4646	0.4634	0.4611	0.4585	0.4562	0.4536	0.4518	0.4507	0.4501	
13	0.4681	0.4656	0.4643	0.4614	0.4597	0.4573	0.4552	0.4536	0.4519	0.4509	0.4502	0.4499	

TABLE 26. Staggered array of turbines tested in the Manchester basin at a tip speed ratio of $\gamma = 4.0$: Depth averaged turbulent kinetic energy. The value for the cells containing the turbines have been underlined

	downstream		stream wise direction ←										
1	1.15e-03	2.06e-03	2.19e-03	2.35e-03	2.52e-03	2.72e-03	2.93e-03	3.17e-03	3.45e-03	3.75e-03	4.09e-03	4.46e-03	4.84e-03
2	1.26e-03	2.31e-03	2.48e-03	2.68e-03	2.91e-03	3.17e-03	3.47e-03	3.82e-03	4.23e-03	4.68e-03	5.17e-03	5.66e-03	6.03e-03
3	1.21e-03	2.21e-03	2.37e-03	2.56e-03	2.77e-03	3.01e-03	3.29e-03	3.60e-03	3.97e-03	4.39e-03	4.87e-03	5.41e-03	5.95e-03
4	1.19e-03	2.14e-03	2.29e-03	2.46e-03	2.64e-03	2.83e-03	3.05e-03	3.27e-03	3.51e-03	3.74e-03	3.96e-03	4.13e-03	4.21e-03
5	1.27e-03	2.19e-03	2.34e-03	2.51e-03	2.71e-03	2.93e-03	3.18e-03	3.46e-03	3.79e-03	4.17e-03	4.60e-03	5.08e-03	5.55e-03
6	1.38e-03	2.35e-03	2.51e-03	2.69e-03	2.90e-03	3.14e-03	3.41e-03	3.72e-03	4.06e-03	4.44e-03	4.83e-03	5.16e-03	5.34e-03
7	1.32e-03	2.12e-03	2.24e-03	2.38e-03	2.53e-03	2.70e-03	2.89e-03	3.10e-03	3.32e-03	3.55e-03	3.79e-03	3.99e-03	4.13e-03
8	1.10e-03	1.61e-03	1.67e-03	1.73e-03	1.79e-03	1.85e-03	1.91e-03	1.95e-03	1.98e-03	1.97e-03	1.94e-03	1.87e-03	1.76e-03
9	7.77e-04	9.59e-04	9.79e-04	1.00e-03	1.02e-03	1.04e-03	1.06e-03	1.07e-03	1.09e-03	1.13e-03	1.17e-03	1.22e-03	1.27e-03
10	6.40e-04	8.49e-04	8.74e-04	9.01e-04	9.31e-04	9.63e-04	9.98e-04	1.04e-03	1.08e-03	1.11e-03	1.16e-03	1.21e-03	1.27e-03
11	6.10e-04	8.14e-04	8.40e-04	8.68e-04	8.98e-04	9.30e-04	9.65e-04	1.00e-03	1.04e-03	1.09e-03	1.14e-03	1.19e-03	1.25e-03
12	6.05e-04	8.11e-04	8.37e-04	8.65e-04	8.95e-04	9.27e-04	9.62e-04	1.00e-03	1.04e-03	1.09e-03	1.14e-03	1.19e-03	1.25e-03
13	6.01e-04	8.05e-04	8.31e-04	8.59e-04	8.89e-04	9.22e-04	9.57e-04	9.95e-04	1.04e-03	1.08e-03	1.13e-03	1.18e-03	1.24e-03
	stream wise direction ←											inlet	
1	5.23e-03	4.91e-03	3.93e-03	3.93e-03	4.75e-03	<u>4.98e-03</u>	4.62e-03	4.16e-03	2.25e-03	2.43e-03	2.67e-03	2.79e-03	
2	6.20e-03	<u>6.00e-03</u>	4.82e-03	3.36e-03	3.73e-03	4.40e-03	3.73e-03	2.75e-03	2.23e-03	2.41e-03	2.65e-03	2.79e-03	
3	6.46e-03	5.79e-03	3.85e-03	3.45e-03	5.04e-03	<u>5.18e-03</u>	4.99e-03	3.96e-03	2.28e-03	2.46e-03	2.68e-03	2.83e-03	
4	4.11e-03	3.55e-03	3.28e-03	3.45e-03	4.97e-03	5.61e-03	5.60e-03	3.85e-03	2.26e-03	2.43e-03	2.68e-03	2.78e-03	
5	5.98e-03	5.26e-03	3.29e-03	2.88e-03	2.57e-03	2.82e-03	2.45e-03	2.22e-03	2.26e-03	2.41e-03	2.65e-03	2.82e-03	
6	5.26e-03	<u>5.01e-03</u>	3.84e-03	2.06e-03	1.88e-03	1.90e-03	1.98e-03	2.11e-03	2.31e-03	2.50e-03	2.69e-03	2.88e-03	
7	4.08e-03	2.91e-03	1.98e-03	1.72e-03	1.66e-03	1.76e-03	1.91e-03	2.08e-03	2.26e-03	2.44e-03	2.65e-03	2.86e-03	
8	1.62e-03	1.54e-03	1.55e-03	1.57e-03	1.65e-03	1.74e-03	1.89e-03	2.07e-03	2.29e-03	2.47e-03	2.67e-03	2.87e-03	
9	1.34e-03	1.43e-03	1.47e-03	1.57e-03	1.63e-03	1.74e-03	1.89e-03	2.07e-03	2.26e-03	2.45e-03	2.65e-03	2.87e-03	
10	1.32e-03	1.41e-03	1.46e-03	1.57e-03	1.63e-03	1.74e-03	1.89e-03	2.07e-03	2.26e-03	2.45e-03	2.64e-03	2.85e-03	
11	1.32e-03	1.41e-03	1.46e-03	1.57e-03	1.42e-03	1.52e-03	1.67e-03	1.87e-03	2.08e-03	2.31e-03	2.63e-03	2.87e-03	
12	1.31e-03	1.41e-03	1.46e-03	1.57e-03	1.65e-03	1.79e-03	1.94e-03	2.11e-03	2.30e-03	2.48e-03	2.67e-03	2.87e-03	
13	1.31e-03	1.41e-03	1.45e-03	1.56e-03	1.63e-03	1.74e-03	1.89e-03	2.07e-03	2.27e-03	2.46e-03	2.66e-03	2.87e-03	

TABLE 27. Staggered array of turbines tested in the Manchester basin at a tip speed ratio of $\gamma = 4.0$: Depth averaged turbulent viscosity. The value for the cells containing the turbines have been underlined

	stream wise direction ←												
downstream													
1	1.1616	1.4326	1.4598	1.4877	1.5163	1.5458	1.5758	1.6062	1.6369	1.6676	1.6978	1.7264	1.7507
2	1.2891	1.5675	1.5979	1.6305	1.6656	1.7032	1.7433	1.7850	1.8258	1.8596	1.8716	1.8272	1.6650
3	1.2090	1.4958	1.5273	1.5603	1.5949	1.6312	1.6693	1.7092	1.7507	1.7932	1.8352	1.8738	1.9022
4	1.2074	1.4852	1.5177	1.5517	1.5866	1.6219	1.6569	1.6903	1.7203	1.7441	1.7572	1.7529	1.7237
5	1.2860	1.4858	1.5096	1.5347	1.5609	1.5881	1.6161	1.6445	1.6729	1.7008	1.7269	1.7480	1.7563
6	1.3667	1.5401	1.5625	1.5869	1.6135	1.6421	1.6722	1.7023	1.7291	1.7451	1.7329	1.6533	1.4467
7	1.2034	1.3322	1.3471	1.3629	1.3793	1.3964	1.4140	1.4315	1.4482	1.4620	1.4721	1.4702	1.4592
8	1.0440	1.1407	1.1445	1.1487	1.1538	1.1575	1.1591	1.1578	1.1527	1.1357	1.1189	1.0954	1.0662
9	0.8855	0.9068	0.9088	0.9104	0.9116	0.9123	0.9126	0.8961	0.8963	0.9087	0.9117	0.9163	0.9225
10	0.7979	0.8665	0.8724	0.8785	0.8850	0.8919	0.8992	0.9071	0.9157	0.9064	0.9163	0.9270	0.9380
11	0.7351	0.8124	0.8198	0.8275	0.8355	0.8438	0.8524	0.8613	0.8706	0.8805	0.8907	0.9015	0.9124
12	0.7253	0.8103	0.8181	0.8262	0.8344	0.8429	0.8518	0.8609	0.8703	0.8803	0.8906	0.9014	0.9123
13	0.7303	0.8143	0.8220	0.8298	0.8379	0.8463	0.8550	0.8640	0.8733	0.8831	0.8933	0.9040	0.9149
	stream wise direction ←												
													inlet
1	1.7690	1.6998	1.5296	1.4334	1.5634	<u>1.2464</u>	0.9777	0.8792	1.0707	1.0988	1.1356	1.0821	
2	1.2751	<u>0.7883</u>	1.2021	1.3087	1.4826	1.5900	1.4238	1.2391	1.0956	1.1146	1.1550	1.1241	
3	1.9153	1.8306	1.5213	1.3178	1.5708	<u>1.3558</u>	1.1112	1.0654	1.1484	1.1751	1.1858	1.1922	
4	1.6478	1.4639	1.3781	1.3590	1.6359	1.7112	1.6653	1.4536	1.1317	1.1453	1.1782	1.1140	
5	1.7422	1.6240	1.3350	1.1865	1.2306	1.2682	1.1652	1.0969	1.0610	1.0364	1.0838	1.0648	
6	1.0369	<u>0.5776</u>	0.9080	1.0325	1.0934	1.0718	1.0648	1.0648	1.1182	1.1698	1.1925	1.2160	
7	1.4219	1.2393	1.0602	0.9810	0.9930	1.0029	1.0224	1.0435	1.0522	1.0690	1.1056	1.1514	
8	1.0310	0.9954	0.9948	0.9737	0.9885	0.9871	1.0076	1.0316	1.0934	1.1188	1.1457	1.1747	
9	0.9415	0.9539	0.9626	0.9682	0.9721	0.9873	1.0077	1.0302	1.0506	1.0736	1.1047	1.1675	
10	0.9247	0.9393	0.9469	0.9636	0.9723	0.9875	1.0080	1.0307	1.0518	1.0754	1.0941	1.1170	
11	0.9244	0.9393	0.9469	0.9706	0.7248	0.7346	0.7506	0.7707	0.7927	0.8227	0.9995	1.1512	
12	0.9244	0.9395	0.9472	0.9657	0.9979	1.0384	1.0601	1.0837	1.1055	1.1286	1.1570	1.1950	
13	0.9270	0.9422	0.9493	0.9661	0.9742	0.9897	1.0108	1.0345	1.0586	1.0850	1.1192	1.1691	

3.3.3. *Tip speed ratio* $\gamma = 4.5$. Figure 33 shows mosaic plots of the binned depth averaged velocity magnitude, turbulent kinetic energy and turbulent viscosity. The bin containing the upstream hubs are at $(2.1,0.0)$ while the downstream hubs are at $(0.0,0.0)$ and it is easily identifiable in the velocity plot showing the expected velocity deficit associated with the flow passing the turbine face. It should be noted that the centre upstream hub lies on the symmetry plane and so only half the rotor plane is used in the simulation. Tables 28 to 30 present the binned mean values with the bin containing the turbine nacelle underlined.

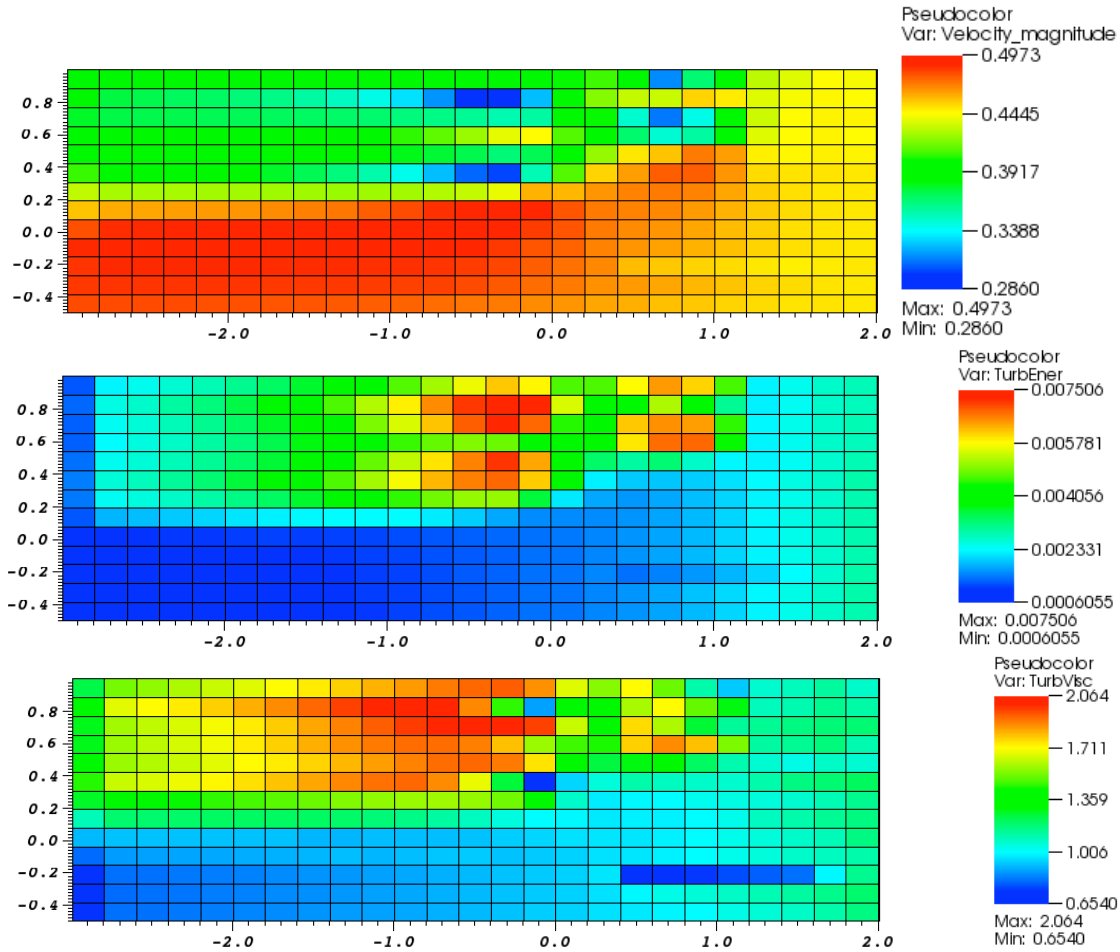


FIGURE 33. Staggered array of turbines tested in the Manchester basin at a tip speed ratio of $\gamma = 4.5$: Mosaic plots showing binned depth averaged velocity magnitude, turbulent kinetic energy and turbulent viscosity.

TABLE 28. Staggered array of turbines tested in the Manchester basin at a tip speed ratio of $\gamma = 4.5$: Depth averaged velocity magnitude. The value for the cells containing the turbines have been underlined

	stream wise direction ←												
downstream													
1	<u>0.3872</u>	0.3883	0.3887	0.3891	0.3897	<u>0.3904</u>	0.3912	0.3922	0.3934	0.3947	0.3963	0.3983	0.4001
2	0.3836	<u>0.3746</u>	0.3730	0.3710	0.3686	0.3657	0.3621	0.3576	0.3517	0.3437	0.3327	0.3176	0.2991
3	0.3792	0.3741	<u>0.3735</u>	0.3728	0.3721	0.3713	0.3705	0.3695	0.3684	0.3669	0.3650	0.3627	0.3597
4	0.3879	0.3861	0.3866	0.3873	0.3882	0.3895	0.3912	0.3935	0.3965	0.4006	0.4065	0.4146	0.4252
5	0.3967	0.3904	0.3899	0.3894	0.3888	0.3882	0.3874	0.3864	0.3850	0.3833	0.3809	0.3773	0.3728
6	0.4084	0.3950	0.3928	0.3901	0.3870	0.3832	0.3785	0.3727	0.3652	0.3556	0.3428	0.3263	0.3085
7	0.4313	0.4280	0.4277	0.4274	0.4269	0.4263	0.4259	0.4255	0.4252	0.4258	0.4264	0.4290	0.4327
8	0.4576	0.4625	0.4634	0.4645	0.4655	0.4667	0.4683	0.4705	0.4731	0.4772	0.4815	0.4872	0.4930
9	0.4801	0.4878	0.4885	0.4892	0.4899	0.4906	0.4913	0.4920	0.4926	0.4936	0.4939	0.4941	0.4938
10	0.4883	0.4921	0.4923	0.4924	0.4924	0.4925	0.4924	0.4924	0.4923	0.4911	0.4908	0.4904	0.4891
11	0.4865	0.4884	0.4885	0.4885	0.4884	0.4883	0.4881	0.4880	0.4877	0.4874	0.4870	0.4861	0.4845
12	0.4850	0.4863	0.4863	0.4862	0.4861	0.4859	0.4857	0.4855	0.4850	0.4845	0.4840	0.4826	0.4809
13	0.4809	0.4813	0.4811	0.4809	0.4806	0.4802	0.4798	0.4792	0.4784	0.4775	0.4763	0.4747	0.4729
	stream wise direction ←												inlet
1	0.4009	0.3998	0.4044	0.4093	0.3878	<u>0.3164</u>	0.3666	0.3976	0.4307	0.4384	0.4442	0.4432	
2	0.2860	<u>0.3263</u>	0.3859	0.4206	0.4324	0.4331	0.4537	0.4487	0.4386	0.4429	0.4466	0.4457	
3	0.3551	0.3571	0.3852	0.4049	0.3482	<u>0.3127</u>	0.3436	0.3946	0.4346	0.4444	0.4474	0.4475	
4	0.4398	0.4449	0.4126	0.4011	0.3670	0.3476	0.3575	0.3932	0.4380	0.4442	0.4473	0.4445	
5	0.3661	0.3725	0.4015	0.4246	0.4498	0.4573	0.4719	0.4649	0.4481	0.4469	0.4480	0.4478	
6	0.3033	<u>0.3540</u>	0.4125	0.4538	0.4647	0.4769	0.4775	0.4665	0.4526	0.4508	0.4504	0.4501	
7	0.4404	0.4607	0.4598	0.4662	0.4694	0.4722	0.4699	0.4633	0.4547	0.4513	0.4502	0.4499	
8	0.4973	0.4901	0.4796	0.4715	0.4694	0.4685	0.4656	0.4609	0.4553	0.4522	0.4507	0.4500	
9	0.4919	0.4847	0.4795	0.4710	0.4682	0.4661	0.4631	0.4593	0.4545	0.4518	0.4504	0.4500	
10	0.4856	0.4798	0.4761	0.4696	0.4667	0.4638	0.4608	0.4577	0.4540	0.4517	0.4504	0.4498	
11	0.4820	0.4771	0.4741	0.4689	0.4589	0.4566	0.4542	0.4521	0.4497	0.4484	0.4491	0.4498	
12	0.4785	0.4743	0.4719	0.4671	0.4656	0.4628	0.4599	0.4572	0.4541	0.4521	0.4508	0.4501	
13	0.4709	0.4681	0.4666	0.4633	0.4613	0.4585	0.4561	0.4542	0.4522	0.4510	0.4503	0.4499	

TABLE 29. Staggered array of turbines tested in the Manchester basin at a tip speed ratio of $\gamma = 4.5$: Depth averaged turbulent kinetic energy. The value for the cells containing the turbines have been underlined

	stream wise direction ←												
downstream													
1	1.25e-03	2.27e-03	2.43e-03	2.61e-03	2.82e-03	3.05e-03	3.31e-03	3.60e-03	3.93e-03	4.31e-03	4.73e-03	5.20e-03	5.68e-03
2	1.35e-03	2.51e-03	2.70e-03	2.93e-03	3.19e-03	3.49e-03	3.84e-03	4.25e-03	4.73e-03	5.28e-03	5.91e-03	6.56e-03	7.10e-03
3	1.30e-03	2.40e-03	2.59e-03	2.80e-03	3.04e-03	3.32e-03	3.64e-03	4.01e-03	4.45e-03	4.96e-03	5.55e-03	6.21e-03	6.89e-03
4	1.29e-03	2.35e-03	2.53e-03	2.72e-03	2.94e-03	3.18e-03	3.44e-03	3.72e-03	4.02e-03	4.32e-03	4.61e-03	4.85e-03	4.98e-03
5	1.39e-03	2.42e-03	2.59e-03	2.79e-03	3.02e-03	3.29e-03	3.59e-03	3.94e-03	4.35e-03	4.82e-03	5.37e-03	5.98e-03	6.60e-03
6	1.51e-03	2.60e-03	2.78e-03	3.00e-03	3.24e-03	3.53e-03	3.86e-03	4.25e-03	4.69e-03	5.20e-03	5.74e-03	6.27e-03	6.64e-03
7	1.47e-03	2.39e-03	2.54e-03	2.71e-03	2.90e-03	3.11e-03	3.35e-03	3.62e-03	3.92e-03	4.25e-03	4.59e-03	4.89e-03	5.13e-03
8	1.24e-03	1.85e-03	1.92e-03	1.99e-03	2.08e-03	2.16e-03	2.24e-03	2.30e-03	2.35e-03	2.34e-03	2.31e-03	2.21e-03	2.03e-03
9	8.43e-04	1.03e-03	1.05e-03	1.06e-03	1.08e-03	1.10e-03	1.12e-03	1.11e-03	1.13e-03	1.16e-03	1.20e-03	1.23e-03	1.28e-03
10	6.62e-04	8.67e-04	8.91e-04	9.18e-04	9.47e-04	9.78e-04	1.01e-03	1.05e-03	1.09e-03	1.12e-03	1.17e-03	1.22e-03	1.28e-03
11	6.19e-04	8.23e-04	8.49e-04	8.76e-04	9.06e-04	9.38e-04	9.72e-04	1.01e-03	1.05e-03	1.10e-03	1.14e-03	1.20e-03	1.25e-03
12	6.13e-04	8.19e-04	8.44e-04	8.72e-04	9.02e-04	9.34e-04	9.69e-04	1.01e-03	1.05e-03	1.09e-03	1.14e-03	1.19e-03	1.25e-03
13	6.05e-04	8.10e-04	8.36e-04	8.64e-04	8.94e-04	9.26e-04	9.61e-04	9.99e-04	1.04e-03	1.09e-03	1.13e-03	1.19e-03	1.25e-03
	stream wise direction ←												inlet
1	6.17e-03	5.85e-03	4.70e-03	4.71e-03	5.81e-03	<u>6.46e-03</u>	6.08e-03	4.67e-03	2.25e-03	2.43e-03	2.67e-03	2.79e-03	
2	7.48e-03	<u>7.41e-03</u>	5.56e-03	3.96e-03	4.43e-03	5.26e-03	4.39e-03	3.02e-03	2.23e-03	2.41e-03	2.65e-03	2.79e-03	
3	7.51e-03	6.78e-03	4.52e-03	4.03e-03	6.16e-03	<u>6.54e-03</u>	6.44e-03	4.57e-03	2.28e-03	2.46e-03	2.68e-03	2.83e-03	
4	4.88e-03	4.19e-03	3.81e-03	4.02e-03	5.94e-03	6.77e-03	6.79e-03	4.47e-03	2.27e-03	2.43e-03	2.68e-03	2.78e-03	
5	7.15e-03	6.37e-03	3.83e-03	3.30e-03	2.94e-03	3.23e-03	2.68e-03	2.28e-03	2.26e-03	2.41e-03	2.65e-03	2.82e-03	
6	6.79e-03	<u>6.15e-03</u>	4.24e-03	2.25e-03	2.00e-03	1.97e-03	2.02e-03	2.12e-03	2.32e-03	2.50e-03	2.69e-03	2.88e-03	
7	5.11e-03	3.52e-03	2.18e-03	1.79e-03	1.67e-03	1.77e-03	1.92e-03	2.09e-03	2.26e-03	2.44e-03	2.65e-03	2.86e-03	
8	1.78e-03	1.59e-03	1.58e-03	1.58e-03	1.65e-03	1.75e-03	1.90e-03	2.07e-03	2.29e-03	2.47e-03	2.67e-03	2.87e-03	
9	1.35e-03	1.43e-03	1.48e-03	1.57e-03	1.64e-03	1.75e-03	1.90e-03	2.07e-03	2.26e-03	2.45e-03	2.65e-03	2.87e-03	
10	1.32e-03	1.42e-03	1.46e-03	1.57e-03	1.63e-03	1.74e-03	1.89e-03	2.07e-03	2.26e-03	2.45e-03	2.64e-03	2.85e-03	
11	1.32e-03	1.41e-03	1.46e-03	1.57e-03	1.42e-03	1.52e-03	1.68e-03	1.87e-03	2.08e-03	2.31e-03	2.63e-03	2.87e-03	
12	1.32e-03	1.41e-03	1.46e-03	1.57e-03	1.65e-03	1.79e-03	1.94e-03	2.11e-03	2.30e-03	2.48e-03	2.67e-03	2.87e-03	
13	1.31e-03	1.41e-03	1.46e-03	1.57e-03	1.63e-03	1.74e-03	1.90e-03	2.07e-03	2.27e-03	2.46e-03	2.66e-03	2.87e-03	

TABLE 30. Staggered array of turbines tested in the Manchester basin at a tip speed ratio of $\gamma = 4.5$: Depth averaged turbulent viscosity. The value for the cells containing the turbines have been underlined

	stream wise direction ←												
downstream													
1	1.2423	1.5405	1.5713	1.6033	1.6366	1.6710	1.7065	1.7428	1.7797	1.8170	1.8538	1.8885	1.9169
2	1.3707	1.6730	1.7065	1.7424	1.7811	1.8231	1.8686	1.9170	1.9667	2.0124	2.0407	2.0180	1.8752
3	1.2833	1.5923	1.6271	1.6639	1.7026	1.7436	1.7870	1.8329	1.8811	1.9309	1.9809	2.0269	2.0588
4	1.2844	1.5821	1.6187	1.6574	1.6978	1.7396	1.7818	1.8232	1.8616	1.8937	1.9142	1.9146	1.8854
5	1.3681	1.5847	1.6123	1.6418	1.6731	1.7062	1.7406	1.7760	1.8119	1.8477	1.8818	1.9097	1.9195
6	1.4542	1.6396	1.6650	1.6932	1.7244	1.7587	1.7959	1.8353	1.8743	1.9067	1.9172	1.8676	1.6869
7	1.2763	1.4088	1.4255	1.4437	1.4630	1.4836	1.5052	1.5274	1.5494	1.5686	1.5842	1.5858	1.5751
8	1.1005	1.1937	1.1975	1.2019	1.2075	1.2114	1.2128	1.2104	1.2040	1.1832	1.1613	1.1298	1.0916
9	0.9165	0.9269	0.9282	0.9290	0.9291	0.9287	0.9279	0.9098	0.9086	0.9190	0.9204	0.9233	0.9279
10	0.8132	0.8760	0.8813	0.8868	0.8926	0.8988	0.9055	0.9126	0.9205	0.9100	0.9195	0.9297	0.9402
11	0.7415	0.8160	0.8232	0.8307	0.8385	0.8465	0.8549	0.8637	0.8729	0.8825	0.8926	0.9032	0.9139
12	0.7284	0.8125	0.8203	0.8282	0.8364	0.8448	0.8536	0.8626	0.8720	0.8819	0.8921	0.9028	0.9135
13	0.7317	0.8156	0.8232	0.8311	0.8391	0.8474	0.8561	0.8651	0.8744	0.8841	0.8942	0.9049	0.9156
	stream wise direction ←												inlet
1	1.9363	1.8629	1.6711	1.5607	1.7135	<u>1.5244</u>	1.1189	0.9378	1.0716	1.0989	1.1356	1.0821	
2	1.4655	<u>0.8824</u>	1.3129	1.4086	1.5990	1.7113	1.5202	1.2892	1.0954	1.1142	1.1549	1.1241	
3	2.0639	1.9734	1.6446	1.4122	1.7652	<u>1.6034</u>	1.2632	1.1418	1.1495	1.1753	1.1859	1.1923	
4	1.8003	1.5841	1.4747	1.4497	1.7821	1.8678	1.8018	1.5458	1.1328	1.1455	1.1783	1.1141	
5	1.8913	1.7539	1.4193	1.2457	1.2917	1.3314	1.2063	1.1112	1.0616	1.0365	1.0838	1.0647	
6	1.2498	<u>0.6540</u>	0.9522	1.0541	1.1221	1.0924	1.0759	1.0671	1.1186	1.1699	1.1925	1.2160	
7	1.5310	1.3117	1.0811	0.9844	0.9972	1.0052	1.0239	1.0442	1.0525	1.0692	1.1057	1.1514	
8	1.0483	1.0018	0.9986	0.9762	0.9897	0.9881	1.0083	1.0321	1.0937	1.1189	1.1458	1.1747	
9	0.9452	0.9559	0.9642	0.9692	0.9729	0.9880	1.0083	1.0305	1.0508	1.0737	1.1048	1.1676	
10	0.9264	0.9404	0.9478	0.9643	0.9729	0.9880	1.0084	1.0310	1.0520	1.0755	1.0942	1.1170	
11	0.9256	0.9402	0.9477	0.9713	0.7251	0.7349	0.7507	0.7708	0.7927	0.8227	0.9995	1.1512	
12	0.9254	0.9403	0.9479	0.9663	0.9984	1.0389	1.0604	1.0839	1.1056	1.1287	1.1571	1.1950	
13	0.9277	0.9427	0.9498	0.9665	0.9747	0.9900	1.0110	1.0346	1.0587	1.0851	1.1193	1.1691	

3.3.4. *Tip speed ratio* $\gamma = 5.5$. Figure 34 shows mosaic plots of the binned depth averaged velocity magnitude, turbulent kinetic energy and turbulent viscosity. The bin containing the upstream hubs are at $(2.1,0.0)$ while the downstream hubs are at $(0.0,0.0)$ and it is easily identifiable in the velocity plot showing the expected velocity deficit associated with the flow passing the turbine face. It should be noted that the centre upstream hub lies on the symmetry plane and so only half the rotor plane is used in the simulation. Tables 31 to 33 present the binned mean values with the bin containing the turbine nacelle underlined.

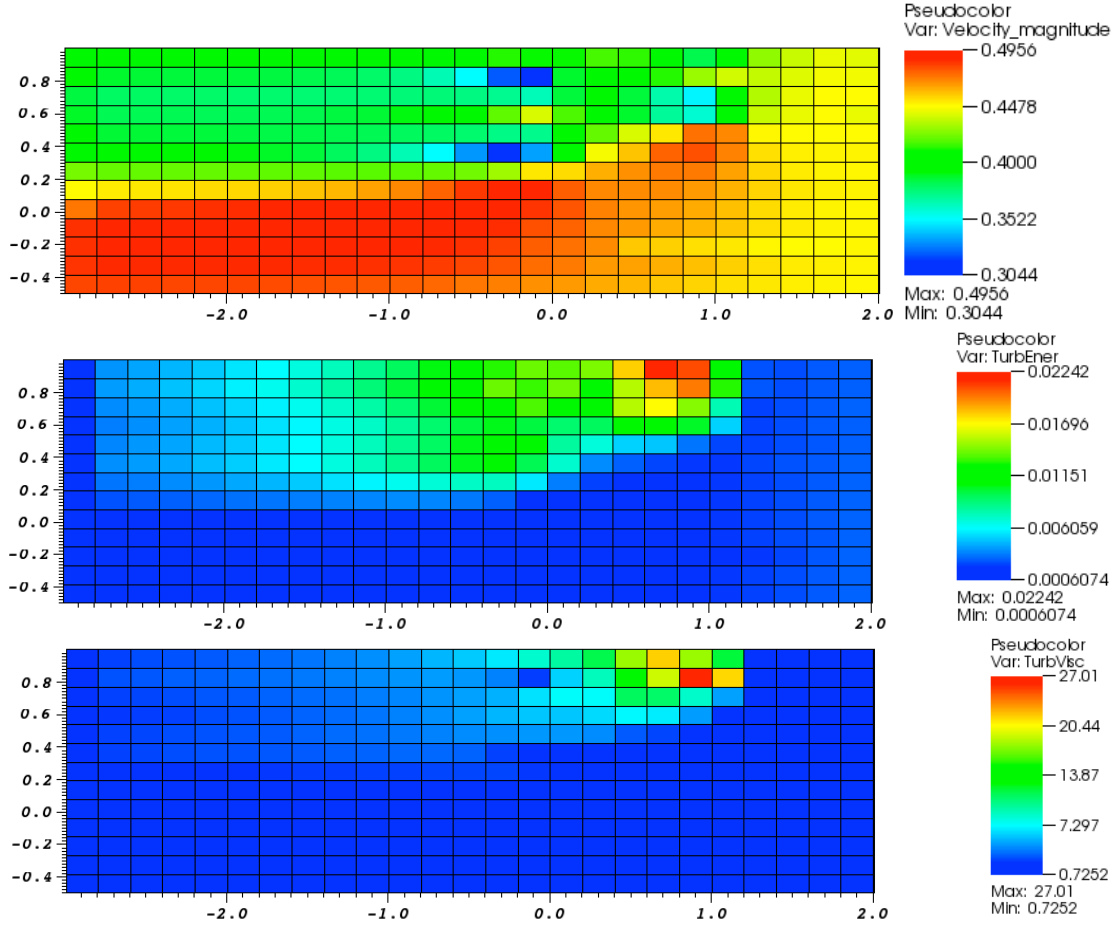


FIGURE 34. Staggered array of turbines tested in the Manchester basin at a tip speed ratio of $\gamma = 5.5$: Mosaic plots showing binned depth averaged velocity magnitude, turbulent kinetic energy and turbulent viscosity.

TABLE 31. Staggered array of turbines tested in the Manchester basin at a tip speed ratio of $\gamma = 5.5$: Depth averaged velocity magnitude. The value for the cells containing the turbines have been underlined

	stream wise direction ←												
downstream													
1	<u>0.3950</u>	0.3949	<u>0.3952</u>	<u>0.3956</u>	<u>0.3961</u>	<u>0.3968</u>	<u>0.3977</u>	<u>0.3990</u>	<u>0.4006</u>	<u>0.4026</u>	<u>0.4051</u>	<u>0.4078</u>	<u>0.4105</u>
2	<u>0.3919</u>	<u>0.3875</u>	<u>0.3870</u>	<u>0.3865</u>	<u>0.3859</u>	<u>0.3852</u>	<u>0.3843</u>	<u>0.3832</u>	<u>0.3815</u>	<u>0.3789</u>	<u>0.3743</u>	<u>0.3660</u>	<u>0.3517</u>
3	<u>0.3847</u>	<u>0.3798</u>	<u>0.3793</u>	<u>0.3789</u>	<u>0.3785</u>	<u>0.3781</u>	<u>0.3777</u>	<u>0.3774</u>	<u>0.3771</u>	<u>0.3769</u>	<u>0.3767</u>	<u>0.3762</u>	<u>0.3749</u>
4	<u>0.3887</u>	<u>0.3826</u>	<u>0.3823</u>	<u>0.3821</u>	<u>0.3820</u>	<u>0.3821</u>	<u>0.3825</u>	<u>0.3833</u>	<u>0.3846</u>	<u>0.3867</u>	<u>0.3903</u>	<u>0.3961</u>	<u>0.4048</u>
5	<u>0.3952</u>	<u>0.3872</u>	<u>0.3866</u>	<u>0.3859</u>	<u>0.3853</u>	<u>0.3847</u>	<u>0.3842</u>	<u>0.3836</u>	<u>0.3830</u>	<u>0.3822</u>	<u>0.3811</u>	<u>0.3796</u>	<u>0.3776</u>
6	<u>0.4060</u>	<u>0.3967</u>	<u>0.3954</u>	<u>0.3940</u>	<u>0.3924</u>	<u>0.3905</u>	<u>0.3882</u>	<u>0.3851</u>	<u>0.3810</u>	<u>0.3751</u>	<u>0.3663</u>	<u>0.3529</u>	<u>0.3335</u>
7	<u>0.4241</u>	<u>0.4217</u>	<u>0.4217</u>	<u>0.4215</u>	<u>0.4212</u>	<u>0.4209</u>	<u>0.4205</u>	<u>0.4202</u>	<u>0.4198</u>	<u>0.4200</u>	<u>0.4200</u>	<u>0.4212</u>	<u>0.4238</u>
8	<u>0.4484</u>	<u>0.4520</u>	<u>0.4529</u>	<u>0.4537</u>	<u>0.4546</u>	<u>0.4557</u>	<u>0.4571</u>	<u>0.4591</u>	<u>0.4614</u>	<u>0.4653</u>	<u>0.4698</u>	<u>0.4764</u>	<u>0.4845</u>
9	<u>0.4732</u>	<u>0.4826</u>	<u>0.4837</u>	<u>0.4848</u>	<u>0.4860</u>	<u>0.4874</u>	<u>0.4888</u>	<u>0.4906</u>	<u>0.4921</u>	<u>0.4940</u>	<u>0.4950</u>	<u>0.4956</u>	<u>0.4953</u>
10	<u>0.4859</u>	<u>0.4921</u>	<u>0.4926</u>	<u>0.4930</u>	<u>0.4935</u>	<u>0.4939</u>	<u>0.4941</u>	<u>0.4943</u>	<u>0.4944</u>	<u>0.4932</u>	<u>0.4929</u>	<u>0.4921</u>	<u>0.4907</u>
11	<u>0.4866</u>	<u>0.4899</u>	<u>0.4900</u>	<u>0.4901</u>	<u>0.4902</u>	<u>0.4902</u>	<u>0.4902</u>	<u>0.4900</u>	<u>0.4898</u>	<u>0.4893</u>	<u>0.4888</u>	<u>0.4877</u>	<u>0.4860</u>
12	<u>0.4857</u>	<u>0.4877</u>	<u>0.4878</u>	<u>0.4878</u>	<u>0.4878</u>	<u>0.4877</u>	<u>0.4875</u>	<u>0.4872</u>	<u>0.4868</u>	<u>0.4862</u>	<u>0.4854</u>	<u>0.4841</u>	<u>0.4822</u>
13	<u>0.4815</u>	<u>0.4824</u>	<u>0.4822</u>	<u>0.4821</u>	<u>0.4819</u>	<u>0.4815</u>	<u>0.4811</u>	<u>0.4805</u>	<u>0.4797</u>	<u>0.4786</u>	<u>0.4773</u>	<u>0.4756</u>	<u>0.4737</u>
	stream wise direction ←												inlet
1	<u>0.4128</u>	<u>0.4117</u>	<u>0.4119</u>	<u>0.4168</u>	<u>0.4141</u>	<u>0.4065</u>	<u>0.3831</u>	<u>0.3946</u>	<u>0.4285</u>	<u>0.4376</u>	<u>0.4441</u>	<u>0.4432</u>	
2	<u>0.3226</u>	<u>0.3092</u>	<u>0.3876</u>	<u>0.4066</u>	<u>0.4105</u>	<u>0.4134</u>	<u>0.4303</u>	<u>0.4397</u>	<u>0.4370</u>	<u>0.4422</u>	<u>0.4464</u>	<u>0.4457</u>	
3	<u>0.3718</u>	<u>0.3651</u>	<u>0.3857</u>	<u>0.4011</u>	<u>0.3863</u>	<u>0.3672</u>	<u>0.3504</u>	<u>0.3932</u>	<u>0.4339</u>	<u>0.4441</u>	<u>0.4473</u>	<u>0.4475</u>	
4	<u>0.4207</u>	<u>0.4416</u>	<u>0.4177</u>	<u>0.4050</u>	<u>0.3878</u>	<u>0.3703</u>	<u>0.3602</u>	<u>0.3923</u>	<u>0.4383</u>	<u>0.4442</u>	<u>0.4473</u>	<u>0.4445</u>	
5	<u>0.3738</u>	<u>0.3730</u>	<u>0.4008</u>	<u>0.4216</u>	<u>0.4412</u>	<u>0.4525</u>	<u>0.4742</u>	<u>0.4695</u>	<u>0.4493</u>	<u>0.4472</u>	<u>0.4481</u>	<u>0.4478</u>	
6	<u>0.3044</u>	<u>0.3352</u>	<u>0.4096</u>	<u>0.4469</u>	<u>0.4596</u>	<u>0.4765</u>	<u>0.4806</u>	<u>0.4702</u>	<u>0.4538</u>	<u>0.4512</u>	<u>0.4505</u>	<u>0.4501</u>	
7	<u>0.4309</u>	<u>0.4529</u>	<u>0.4550</u>	<u>0.4628</u>	<u>0.4682</u>	<u>0.4728</u>	<u>0.4718</u>	<u>0.4654</u>	<u>0.4558</u>	<u>0.4517</u>	<u>0.4503</u>	<u>0.4499</u>	
8	<u>0.4934</u>	<u>0.4902</u>	<u>0.4784</u>	<u>0.4702</u>	<u>0.4687</u>	<u>0.4689</u>	<u>0.4668</u>	<u>0.4622</u>	<u>0.4562</u>	<u>0.4526</u>	<u>0.4509</u>	<u>0.4500</u>	
9	<u>0.4934</u>	<u>0.4855</u>	<u>0.4797</u>	<u>0.4705</u>	<u>0.4679</u>	<u>0.4664</u>	<u>0.4639</u>	<u>0.4602</u>	<u>0.4551</u>	<u>0.4521</u>	<u>0.4505</u>	<u>0.4500</u>	
10	<u>0.4869</u>	<u>0.4805</u>	<u>0.4765</u>	<u>0.4695</u>	<u>0.4667</u>	<u>0.4640</u>	<u>0.4613</u>	<u>0.4583</u>	<u>0.4544</u>	<u>0.4519</u>	<u>0.4504</u>	<u>0.4498</u>	
11	<u>0.4831</u>	<u>0.4778</u>	<u>0.4746</u>	<u>0.4689</u>	<u>0.4590</u>	<u>0.4568</u>	<u>0.4545</u>	<u>0.4524</u>	<u>0.4499</u>	<u>0.4486</u>	<u>0.4492</u>	<u>0.4498</u>	
12	<u>0.4794</u>	<u>0.4749</u>	<u>0.4723</u>	<u>0.4672</u>	<u>0.4657</u>	<u>0.4630</u>	<u>0.4601</u>	<u>0.4575</u>	<u>0.4543</u>	<u>0.4522</u>	<u>0.4509</u>	<u>0.4501</u>	
13	<u>0.4716</u>	<u>0.4685</u>	<u>0.4669</u>	<u>0.4635</u>	<u>0.4615</u>	<u>0.4586</u>	<u>0.4562</u>	<u>0.4543</u>	<u>0.4523</u>	<u>0.4510</u>	<u>0.4503</u>	<u>0.4499</u>	

TABLE 32. Staggered array of turbines tested in the Manchester basin at a tip speed ratio of $\gamma = 5.5$: Depth averaged turbulent kinetic energy. The value for the cells containing the turbines have been underlined

	downstream			stream wise direction ←									
1	<u>1.86e-03</u>	3.85e-03	4.19e-03	4.57e-03	5.00e-03	5.49e-03	6.05e-03	6.70e-03	7.45e-03	8.31e-03	9.30e-03	1.04e-02	1.17e-02
2	1.99e-03	4.08e-03	4.43e-03	4.83e-03	5.28e-03	5.80e-03	6.39e-03	7.07e-03	7.87e-03	8.81e-03	9.92e-03	1.12e-02	1.27e-02
3	1.84e-03	3.72e-03	4.04e-03	4.39e-03	4.80e-03	5.26e-03	5.79e-03	6.39e-03	7.10e-03	7.92e-03	8.88e-03	1.00e-02	1.13e-02
4	1.77e-03	3.50e-03	3.79e-03	4.12e-03	4.49e-03	4.91e-03	5.39e-03	5.95e-03	6.58e-03	7.30e-03	8.11e-03	8.96e-03	9.76e-03
5	1.95e-03	3.67e-03	3.95e-03	4.26e-03	4.62e-03	5.03e-03	5.51e-03	6.05e-03	6.69e-03	7.43e-03	8.30e-03	9.29e-03	1.03e-02
6	2.05e-03	3.77e-03	4.04e-03	4.35e-03	4.70e-03	5.10e-03	5.56e-03	6.10e-03	6.72e-03	7.47e-03	8.33e-03	9.33e-03	1.03e-02
7	1.91e-03	3.28e-03	3.49e-03	3.72e-03	3.99e-03	4.28e-03	4.61e-03	4.99e-03	5.41e-03	5.86e-03	6.37e-03	6.86e-03	7.28e-03
8	1.57e-03	2.55e-03	2.68e-03	2.81e-03	2.96e-03	3.12e-03	3.28e-03	3.43e-03	3.58e-03	3.66e-03	3.71e-03	3.62e-03	3.35e-03
9	1.12e-03	1.44e-03	1.47e-03	1.49e-03	1.51e-03	1.53e-03	1.53e-03	1.47e-03	1.46e-03	1.41e-03	1.39e-03	1.37e-03	1.36e-03
10	7.96e-04	9.87e-04	1.00e-03	1.02e-03	1.04e-03	1.06e-03	1.08e-03	1.11e-03	1.14e-03	1.14e-03	1.19e-03	1.23e-03	1.28e-03
11	6.60e-04	8.43e-04	8.66e-04	8.92e-04	9.19e-04	9.50e-04	9.82e-04	1.02e-03	1.06e-03	1.10e-03	1.15e-03	1.20e-03	1.26e-03
12	6.24e-04	8.24e-04	8.49e-04	8.76e-04	9.06e-04	9.37e-04	9.72e-04	1.01e-03	1.05e-03	1.10e-03	1.14e-03	1.20e-03	1.25e-03
13	6.07e-04	8.11e-04	8.37e-04	8.65e-04	8.95e-04	9.27e-04	9.63e-04	1.00e-03	1.04e-03	1.09e-03	1.14e-03	1.19e-03	1.25e-03
	stream wise direction ←										inlet		
1	1.30e-02	1.41e-02	1.38e-02	1.44e-02	1.80e-02	<u>2.24e-02</u>	2.08e-02	1.15e-02	2.52e-03	2.43e-03	2.67e-03	2.79e-03	
2	1.41e-02	<u>1.33e-02</u>	1.42e-02	1.22e-02	1.55e-02	1.85e-02	1.98e-02	1.30e-02	2.57e-03	2.41e-03	2.65e-03	2.79e-03	
3	1.27e-02	1.35e-02	1.17e-02	1.07e-02	1.55e-02	<u>1.71e-02</u>	1.45e-02	7.67e-03	2.30e-03	2.46e-03	2.68e-03	2.83e-03	
4	1.03e-02	9.74e-03	8.96e-03	9.31e-03	1.17e-02	1.25e-02	1.02e-02	5.17e-03	2.27e-03	2.43e-03	2.68e-03	2.78e-03	
5	1.13e-02	1.10e-02	8.06e-03	6.77e-03	5.16e-03	4.95e-03	3.29e-03	2.33e-03	2.26e-03	2.41e-03	2.65e-03	2.82e-03	
6	1.08e-02	<u>9.55e-03</u>	7.01e-03	3.68e-03	2.75e-03	2.32e-03	2.09e-03	2.13e-03	2.32e-03	2.50e-03	2.69e-03	2.88e-03	
7	7.38e-03	5.56e-03	3.43e-03	2.27e-03	1.70e-03	1.78e-03	1.92e-03	2.09e-03	2.26e-03	2.44e-03	2.65e-03	2.86e-03	
8	2.78e-03	1.95e-03	1.81e-03	1.62e-03	1.65e-03	1.75e-03	1.90e-03	2.08e-03	2.29e-03	2.47e-03	2.67e-03	2.87e-03	
9	1.38e-03	1.44e-03	1.48e-03	1.57e-03	1.64e-03	1.75e-03	1.90e-03	2.07e-03	2.26e-03	2.45e-03	2.65e-03	2.87e-03	
10	1.33e-03	1.42e-03	1.46e-03	1.57e-03	1.64e-03	1.75e-03	1.89e-03	2.07e-03	2.26e-03	2.45e-03	2.64e-03	2.85e-03	
11	1.32e-03	1.42e-03	1.46e-03	1.57e-03	1.42e-03	1.52e-03	1.68e-03	1.87e-03	2.09e-03	2.31e-03	2.63e-03	2.87e-03	
12	1.32e-03	1.41e-03	1.46e-03	1.57e-03	1.66e-03	1.79e-03	1.94e-03	2.11e-03	2.30e-03	2.48e-03	2.67e-03	2.87e-03	
13	1.31e-03	1.41e-03	1.46e-03	1.57e-03	1.63e-03	1.74e-03	1.90e-03	2.07e-03	2.27e-03	2.46e-03	2.66e-03	2.87e-03	

TABLE 33. Staggered array of turbines tested in the Manchester basin at a tip speed ratio of $\gamma = 5.5$: Depth averaged turbulent viscosity. The value for the cells containing the turbines have been underlined

	stream wise direction ←												
downstream													
1	1.7451	2.7498	2.8967	3.0598	3.2415	3.4452	3.6747	3.9348	4.2320	4.5752	4.9757	5.4506	6.0019
2	1.9549	3.0044	3.1470	3.3014	3.4684	3.6485	3.8419	4.0473	4.2619	4.4789	4.6825	4.8339	4.8316
3	1.7783	2.7005	2.8274	2.9657	3.1168	3.2820	3.4629	3.6611	3.8781	4.1161	4.3775	4.6657	4.9720
4	1.7363	2.5391	2.6507	2.7741	2.9113	3.0651	3.2388	3.4363	3.6630	3.9253	4.2310	4.5870	4.9806
5	1.9436	2.6968	2.7950	2.9021	3.0193	3.1479	3.2897	3.4461	3.6187	3.8079	4.0126	4.2254	4.4222
6	2.0455	2.7345	2.8144	2.8989	2.9882	3.0820	3.1800	3.2811	3.3826	3.4789	3.5557	3.5756	3.4388
7	1.7486	2.2233	2.2748	2.3296	2.3871	2.4472	2.5098	2.5744	2.6404	2.7022	2.7646	2.8108	2.8393
8	1.4222	1.7493	1.7768	1.8072	1.8414	1.8752	1.9077	1.9346	1.9575	1.9582	1.9503	1.9071	1.8236
9	1.1921	1.2676	1.2695	1.2686	1.2642	1.2555	1.2413	1.1910	1.1626	1.1190	1.0809	1.0399	1.0014
10	0.9803	1.0049	1.0010	0.9963	0.9909	0.9850	0.9790	0.9733	0.9683	0.9364	0.9373	0.9405	0.9460
11	0.8078	0.8420	0.8455	0.8494	0.8540	0.8591	0.8650	0.8714	0.8786	0.8867	0.8955	0.9051	0.9150
12	0.7491	0.8170	0.8240	0.8313	0.8390	0.8470	0.8553	0.8641	0.8732	0.8829	0.8929	0.9034	0.9140
13	0.7328	0.8161	0.8237	0.8315	0.8395	0.8478	0.8564	0.8654	0.8747	0.8844	0.8945	0.9051	0.9158

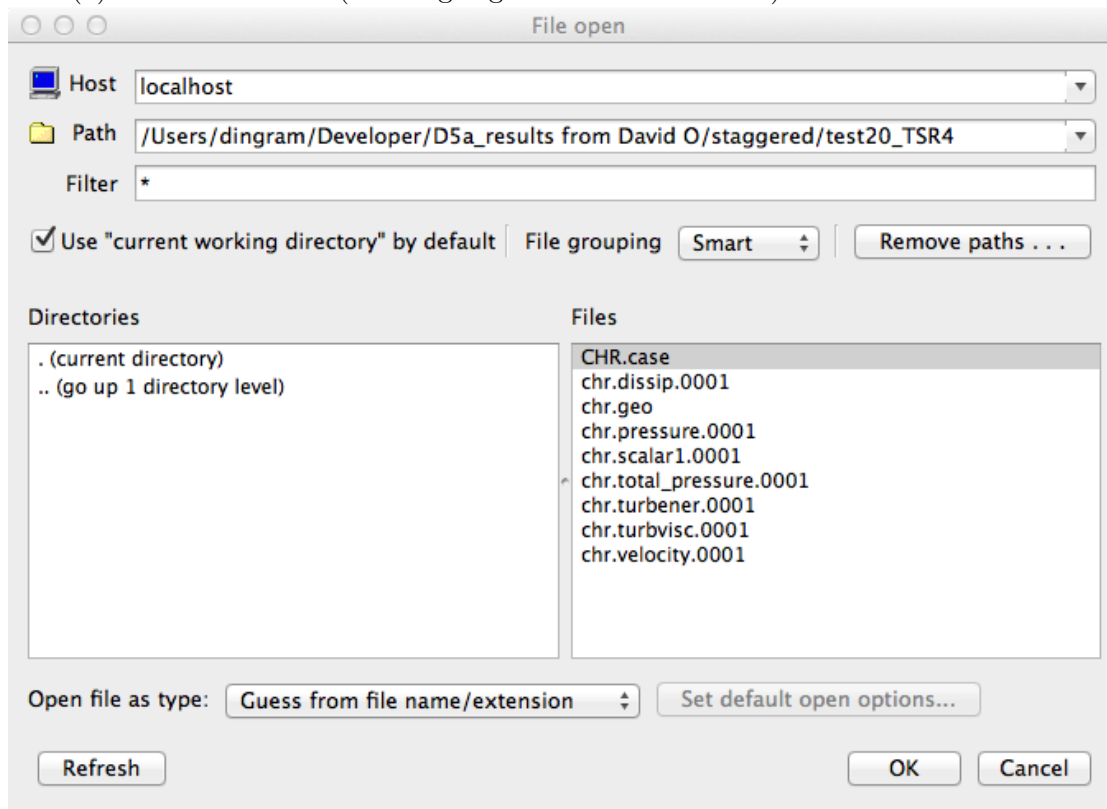
	stream wise direction ←												inlet
1	6.7741	8.4644	9.6035	11.6020	18.0305	<u>21.7528</u>	18.0301	11.9974	1.4768	1.0991	1.1356	1.0821	
2	4.2548	<u>2.6240</u>	6.2387	8.9856	14.2758	19.2166	27.0143	21.5306	1.6216	1.1139	1.1548	1.1240	
3	5.3576	6.5082	7.4222	7.5011	11.2145	<u>10.8921</u>	8.5757	4.9644	1.1691	1.1754	1.1859	1.1923	
4	5.4531	5.9155	5.9124	6.4353	7.0980	6.7952	4.9227	2.1941	1.1339	1.1457	1.1784	1.1141	
5	4.5717	4.8230	4.7604	4.4237	3.2210	2.7884	1.7257	1.1256	1.0623	1.0367	1.0838	1.0647	
6	2.7403	<u>1.3912</u>	2.4266	2.3772	1.7604	1.3885	1.1358	1.0691	1.1192	1.1701	1.1926	1.2160	
7	2.8187	2.5479	2.0149	1.4312	1.0240	1.0118	1.0256	1.0448	1.0528	1.0693	1.1057	1.1514	
8	1.6610	1.3139	1.2077	1.0176	0.9912	0.9889	1.0088	1.0323	1.0939	1.1191	1.1458	1.1747	
9	0.9770	0.9634	0.9685	0.9708	0.9733	0.9883	1.0085	1.0307	1.0509	1.0737	1.1048	1.1676	
10	0.9284	0.9413	0.9486	0.9647	0.9731	0.9881	1.0085	1.0311	1.0521	1.0756	1.0942	1.1170	
11	0.9263	0.9406	0.9481	0.9715	0.7252	0.7350	0.7508	0.7708	0.7927	0.8227	0.9996	1.1512	
12	0.9257	0.9405	0.9480	0.9664	0.9985	1.0390	1.0605	1.0840	1.1057	1.1287	1.1571	1.1950	
13	0.9278	0.9428	0.9499	0.9666	0.9747	0.9901	1.0111	1.0347	1.0587	1.0850	1.1193	1.1691	

APPENDIX A

Production of Depth averaged data using VisIt

The following set of instructions demonstrate the procedure for generating depth averaged distributions from results files from `code_saturne` simulations using the VisIt visualisation software which can be freely downloaded from Lawrence Livermore National Laboratory¹. These procedures utilise version 2.5.2 of VisIt.

- (1) load the datafile (an ensight gold format `.case` file) into VisIt.



- (2) Add a *Pseudo-colour* plot for the selected variable (in this case `Velocity_magnitude`).
- (3) Add a *Data-binning* operator to the plot, this can be found on the `Operator Attributes` menu in the `Analysis` sub menu. Once selected the `dataBinning` window will open.

¹<https://wci.llnl.gov/codes/visit/>

Bin Definitions

Dimensions: 1D

Dimension 1 | Dimension 2 | Dimension 3

Bin based on: Variable (default) X Y Z

Number of bins: 50

Specify range

Min: 0

Max: 1

Behavior for data outside range: Clamp Discard

Reduction

Reduction Operator: Average

Variable: default

Value for bins with no data: 0

Buttons: Make default, Apply, Load, Save, Reset, Post, Dismiss

- (4) Choose 2D and the select the z ordinate for the **dimension 1** binning variable. Ensure that the specify range box is ticked and that the required range is entered.

Bin Definitions

Dimensions: 1D

Dimension 1 | Dimension 2 | Dimension 3

Bin based on: Variable (default) X Y Z

Number of bins: 25

Specify range

Min: -3.0

Max: 2.0

Behavior for data outside range: Clamp Discard

Reduction

Reduction Operator: Average

Variable: default

Value for bins with no data: 0

Buttons: Make default, Apply, Load, Save, Reset, Post, Dismiss

- (5) Choose **Dimension 2** and set the x ordinate as the binning variable. If needed tick the specify range box is ticked and enter the required range.

DataBinning operator attributes

Bin Definitions

Dimensions: 2D

Dimension 1 | Dimension 2 | Dimension 3

Bin based on: Variable X Y Z

Number of bins: 13

Specify range

Min: -0.5

Max: 1

Behavior for data outside range: Clamp Discard

Reduction

Reduction Operator: Average

Variable: default

Value for bins with no data: 0

Buttons: Make default, Load, Save, Reset, Apply, Post, Dismiss

- (6) Choose the **Average** reduction operator and change the selected variable from **default** to the same variable as was selected in step 2. All of the solution variables can be found under the **Scalars** entry in the **Variables** menu. Set the *Value for bins with no data* to -99

DataBinning operator attributes

Bin Definitions

Dimensions: 2D

Dimension 1 | Dimension 2 | Dimension 3

Bin based on: Variable X Y Z

Number of bins: 13

Specify range

Min: -0.5

Max: 1

Behavior for data outside range: Clamp Discard

Reduction

Reduction Operator: Average

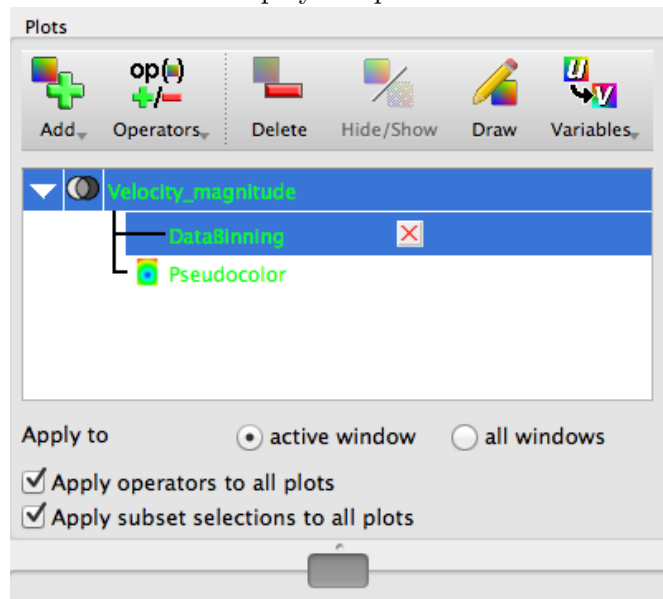
Variable: Velocity_magnitude

Value for bins with no data: -99

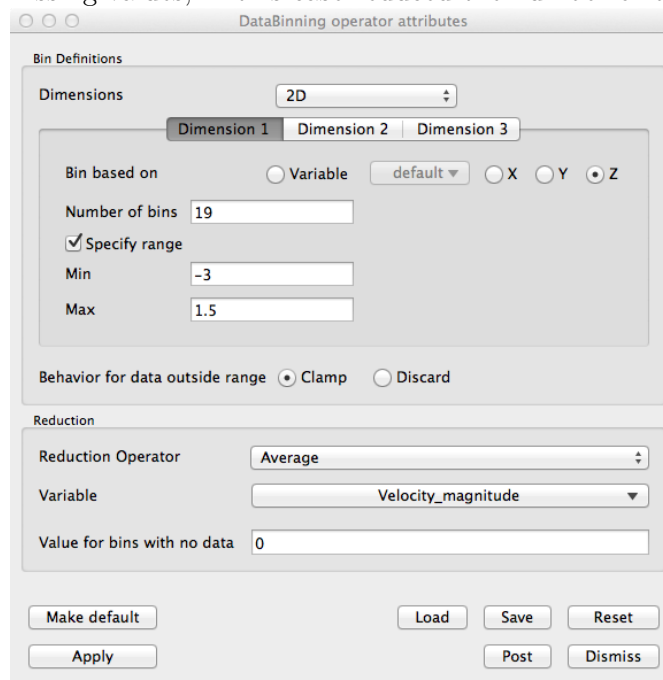
Buttons: Make default, Load, Save, Reset, Apply, Post, Dismiss

(7) click on Apply and Dismiss

(8) click on the Draw icon to display the plot.



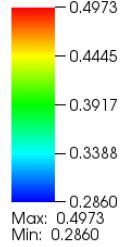
If the plot contains values of -99 then there the bins are too small and some contain missing values, in this case reduced the number of bins are try again.



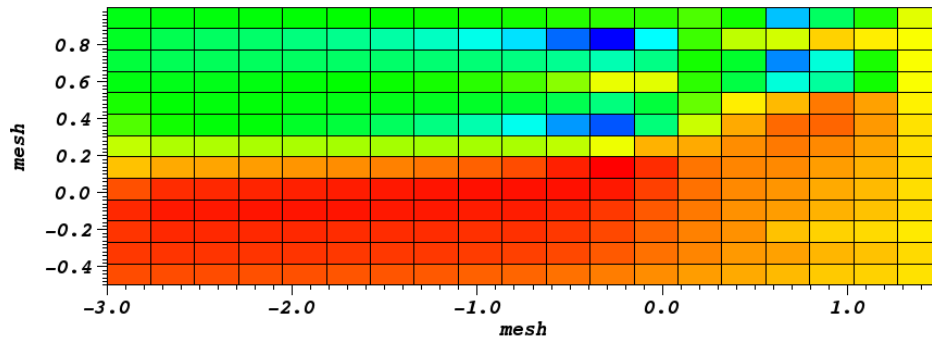
(9) Add a *Mesh* plot to the plotting window.

DB: CHR.case
Cycle: 0 Time: 1

Pseudocolor
Var: Velocity_magnitude



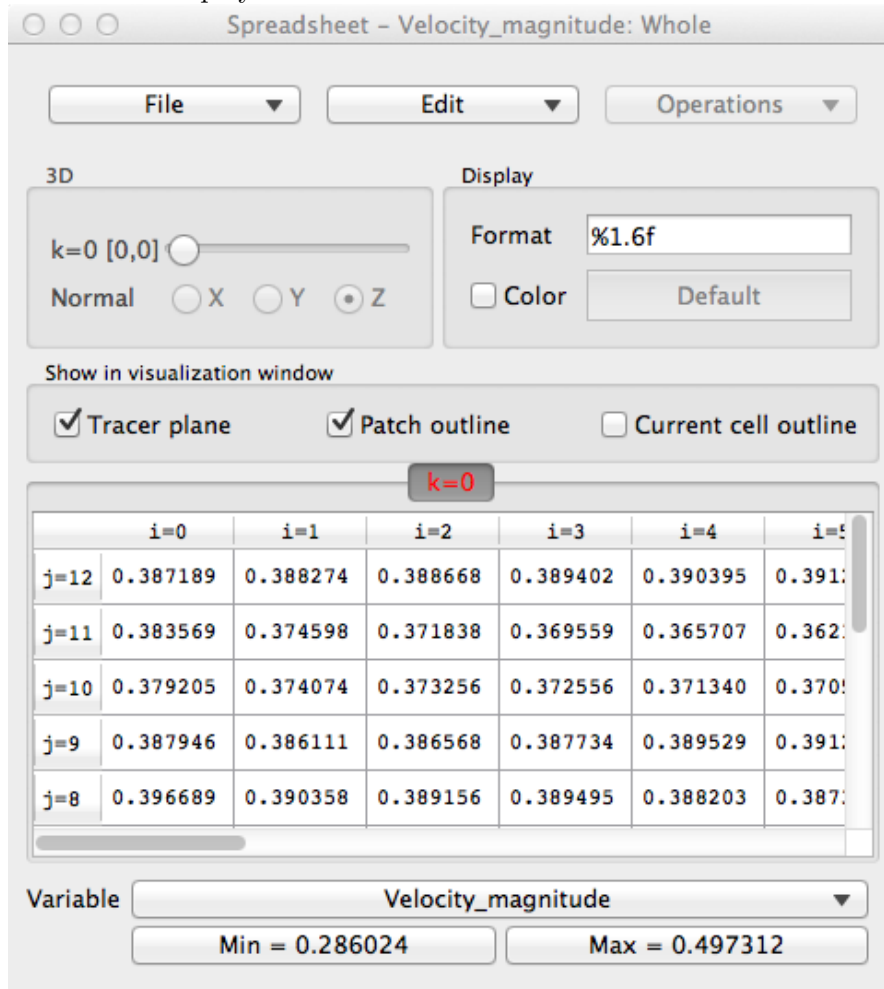
Mesh
Var: mesh



user: dingram
Tue Aug 28 15:09:32 2012

To export the depth averaged information to a text file a *spreadsheet* plot can be used.

- (1) Add a *Spreadsheet* plot and choose the same variable as that used for binning the data from the list of variables on the sub-menu. The *Spreadsheet* window will now be displayed.



- (2) Enter the required numerical format in the *Format* box and press enter - for all the tables included in this report either %1.4f, 4 decimal places floating point, or %1.2e, 2 decimal places exponent format, have been used.
- (3) uncheck the *Tracer plane* and *Patch outline* boxes.
- (4) Select the part of the table to be output, either by dragging the mouse over the cells or by using the *Select All* item on the *Edit* menu.
- (5) Use the *Save as text ...* item on the file menu to save the text file containing the spreadsheet.

APPENDIX B

Contents of the Accompanying CD

The data needed to run the cases presented in this report are included on an accompanying CD, which is also available as a .zip file. The following files are on the CD.

README: Description of the data on the CD

D5a.pdf: a .pdf file containing this report.

Single: directory containing the simulations for a single turbine tested in the EDF flume.

D5_Case.xml: Code_Saturne case file

usinv.f90: User subroutine initialising the single turbine case

ustsns.f90: User subroutine specifying the source terms for the actuator disks.

blade.txt: Blade definition file.

Circle.txt: Aerodynamic coefficients for a circular cylinder.

4415.txt: Aerodynamic coefficients for a NACA 4415 airfoil.

single.cgns: CGNS format grid file.

TSRx.x: subdirectory containing results for the simulation at a tip speed ratio of $\gamma = x.x$.

Double: directory containing the simulations for an infinite width array of two rows of turbines in series, tested by Manchester. Utilising symmetry planes to restrict the simulation to a single column of the array.

D5_Case.xml: Code_Saturne case file

usinv.f90: User subroutine initialising the double turbine case

ustsns.f90: User subroutine specifying the source terms for the actuator disks.

blade.txt: Blade definition file.

Circle.txt: Aerodynamic coefficients for a circular cylinder.

Goe804.txt: Aerodynamic coefficients for a GOE 804 airfoil.

test19.cgns: CGNS format grid file.

TSR $x.x$: subdirectory containing results for the simulation at a tip speed ratio of $\gamma = x.x$.

Staggered: directory containing the simulations for a seven turbine array of two rows of turbines in a staggered arrangement, tested by Manchester. But utilising a symmetry plane to halve the computational domain.

D5_Case.xml: Code_Saturne case file

usinv.f90: User subroutine initialising the double turbine case

ustsns.f90: User subroutine specifying the source terms for the actuator disks.

blade.txt: Blade definition file.

Circle.txt: Aerodynamic coefficients for a circular cylinder.

Goe804.txt: Aerodynamic coefficients for a GOE 804 airfoil.

test20.cgns: CGNS format grid file.

TSR $x.x$: subdirectory containing results for the simulation at a tip speed ratio of $\gamma = x.x$.

Double: directory containing the simulations for an infinite width array of two rows of turbines in series, tested by Manchester. Utilising symmetry planes to restrict the simulation to a single column of the array.

Staggered: directory containing the simulations for a seven turbine array of two rows of turbines in a staggered arrangement, tested by Manchester. But utilising a symmetry plane to halve the computational domain.

APPENDIX C

usinv.f90

```
!-----  
!  
!           Code_Saturne version 2.0.0-rc1  
!  
!  
! This file is part of the Code_Saturne Kernel, element of the  
! Code_Saturne CFD tool.  
  
! Copyright (C) 1998-2008 EDF S.A., France  
  
! contact: saturne-support@edf.fr  
  
! The Code_Saturne Kernel is free software; you can redistribute it  
! and/or modify it under the terms of the GNU General Public License  
! as published by the Free Software Foundation; either version 2 of  
! the License, or (at your option) any later version.  
  
! The Code_Saturne Kernel is distributed in the hope that it will be  
! useful, but WITHOUT ANY WARRANTY; without even the implied warranty  
! of MERCHANTABILITY or FITNESS FOR A PARTICULAR PURPOSE. See the  
! GNU General Public License for more details.  
  
! You should have received a copy of the GNU General Public License  
! along with the Code_Saturne Kernel; if not, write to the  
! Free Software Foundation, Inc.,  
! 51 Franklin St, Fifth Floor,  
! Boston, MA 02110-1301 USA  
  
!-----  
  
Module connectivity  
  Integer(8)      :: nbccl(1000000,6)  
  Integer(8)      con(1000000,6)  
  double precision clcd_val(1000)  
contains  
  subroutine error_message(text)  
    character (*) :: text  
    !if (irangp.le.0) then  
      print*,text  
    !endif  
    stop  
  end subroutine error_message  
End Module connectivity
```

```

Module turbine_design
  integer      n_be
  Integer      :: nMax_elms_start(2)
  Integer      :: nMax_elms_stop(2)
  double precision  :: rotor_radius
  double precision  :: blade_scale
  double precision  :: Frontal_Area(2)
  type :: b_section
    double precision  :: alpha
    double precision  :: cl
    double precision  :: cd
    type(b_section), pointer  :: next
  end type b_section
  type :: blade_element
    double precision  :: rad
    double precision  :: theta
    double precision  :: chord
    integer           :: rec_count
    character(30),pointer  :: Bsection
    type (b_section), pointer  :: ptr_bsection
  end type blade_element
  type :: AD_element
    double precision  :: rad
    double precision  :: chord
    double precision  :: twist
    double precision  :: elm_area
    double precision  :: azim_deg
    double precision  :: dFX
    double precision  :: dFY
    double precision  :: dFZ
    double precision  :: frac_v
    integer           :: nCel ! code saturne cell number
    integer           :: Nrec1
    integer           :: Nrec2
    type (b_section), pointer  :: ptr_Belement1
    type (b_section), pointer  :: ptr_Belement2
  end type AD_element
  type(AD_element), allocatable  :: AD_position(:)
  type(blade_element), allocatable  :: blade_position(:)
End Module turbine_design

```

```

subroutine usiniv &
  !=====
  ( idbia0 , idbra0 , &
  ndim , ncelet , ncel , nfac , nfabor , nfml , nprfml , &
  nmod , lndfac , lndfbr , ncelbr , &
  nvar , nscal , nphas , &
  nideve , nrdeve , nituse , nrtuse , &
  ifacel , ifabor , ifmfbr , ifmcel , iprfml , maxelt , lstelt , &
  ipnfac , nodfac , ipnfbr , nodfbr , &

```

```

    ideovel , ituser , ia      ,                                &
    xyzcen , surfac , surfbo , cdgfac , cdgfb , xyznod , volume , &
    dt      , rtp      , propce , propfa , propfb , coefa  , coefb , &
    rdevel , rtuser , ra      )

use turbine_design
use connectivity
!=====
! Purpose:
! -----

!   User subroutine.

!   Initialize variables

! This subroutine is called at beginning of the computation
! (restart or not) before the loop time step

! This subroutine enables to initialize or modify (for restart)
!   unknown variables and time step values

! rom and viscl values are equal to ro0 and viscl0 or initialize
! by reading the restart file
! viscls and cp variables (when there are defined) have no value
! excepted if they are read from a restart file

! Physical quantities are defined in the following arrays:
! propce (physical quantities defined at cell center),
! propfa (physical quantities defined at interior face center),
! propfb (physical quantities defined at border face center).
!
! Examples:
! propce(iel, iproc(irom (iphas))) means rom (iel, iphas)
! propce(iel, iproc(iviscl(iphas))) means viscl(iel, iphas)
! propce(iel, iproc(icp (iphas))) means cp (iel, iphas)
! propce(iel, iproc(ivisls(iscal))) means visls(iel, iscal)
! propfa(ifac, iprof(ifluma(ivar))) means flumas(ifac, ivar)
! propfb(ifac, iprob(irom (iphas))) means romb (ifac, iphas)
! propfb(ifac, iprob(ifluma(ivar))) means flumab(ifac, ivar)

! Modification of the behaviour law of physical quantities (rom, viscl,
! viscls, cp) is not done here. It is the purpose of the user subroutine
! usphyv

! Cells identification
! =====

! Cells may be identified using the 'getcel' subroutine.
! The syntax of this subroutine is described in the 'usclim' subroutine,
! but a more thorough description can be found in the user guide.

!-----

```

```

! Arguments
!-----!
! name      !type!mode ! role
!-----!
! idbia0    ! i  ! <-- ! number of first free position in ia
! idbra0    ! i  ! <-- ! number of first free position in ra
! ndim      ! i  ! <-- ! spatial dimension
! ncelet    ! i  ! <-- ! number of extended (real + ghost) cells
! ncel      ! i  ! <-- ! number of cells
! nfac      ! i  ! <-- ! number of interior faces
! nfabor    ! i  ! <-- ! number of boundary faces
! nfml      ! i  ! <-- ! number of families (group classes)
! nprfml    ! i  ! <-- ! number of properties per family (group class)
! nnod      ! i  ! <-- ! number of vertices
! lndfac    ! i  ! <-- ! size of nodfac indexed array
! lndfbr    ! i  ! <-- ! size of nodfbr indexed array
! ncelbr    ! i  ! <-- ! number of cells with faces on boundary
! nvar      ! i  ! <-- ! total number of variables
! nscal     ! i  ! <-- ! total number of scalars
! nphas     ! i  ! <-- ! number of phases
! nideve, nrdeve ! i  ! <-- ! sizes of idevel and rdevel arrays
! nituse, nrtuse ! i  ! <-- ! sizes of ituser and rtuser arrays
! ifacel(2, nfac) ! ia ! <-- ! interior faces -> cells connectivity
! ifabor(nfabor) ! ia ! <-- ! boundary faces -> cells connectivity
! ifmfbr(nfabor) ! ia ! <-- ! boundary face family numbers
! ifmcel(ncelet) ! ia ! <-- ! cell family numbers
! iprfml    ! ia ! <-- ! property numbers per family
! (nfml, nprfml) !   !   !
! maxelt    ! i  ! <-- ! max number of cells and faces (int/boundary)
! lstelt(maxelt) ! ia ! --- ! work array
! ipnfac(nfac+1) ! ia ! <-- ! interior faces -> vertices index (optional)
! nodfac(lndfac) ! ia ! <-- ! interior faces -> vertices list (optional)
! ipnfbr(nfabor+1) ! ia ! <-- ! boundary faces -> vertices index (optional)
! nodfbr(lndfbr) ! ia ! <-- ! boundary faces -> vertices list (optional)
! idevel(nideve) ! ia ! <-> ! integer work array for temporary development
! ituser(nituse) ! ia ! <-> ! user-reserved integer work array
! ia(*)     ! ia ! --- ! main integer work array
! xyzcen    ! ra ! <-- ! cell centers
! (ndim, ncelet) !   !   !
! surfac    ! ra ! <-- ! interior faces surface vectors
! (ndim, nfac) !   !   !
! surfbo    ! ra ! <-- ! boundary faces surface vectors
! (ndim, nfabor) !   !   !
! cdgfac    ! ra ! <-- ! interior faces centers of gravity
! (ndim, nfac) !   !   !
! cdgfo     ! ra ! <-- ! boundary faces centers of gravity
! (ndim, nfabor) !   !   !
! xyznod    ! ra ! <-- ! vertex coordinates (optional)
! (ndim, nnod) !   !   !
! volume(ncelet) ! ra ! <-- ! cell volumes
! dt(ncelet) ! ra ! <-- ! time step (per cell)
! rtp(ncelet, *) ! ra ! <-- ! computed variables at cell centers at current
!           !   !   ! time steps

```

```

! propce(ncelet, *)! ra ! <-- ! physical properties at cell centers      !
! propfa(nfac, *) ! ra ! <-- ! physical properties at interior face centers !
! propfb(nfabor, *)! ra ! <-- ! physical properties at boundary face centers !
! coefa, coefb    ! ra ! <-- ! boundary conditions                    !
! (nfabor, *)     !     !                                           !
! rdevel(nrdeve)  ! ra ! <-> ! real work array for temporary development !
! rtuser(nrtuse)  ! ra ! <-> ! user-reserved real work array           !
! ra(*)           ! ra ! --- ! main real work array                     !
!-----!-----!-----!-----!

```

```

!      Type: i (integer), r (real), s (string), a (array), l (logical),
!            and composite types (ex: ra real array)
!      mode: <-- input, --> output, <-> modifies data, --- work array
!=====

```

```
implicit none
```

```

!=====
! Common blocks
!=====

```

```

include "paramx.h"
include "pointe.h"
include "numvar.h"
include "optcal.h"
include "cstphy.h"
include "entsor.h"
include "parall.h"
include "period.h"

```

```
!=====
```

```
! Arguments
```

```

integer      ilelt, nlelt, nlelt2
integer      idbia0 , idbra0
integer      ndim  , ncelet , ncel  , nfac  , nfabor
integer      nfml  , nprfml
integer      nnod  , lndfac , lndfbr , ncelbr
integer      nvar  , nscal  , nphas
integer      nideve , nrdeve , nituse , nrtuse

```

```

integer      ifacel(2,nfac) , ifabor(nfabor)
integer      ifmfbr(nfabor) , ifmcel(ncelet)
integer      iprfml(nfml,nprfml), maxelt, lstelt(maxelt)
integer      ipnfac(nfac+1), nodfac(lndfac)
integer      ipnfbr(nfabor+1), nodfbr(lndfbr)
integer      idevel(nideve), ituser(nituse), ia(*)

```

```

double precision xyzcen(ndim,ncelet)
double precision surfac(ndim,nfac), surfbo(ndim,nfabor)
double precision cdgfac(ndim,nfac), cdgfbo(ndim,nfabor)
double precision xyznod(ndim,nnod), volume(ncelet)

```



```

double precision dt(ncelet), rtp(ncelet,*), propce(ncelet,*)
double precision propfa(nfac,*), propfb(nfabor,*)
double precision coefa(nfabor,*), coefb(nfabor,*)
double precision rdevel(nrdeve), rtuser(nrtuse), ra(*)

! Local variables

logical :: switch1,switch2
real    :: random
double precision, parameter :: pi = 3.1415926535897932384626433832795028841971693993751058209749445923
double precision, parameter :: RotorR = 0.135 ! metres
double precision zmax, zmin
double precision angle_switch
double precision temprtp(ncelet,1)
double precision x_dist, y_dist, z_dist, radius, disc_patch,area_sum
integer         idebia, idebra,impout(6),ii
integer         ielt,iel, iutile, iel1,iel2, i, j, ival,ival2
integer         ifac, inb, inb2, itest, n_passes, ipass,n,nbe,Nrec,Nfarm
integer(8)      ihuge
integer, parameter      :: Nfarmax = 2 ! number of turbines modelled

double precision chord1, chord2, twist1, twist2, frac_val1,frac_val,radius1,radius2, v_small
double precision deg2rad, dist_diff, cell_size
Integer         ifac2, n_of_f, jmax,jmin,isnbb,Number_Of_Faces,ifbn,nbelm
Logical         ifind, iswitch1,iswitch2
type (b_section), pointer :: current, bucket
!=====
! 1. Initialization of local variables
!=====
idebia = idbia0
idebra = idbra0
ihuge = 2.0e10
v_small = 1.0d-6
deg2rad = pi/180.0
rotor_radius = RotorR ! metres
do i = 1, ncel
  do j = 1, 6
    con(i,j) = -ihuge
    nbcell(i,j) = -ihuge
  enddo
enddo

!*****Find smallest cell size at inlet
cell_size = huge(1.0)
call getfbr('INLET', nlelt, lstelt)
nlelt2 = nlelt - 1
do ielt = 1, nlelt2
  ifac = lstelt(ielt)
  ifac2 =lstelt(ielt + 1)
  dist_diff = dabs( cdgfb(2,ifac) - cdgfb(2,ifac2) )
  if (cell_size > dist_diff) then
    cell_size = dist_diff
  endif
endif

```

```

enddo
print*, 'smallest cell size = ', cell_size
!*****
!=====
! 2. Unknown variables initialization:
!     ONLY done if there is no restart computation
!=====

! --- Example:  isca(1) is the variable number in RTP related to the first
!                user-defined scalar variable
!                rtp(iel,isca(1)) is the value of this variable in cell number
!                iel.

!***** isuite if block*****
if (isuite.eq.0) then
  ! do ii = 1, 1

  !  impout(ii) = impusr(ii)

  !enddo
  !open(impout(1),file='test_result.dat')

!=====
! 3. Building connectivity between particular indexed cell in the flow field and
!     its local neighbour cells. For a hexahedral cell this involves 6 neighbours
!=====
  do ifac = 1, nfac
    iel1 = ifacel(1, ifac)
    iel2 = ifacel(2,ifac)
    switch1 = .true.
    switch2 = .true.
    do i = 1, 6
      if ((switch1).and.(con(iel1,i).eq.(-ihuge) )) then
        con(iel1,i) = ifac
        switch1 = .false.
      endif
      if ((switch2).and.(con(iel2,i).eq.(-ihuge) )) then
        con(iel2,i) = ifac
        switch2 = .false.
      endif
    endif
  enddo
enddo

!*****
!Create 'nbccl(iel,Number_Of_Faces)' which provides connectivity between a cell centre of cell 'iel'
!and 1 to 'Number_Of_Faces' neighbour cells over 1 to ncel mesh cells in the flow field for any general
!polyhedral mesh (note in this case this is hexahedral)
!*****
do iel = 1, ncel
  rtp(iel,isca(1)) = 0.0
  do ifac = 1,6
    if (con(iel,ifac).gt.(-ihuge)) then

```

```

        iel2 = ifacel(2,con(iel,ifac))
        iel1 = ifacel(1,con(iel,ifac))
        if (iel1.ne.iel) then
            nbcell(iel,ifac) = iel1
        endif
        if (iel2.ne.iel) then
            nbcell(iel,ifac) = iel2
        endif
    endif
enddo
enddo
!*****
do i = 1, ncel
    rtp(iel, isca(1) ) = 0.0
enddo
! -----
! Now setup rotor blade design associated with all turbines of the farm
! -----

blade_scale = 1.0
allocate(AD_position(10000))
allocate(blade_position(100))
call read_blade_design(n_be)
nbelm = 0
! -----
!     Setup each of the Nfarm turbines associated with modelled tidal turbine farm
! -----
do Nfarm = 1,Nfarmax
nMax_elms_start(Nfarm) = nbelm + 1
area_sum = 0.d0
if (Nfarm == 1) then
    call getcel('X < 0.135 and X > -0.135 and Y > -0.135 &
                and Y < 0.135 and Z > -0.0014 and Z < 0.0014',    &
                nlelt,lstelt)
    zmin = -0.001401 ;zmax = 0.001401
else if (Nfarm == 2) then
    call getcel('X < 0.135 and X > -0.135 and Y > -0.135 &
                and Y < 0.135 and Z > 2.1586 and Z < 2.1614',    &
                nlelt,lstelt)
    zmin = 2.1586 ;zmax = 2.1614
endif
do ilelt = 1, nlelt
    iel = lstelt(ilelt)
    x_dist = xyzcen(1,iel)
    y_dist = xyzcen(2,iel)
    z_dist = xyzcen(3,iel)
    radius = dsqrt((x_dist * x_dist) + (y_dist * y_dist) )
    if ((radius <= rotor_radius).and.(z_dist > zmin).and.(z_dist < zmax)) then
        do i = 1, 6
            !*****
            if (con(iel,i) > -1) then
                disc_patch = surfac(3,con(iel,i))
                if (disc_patch > 0.d0) then

```

```

        area_sum = area_sum + disc_patch * 0.5
                ! used as a maker in debugging
        rtp(iel, isca(1) ) = 10.0
    endif
endif
!*****
enddo
endif
enddo

```

```

Frontal_Area(Nfarm) = area_sum
print*, 'time zero   area_sum = ', Frontal_Area(Nfarm), ' Turbine number = ', Nfarm

```

```

! -----
! Now setup the Actuator Disc
! -----

if (Nfarm == 1) then
    call getcel('X < 0.135 and X > -0.135 and Y > -0.135 &
                and Y < 0.135 and Z > -0.0014 and Z < 0.0014', &
                nlelt, lstelt)
    zmin = -0.001401 ; zmax = 0.001401
else if (Nfarm == 2) then
    call getcel('X < 0.135 and X > -0.135 and Y > -0.135 &
                and Y < 0.135 and Z > 2.1586 and Z < 2.1614', &
                nlelt, lstelt)
    zmin = 2.1586 ; zmax = 2.1614
endif
do ilelt = 1, nlelt
    iel = lstelt(ilelt)
    x_dist = xyzcen(1, iel)
    y_dist = xyzcen(2, iel)
    z_dist = xyzcen(3, iel)
    radius = dsqrt((x_dist * x_dist) + (y_dist * y_dist) )
    ! -----
    ! ~~~~~Create Actuator Disc from avialable mesh cells~~~~~
    ! -----
    if ((radius <= rotor_radius).and.(z_dist > zmin).and.(z_dist < zmax)) then
        nbelm = nbelm + 1
        AD_position(nbelm)%nCel = iel
        AD_position(nbelm)%rad = radius
        ! -----
        ! find frontal area of cell and azimuthal angles
        ! about the centre on the actuator disc
        ! -----
        area_sum = 0.d0
        do i = 1, 6
            if (con(iel, i) > -1) then
                disc_patch = surfac(3, con(iel, i))
                if (disc_patch > 0.d0) then

```

```

        area_sum = area_sum + disc_patch * 0.5
    endif
endif
enddo
AD_position(nbelm)%elm_area = area_sum
AD_position(nbelm)%azim_deg = datan2(y_dist,x_dist)
AD_position(nbelm)%frac_v = 0.0
! -----
! Calculate blade design chord and twist from blade
! design table
! -----
ifind = .true.
do n = 1, n_be - 1
    radius1 = blade_scale * (blade_position(n)%rad)
    radius2 = blade_scale * (blade_position(n + 1)%rad)
    ! ----- set up Actuator Disc elements-----
    if ( (radius >= radius1) .and. (radius <= radius2)) then
        ifind = .false.
        frac_val1 = radius2 - radius1
        if (dabs(frac_val1) < v_small) then
            call error_message("Error with blade design table")
        endif
        frac_val = (radius - radius1)/frac_val1
        AD_position(nbelm)%frac_v = frac_val
        chord1 = blade_scale * (blade_position(n)%chord)
        chord2 = blade_scale * (blade_position(n+1)%chord)
        AD_position(nbelm)%chord = chord1 + (chord2 - chord1) * frac_val
        twist1 = deg2rad * (blade_position(n)%theta)
        twist2 = deg2rad * (blade_position(n+1)%theta)
        AD_position(nbelm)%twist = twist1 + (twist2 - twist1) * frac_val
        ! -----
        nullify(AD_position(nbelm)%ptr_Belement1)
        allocate(AD_position(nbelm)%ptr_Belement1)
        AD_position(nbelm)%ptr_Belement1 = blade_position(n)%ptr_bsection
        Nrec = blade_position(n)%rec_count
        AD_position(nbelm)%Nrec1 = Nrec
        current => AD_position(nbelm)%ptr_Belement1
        bucket => blade_position(n)%ptr_bsection
        do i = 1, Nrec
            current%alpha = deg2rad * bucket%alpha
            current%c1 = bucket%c1
            current%cd = bucket%cd
            allocate(current%next)
            nullify( current%next%next )
            current => current%next
            bucket => bucket%next
        enddo
        ! -----
        nullify(AD_position(nbelm)%ptr_Belement2)
        allocate(AD_position(nbelm)%ptr_Belement2)
        AD_position(nbelm)%ptr_Belement2 = blade_position(n+1)%ptr_bsection
        Nrec = blade_position(n+1)%rec_count
        AD_position(nbelm)%Nrec2 = Nrec
    enddo
enddo

```

```

current => AD_position(nbelm)%ptr_Belement2
bucket => blade_position(n+1)%ptr_bsection
do i = 1, Nrec
  current%alpha = deg2rad * bucket%alpha
  current%c1    = bucket%c1
  current%cd    = bucket%cd
  allocate(current%next)
  nullify( current%next%next )
  current => current%next
  bucket  => bucket%next
enddo
! -----
exit
else if (radius < radius1) then
  AD_position(nbelm)%chord = blade_scale * blade_position(1)%chord
  AD_position(nbelm)%twist = deg2rad * blade_position(1)%theta
  ! -----
  nullify(AD_position(nbelm)%ptr_Belement1)
  allocate(AD_position(nbelm)%ptr_Belement1)
  AD_position(nbelm)%ptr_Belement1 = blade_position(1)%ptr_bsection
  Nrec = blade_position(1)%rec_count
  AD_position(nbelm)%Nrec1 = Nrec
  current => AD_position(nbelm)%ptr_Belement1
  bucket  => blade_position(1)%ptr_bsection
  do i = 1, Nrec
    current%alpha = deg2rad * bucket%alpha
    current%c1    = bucket%c1
    current%cd    = bucket%cd
    allocate(current%next)
    nullify( current%next%next )
    current => current%next
    bucket  => bucket%next
  enddo
  ! -----
  nullify(AD_position(nbelm)%ptr_Belement2)
  allocate(AD_position(nbelm)%ptr_Belement2)
  AD_position(nbelm)%ptr_Belement2 = blade_position(1)%ptr_bsection
  Nrec = blade_position(1)%rec_count
  AD_position(nbelm)%Nrec2 = Nrec
  current => AD_position(nbelm)%ptr_Belement2
  bucket  => blade_position(1)%ptr_bsection
  do i = 1, Nrec
    current%alpha = deg2rad * bucket%alpha
    current%c1    = bucket%c1
    current%cd    = bucket%cd
    allocate(current%next)
    nullify( current%next%next )
    current => current%next
    bucket  => bucket%next
  enddo
  ! -----
endif
! -----

```

```

        enddo
!   if (ifind) then
!       print*, 'element ',nbelm,' at radius = ',AD_position(nbelm)%rad
!   endif
endif
-----
! -----
! -----
! -----
enddo
!-----
!   enddo -- Setup each of the Nfarm turbines associated with modelled tidal turbine farm
!-----
! ----start and stop element no for each turbine
nMax_elms_stop(Nfarm) = nbelm
!-----
print*, ' Turbine number of farm = ',Nfarm
print*, ' nMax_elms start = ',nMax_elms_start(Nfarm)
print*, ' nMax_elms stop = ',nMax_elms_stop(Nfarm)
enddo

! do n = 1,nMax_elms
!   Nrec   =   AD_position(n)%Nrec1
!   radius =   AD_position(n)%rad
!   current => AD_position(n)%ptr_Belement1
!   do i = 1, Nrec
!       write(impout(1),"(4g17.9)") radius,current%alpha, &
!           current%cl,current%cd
!       current => current%next
!       print*, radius,current%alpha, &
!           current%cl,current%cd
!       current => current%next
!   enddo
! enddo
! -----
! Close files at final time step
! -----
!if (irangp.le.0) then

!do ii = 1, 1

!   close(impout(ii))

! enddo

!endif
! -----
! Close files at final time step
! -----
!***** isuite if block*****
endif ! *****end of if block of isuite if block
print*, 'end of usinv'
return
contains

```

```

subroutine read_blade_design(n)
  use turbine_design
  implicit none

  type(b_section), pointer :: current,previous
  double precision rad,theta,chord,dummy
  integer n, itd ,ic,isec
  character a_nam1 * 30
  character a_nam2 * 30

  rad = 1.0
  n = 0
  open(unit=9,FILE='blade.txt',status='old')
  do while(rad > 0)
    read(9,*)rad,theta,chord,dummy,a_nam1,a_nam2
    if (rad > 0) then
      n = n + 1
      blade_position(n)%rad = rad
      blade_position(n)%theta = theta
      blade_position(n)%chord = chord
      dummy = dummy * 100.0
      if (mod(dummy,1.0) < 0.5) then
        itd = int(dummy)
      else
        itd = int(dummy) + 1
      endif
      allocate(blade_position(n)%Bsection)
      blade_position(n)%Bsection = a_nam1
      call read_blade_section(n,itd,blade_position(n))
    endif
  enddo
  close(unit=9)
  return
end subroutine read_blade_design
!=====
subroutine read_blade_section(ibdpos,ithk, bld_ptr)
  use turbine_design
  implicit none
  type(blade_element)      :: bld_ptr
  type (b_section), pointer :: current
  double precision alpha,cl,cd
  integer    count, ithk_chd,ithk,ibld, ichks,ic2
  integer    new_cnt,ithknew,ibdpos
  character  nam_given *20
  character  file_type *6
  character  file_name * 30
  character  file_name1 * 30
  character  icode * 2
  logical ex, swit
  integer, parameter :: no_of_bsecs = 2
  integer, parameter :: lift_first = 1 ! 1 is for yes otherwise no

  file_type = '.txt'

```



```

swit      = .true.
nam_given = bld_ptr%Bsection
count = index(nam_given,' ') - 1
file_name = nam_given(1:count) // file_type
if ((ithk > 9).and.(ithk < 100)) then
  icheck   = nam_given(count-1:count)
  read(icheck,*) ithk_chd
  write(icheck,'(i2)')ithk_chd
  file_name = nam_given(1:count-2) &
    // icheck// file_type
else
  ithk_chd = ithk
  swit     = .false.
  inquire(FILE= file_name,exist= ex)
  if (ex.eqv..true.) then
    print*,file_name,' found'
  else
    print*,'Error no ',file_name,' file included'
    stop
  endif
endif
!~~~~~Select the necessary blade section files~~~~~
if (swit) then
  do ichks = 1, no_of_bsecs
    ithknew = ithk_chd
    do while(ithknew > 9)
      inquire(FILE= file_name,exist= ex)
      if (ex.eqv..true.) then
        print*,file_name,' found'
        exit
      endif
      ithknew = ithknew - 1
      write(icheck,'(i2)')ithknew
      file_name = nam_given(1:count-2) &
        // icheck// file_type
    enddo
    if (ex .eqv..false.) then
      print*,'warning ',file_name,ibdpos
    else
      exit
    endif
  enddo
endif
!~~~~~
allocate(bld_ptr%ptr_bsection)
if (ex) then
  !print*,'the file is ',file_name
  open(unit=10,FILE= file_name,status='old')
  current => bld_ptr%ptr_bsection
  alpha = 0.0
  count = 1
  do
    if ( lift_first == 1) then

```

```

        read(10,*)alpha,c1,cd
    else
        read(10,*)alpha,cd,c1
    endif
    if (alpha == -999) then
        count = count - 1
        exit
    endif
    current%alpha = alpha
    current%c1    = c1
    current%cd    = cd
    allocate( current%next )
    count = count + 1
    current%next%alpha = -999
    current%next%c1    = -999
    current%next%cd    = -999
    nullify( current%next%next )
    current => current%next
enddo
close(unit=10)
else
    count = 0
    current => bld_ptr%ptr_bsection
    current%alpha = -999
    current%c1    = -999
    current%cd    = -999
    allocate( current%next )
    nullify( current%next%next )
endif
!~~~~~
bld_ptr%rec_count = count
return
end subroutine read_blade_section
!=====
end subroutine usinv

```


APPENDIX D

ustsns.f90

```
!-----
!  
!           Code_Saturne version 2.0.1  
!-----  
  
!   This file is part of the Code_Saturne Kernel, element of the  
!   Code_Saturne CFD tool.  
  
!   Copyright (C) 1998-2009 EDF S.A., France  
  
!   contact: saturne-support@edf.fr  
  
!   The Code_Saturne Kernel is free software; you can redistribute it  
!   and/or modify it under the terms of the GNU General Public License  
!   as published by the Free Software Foundation; either version 2 of  
!   the License, or (at your option) any later version.  
  
!   The Code_Saturne Kernel is distributed in the hope that it will be  
!   useful, but WITHOUT ANY WARRANTY; without even the implied warranty  
!   of MERCHANTABILITY or FITNESS FOR A PARTICULAR PURPOSE. See the  
!   GNU General Public License for more details.  
  
!   You should have received a copy of the GNU General Public License  
!   along with the Code_Saturne Kernel; if not, write to the  
!   Free Software Foundation, Inc.,  
!   51 Franklin St, Fifth Floor,  
!   Boston, MA 02110-1301 USA  
  
!-----  
  
subroutine ustsns &  
!=====
```

(idbia0 , idbra0 ,	&
ndim , ncelet , ncel , nfac , nfavor , nfml , nprfml ,	&
nnod , lndfac , lndfbr , ncelbr ,	&
nvar , nscal , nphas , ncepdp , ncesmp ,	&
nideve , nrdeve , nituse , nrtuse ,	&
ivar , iphas ,	&
ifacel , ifabor , ifmfbr , ifmcel , iprfml , maxelt , lstelt ,	&
ipnfac , nodfac , ipnfbr , nodfbr ,	&
icepdc , icetsm , itypsm ,	&
idevel , ituser , ia ,	&

```

xyzcen , surfac , surfbo , cdgfac , cdgfb , xyznod , volume , &
dt      , rtpa   , propce , propfa , propfb ,           &
coefa   , coefb  , ckupdc , smacel ,                   &
crvexp  , crvimp ,                                           &
dam     , xam    ,                                           &
w1      , w2    , w3    , w4    , w5    , w6    ,       &
rdevel  , rtuser , ra    )

=====
! Purpose:
! -----

!   User subroutine.

!   Additional right-hand side source terms for velocity components equation
!   (Navier-Stokes)

!
! Usage
! -----
! The routine is called for each velocity component. It is therefore necessary
! to test the value of the variable ivar to separate the treatments of the
! components iu(iphas), iv(iphas) or iw(iphas).
!
! The additional source term is decomposed into an explicit part (crvexp) and
! an implicit part (crvimp) that must be provided here.
! The resulting equation solved by the code for a velocity component u is:
!
! rho*volume*du/dt + .... = crvimp*u + crvexp
!
! Note that crvexp and crvimp are defined after the Finite Volume integration
! over the cells, so they include the "volume" term. More precisely:
! - crvexp is expressed in kg.m/s2
! - crvimp is expressed in kg/s
!
! The crvexp and crvimp arrays are already initialized to 0 before entering the
! the routine. It is not needed to do it in the routine (waste of CPU time).
!
! For stability reasons, Code_Saturne will not add -crvimp directly to the
! diagonal of the matrix, but Max(-crvimp,0). This way, the crvimp term is
! treated implicitly only if it strengthens the diagonal of the matrix.
! However, when using the second-order in time scheme, this limitation cannot
! be done anymore and -crvimp is added directly. The user should therefore test
! the negativity of crvimp by himself.
!
! When using the second-order in time scheme, one should supply:
! - crvexp at time n
! - crvimp at time n+1/2
!
!
! The selection of cells where to apply the source terms is based on a getcel
! command. For more info on the syntax of the getcel command, refer to the
! user manual or to the comments on the similar command getfbr in the routine

```

! usclim.

```

-----
! Arguments
-----
! name          !type!mode ! role
-----
! idbia0        ! i  ! <-- ! number of first free position in ia
! idbra0        ! i  ! <-- ! number of first free position in ra
! ndim          ! i  ! <-- ! spatial dimension
! ncelet        ! i  ! <-- ! number of extended (real + ghost) cells
! ncel          ! i  ! <-- ! number of cells
! nfac          ! i  ! <-- ! number of interior faces
! nfabor        ! i  ! <-- ! number of boundary faces
! nfml          ! i  ! <-- ! number of families (group classes)
! nprfml        ! i  ! <-- ! number of properties per family (group class)
! nnod          ! i  ! <-- ! number of vertices
! lndfac        ! i  ! <-- ! size of nodfac indexed array
! lndfbr        ! i  ! <-- ! size of nodfbr indexed array
! ncelbr        ! i  ! <-- ! number of cells with faces on boundary
! nvar          ! i  ! <-- ! total number of variables
! nscal         ! i  ! <-- ! total number of scalars
! nphas         ! i  ! <-- ! number of phases
! ncepdp        ! i  ! <-- ! number of cells with head loss terms
! ncssmp        ! i  ! <-- ! number of cells with mass source terms
! nideve, nrdeve ! i  ! <-- ! sizes of idevel and rdevel arrays
! nituse, nrtuse ! i  ! <-- ! sizes of ituser and rtuser arrays
! ivar          ! i  ! <-- ! index number of the current variable
! iphas         ! i  ! <-- ! index number of the current phase
! ifacel(2, nfac) ! ia ! <-- ! interior faces -> cells connectivity
! ifabor(nfabor) ! ia ! <-- ! boundary faces -> cells connectivity
! ifmfbr(nfabor) ! ia ! <-- ! boundary face family numbers
! ifmcel(ncelet) ! ia ! <-- ! cell family numbers
! iprfml        ! ia ! <-- ! property numbers per family
! (nfml, nprfml) !   !   !
! maxelt        ! i  ! <-- ! max number of cells and faces (int/boundary)
! lstelt(maxelt) ! ia ! --- ! work array
! ipnfac(nfac+1) ! ia ! <-- ! interior faces -> vertices index (optional)
! nodfac(lndfac) ! ia ! <-- ! interior faces -> vertices list (optional)
! ipnfbr(nfabor+1) ! ia ! <-- ! boundary faces -> vertices index (optional)
! nodfbr(lndfbr) ! ia ! <-- ! boundary faces -> vertices list (optional)
! icepdc(ncepdp) ! ia ! <-- ! index number of cells with head loss terms
! icetsm(ncesmp) ! ia ! <-- ! index number of cells with mass source terms
! itypsm        ! ia ! <-- ! type of mass source term for each variable
! (ncesmp,nvar) !   !   ! (see ustsma)
! idevel(nideve) ! ia ! <-- ! integer work array for temporary developpement
! ituser(nituse) ! ia ! <-- ! user-reserved integer work array
! ia(*)         ! ia ! --- ! main integer work array
! xyzcen        ! ra ! <-- ! cell centers
! (ndim, ncelet) !   !   !
! surfac        ! ra ! <-- ! interior faces surface vectors
! (ndim, nfac)  !   !   !
! surfbo        ! ra ! <-- ! boundary faces surface vectors

```

```

! (ndim, nfavor) ! ! ! !
! cdgfac ! ra ! <-- ! interior faces centers of gravity !
! (ndim, nfac) ! ! ! !
! cdgfbo ! ra ! <-- ! boundary faces centers of gravity !
! (ndim, nfabor) ! ! ! !
! xyznod ! ra ! <-- ! vertex coordinates (optional) !
! (ndim, nmod) ! ! ! !
! volume(ncelet) ! ra ! <-- ! cell volumes !
! dt(ncelet) ! ra ! <-- ! time step (per cell) !
! rtpa ! ra ! <-- ! calculated variables at cell centers !
! (ncelet, *) ! ! ! ! (preceding time steps) !
! propce(ncelet, *) ! ra ! <-- ! physical properties at cell centers !
! propfa(nfac, *) ! ra ! <-- ! physical properties at interior face centers !
! propfb(nfabor, *) ! ra ! <-- ! physical properties at boundary face centers !
! coefa, coefb ! ra ! <-- ! boundary conditions !
! (nfabor, *) ! ! ! !
! ckupdc(ncepdp,6) ! ra ! <-- ! head loss coefficient !
! smacel ! ra ! <-- ! value associated to each variable in the mass !
! (ncesmp,nvar) ! ! ! ! source terms or mass rate (see ustsma) !
! crvexp ! ra ! --> ! explicit part of the source term !
! crvimp ! ra ! --> ! implicit part of the source term !
! dam(ncelet) ! ra ! --- ! work array !
! xam(nfac,2) ! ra ! --- ! work array !
! w1,2,3,4,5,6 ! ra ! --- ! work arrays !
! (ncelet) ! ! ! ! (computation of pressure gradient) !
! rdevel(nrdeve) ! ra ! <-> ! real work array for temporary developpement !
! rtuser(nituse) ! ra ! <-- ! user-reserved real work array !
! ra(*) ! ra ! --- ! main real work array !
!-----!-----!-----!-----!-----!-----!-----!-----!-----!-----!

```

```

! Type: i (integer), r (real), s (string), a (array), l (logical),
! and composite types (ex: ra real array)
! mode: <-- input, --> output, <-> modifies data, --- work array
!=====

```

```

use turbine_design
use connectivity
implicit none

```

```

!=====
! Common blocks
!=====

```

```

include "paramx.h"
include "pointe.h"
include "numvar.h"
include "entsor.h"
include "optcal.h"
include "cstphy.h"
include "parall.h"
include "period.h"

```

```

!=====

```

! Arguments

```
integer      idbia0 , idbra0
integer      ndim  , ncelet , ncel  , nfac  , nfabor
integer      nfml  , nprfml
integer      nnod  , lndfac , lndfbr , ncelbr
integer      nvar  , nscal , nphas
integer      ncepdp , ncesmp
integer      nideve , nrdeve , nituse , nrtuse
integer      ivar  , iphas
```

```
integer      ifacel(2,nfac) , ifabor(nfabor)
integer      ifmibr(nfabor) , ifmcel(ncelet)
integer      iprfml(nfml,nprfml), maxelt, lstelt(maxelt)
integer      ipnfac(nfac+1), nodfac(lndfac)
integer      ipnfbr(nfabor+1), nodfbr(lndfbr)
integer      icepdc(ncepdp)
integer      icetsm(ncesmp), itypsm(ncesmp,nvar)
integer      idevel(nideve), ituser(nituse), ia(*)
```

```
double precision xyzcen(ndim,ncelet)
double precision surfac(ndim,nfac), surfbo(ndim,nfabor)
double precision cdgfac(ndim,nfac), cdgfb(ndim,nfabor)
double precision xyznod(ndim,nnod), volume(ncelet)
double precision dt(ncelet), rtpa(ncelet,*)
double precision propce(ncelet,*)
double precision propfa(nfac,*), propfb(nfabor,*)
double precision coefa(nfabor,*), coefb(nfabor,*)
double precision ckupdc(ncepdp,6), smacel(ncesmp,nvar)
double precision crvexp(ncelet), crvimp(ncelet)
double precision dam(ncelet), xam(nfac,2)
double precision w1(ncelet), w2(ncelet), w3(ncelet)
double precision w4(ncelet), w5(ncelet), w6(ncelet)
double precision rdevel(nrdeve), rtuser(nrtuse), ra(*)
```

! Local variables

```
character*80  chaine
integer      idebia, idebra
integer      iel, ipcrom, ipp, iutile, ifac,i,Nfarm
integer      ilelt, nlelt, iel1, iel2, nold_tstep, Nrec, ii, impout(6)
integer      :: ncall = 0 ! fortran static variable
double precision ckp, qdm, x_dist, y_dist, radius, disc_patch, z_dist
double precision F_prandtl, tval1, tval2, density, chord, frac_val, elm_area, azim_ang
double precision ux, uy, uz, u_theta, phi, cl, cd, cl1, cl2, cd1
double precision cd2, alpha, alpha1
double precision rad2deg, val_d, W_rel2, W_rel
double precision Cn_2D, Ct_2D, Cn_3D, Ct_3D, dF_theta, dF_z, dF_cel_theta, dF_cel_z, k_value
double precision accm_T, accm_P, C_T, C_p
double precision, parameter :: pi = 3.1415926535897932384626433832795028841971693993751058209749445923078164062
double precision, parameter :: U_inf = 0.45 ! m/s
double precision, parameter :: omega = 15.0 ! rotational speed of turbine in radians per second
integer, parameter      :: Nb = 3 ! number of blades with the turbine
```



```

integer, parameter      :: Nfarmax   = 2 ! number of turbines modelled
Logical, parameter     :: iflow     = .true. ! clockwise rotation from upstream & axial flow in
type (b_section), pointer :: ptr_bsection
Logical                ichk

! blade design variables
integer n, nbelm
type(b_section), pointer :: current,previous,check

!=====

! -- setup output files --
do ii = 1,3

    impout(ii) = impusr(ii)

enddo
open(impout(1),file='CT_Cp_results1.dat')
open(impout(2),file='CT_Cp_results2.dat')
open(impout(3),file='Clcdmap.dat')
! -----

!=====
! 1. Initialization
!=====

idebia = idbia0
idebra = idbra0
ncall = ncall + 1
rad2deg = 180.0/pi
ipp     = ipprtp(ivar)
iphas  = 1
if(iwarni(ivar).ge.1) then
    chaine = nomvar(ipp)
    write(nfecra,1000) chaine(1:8)
endif

ipcrom = ipproc(irom (iphas))
!=====
! 2. Calculating current momentum blade element forces
!=====

if ( ncall == 1) then
do Nfarm = 1, Nfarmax
    accm_T = 0.0
    accm_P = 0.0
    do nbelm = nMax_elms_start(Nfarm), nMax_elms_stop(Nfarm)
        iel      = AD_position(nbelm)%nCel
        x_dist   = xyzcen(1,iel)
        y_dist   = xyzcen(2,iel)
        z_dist   = xyzcen(3,iel)
        density  = propce(iel,ipcrom)
    enddo
enddo

```

```

radius  = AD_position(nbelm)%rad
chord   = AD_position(nbelm)%chord
frac_val = AD_position(nbelm)%frac_v
elm_area = AD_position(nbelm)%elm_area
azim_ang = AD_position(nbelm)%azim_deg
! -----
! Calculate blade element forces in blade fixed coordinates
! -----

! -----
! Note ux,uy,uz are in flow fixed coords
! -----
ux      = rtpa(iel, iu(iphas) )
uy      = rtpa(iel, iv(iphas) )
uz      = rtpa(iel, iw(iphas) )
! -----
! Note u_theta is equiv to uy in in blade fixed coordinates
! -----
if (iflow) then
  uz = -uz
endif
!if(ntcabs > 137) then
!print*, 'step1', radius, frac_val, ux, uy, uz
!endif
  u_theta = - (uy * dcos(azim_ang)) + (ux * dsin(azim_ang) ) + (omega * radius)
  phi     = datan2(uz, u_theta)
  alpha   = phi - AD_position(nbelm)%twist
  Nrec    = AD_position(nbelm)%Nrec1
  if (Nrec == 0) then
    print*, 'Nrec = ', Nrec
    print*, 'radius = ', radius, ' twist = ', AD_position(nbelm)%twist, &
      'phi = ', phi, ' nbelm = ', nbelm
    stop
  endif
  ptr_bsection => AD_position(nbelm)%ptr_Belement1
!if(ntcabs > 137) then
!print*, 'step2', u_theta, phi, alpha
!endif
  call find_cl_cd(alpha, Nrec, ptr_bsection, cl1, cd1, ichk)
  !if (ichk) then
  ! print*, '1st ptr'
  ! print*, 'radius = ', radius
  !endif
  Nrec    = AD_position(nbelm)%Nrec2
  if (Nrec == 0) then
    print*, 'Nrec = ', Nrec
    print*, 'radius = ', radius, ' twist = ', AD_position(nbelm)%twist, &
      'phi = ', phi, ' nbelm = ', nbelm
    stop
  endif
!if(ntcabs > 137) then
!print*, 'step3', cl1, cd1
!endif

```

```

ptr_bsection => AD_position(nbelm)%ptr_Belement2
call find_cl_cd(alpha,Nrec,ptr_bsection,cl2,cd2,ichk)
!if (ichk) then
!  print*, '2nd ptr'
!  mpout(1), "(i5,2g17.9)") ntcabs,C_T,C_pprint*, 'radius = ', radius
!endif
cl = cl1 + frac_val * (cl2 - cl1)
cd = cd1 + frac_val * (cd2 - cd1)
!***** recoding L/D values on the disc *****
if (cd > 0.0) then
  clcd_val(nbelm) = cl/cd
else
  clcd_val(nbelm) = 0.0
endif
!*****
Cn_2D = cl * dcos(phi) + cd * dsin(phi)
Ct_2D = cl * dsin(phi) - cd * dcos(phi)
! -----
!  Calculating the Prandtl Tip Loss factor F_prandtl
! -----
if (dabs(radius) < tiny(1.0)) call error_message("error1 ustsns function")
tval1 = Nb * (1.0 - rotor_radius/radius)
tval2 = 2.0 * dsin(phi)
!if(ntcabs > 137) then
!print*, 'step4', Cn_2D, Ct_2D, tval1, tval2
!endif
  if (dabs(tval2) > tiny(1.0)) then
    F_prandtl = (2.0/pi) * dacos(dexp(tval1/tval2))
    if ((F_prandtl < 0).or.(F_prandtl > 1.0)) call error_message("error2 ustsns function")
  else
    F_prandtl = 1.0
  endif
!if(ntcabs > 137)then
!print*, 'step5', F_prandtl
!endif
  Cn_3D = F_prandtl * Cn_2D
  Ct_3D = F_prandtl * Ct_2D
! -----
!  Note W_rel2 = (uz * uz) + (u_theta * u_theta) has not been included here
!  since source terms crimpi & crvexpi require k * W_rel2 format for forces
! -----
  dF_theta = 0.5 * chord * density * Ct_3D
  dF_z = 0.5 * chord * density * Cn_3D
!if(ntcabs > 137)then
!print*, 'step6', radius
!endif
  dF_cel_theta = Nb * dF_theta * elm_area/(2.0 * pi * radius)
  dF_cel_z = Nb * dF_z * elm_area/(2.0 * pi * radius)
! -----
!  Convert blade element forces into flow fixed coordinates
! -----
  AD_position(nbelm)%dFX = - dF_cel_theta * dsin(azim_ang)
  AD_position(nbelm)%dFY = dF_cel_theta * dcos(azim_ang)

```

```

if (iflow) then
  AD_position(nbelm)%dFZ = dF_cel_z
else
  AD_position(nbelm)%dFZ = - dF_cel_z
endif
W_rel2 = (u_theta * u_theta) + (uz * uz)
accm_T = accm_T + ( dF_cel_z * W_rel2 )
accm_P = accm_P + ( radius * omega * dF_cel_theta * W_rel2 )
enddo
C_T = accm_T/(0.5 * density * Frontal_Area(Nfarm) * U_inf * U_inf)
C_p = accm_P/(0.5 * density * Frontal_Area(Nfarm) * U_inf * U_inf * U_inf)
if (Nfarm == 1) then
  write(impout(1),"(2i5,2g17.9)") ntcabs,Nfarm,C_T,C_p
else
  write(impout(2),"(2i5,2g17.9)") ntcabs,Nfarm,C_T,C_p
endif

enddo ! end of loop for Nfarm
endif

!=====
! 2. Example of arbitrary source term for component u:

!
!           S = A * u + B
!
!   appearing in the equation under the form:
!
!           rho*du/dt = S (+ standard Navier-Stokes terms)

!In the following example:
! A = -rho*CKP
! B = XMMT
!
!with:
! CKP = 1.DO [1/s      ] (return term on velocity)
! MMT = 100.DO [kg/m2/s2] (momentum production by volume and time unit)
!
!which yields:
!   crvimp(iel) = volume(iel)* A = - volume(iel)*(rho*CKP )
!   crvexp(iel) = volume(iel)* B =  volume(iel)*(XMMT   )

! -----

! It is quite frequent to forget to remove this example when it is
! not needed. Therefore the following test is designed to prevent
! any bad surprise.

!iutile = 0

!if(iutile.eq.0) return

```

```

! -----
! -----
! Calculate the momentum source terms Sx, Sy and Sz for actuator disc representation
! -----
!if(ntcabs > 137) then
!print*, 'step7'
!endif
do nbelm = 1, nMax_elms_stop(Nfarmax)
  iel      = AD_position(nbelm)%nCel
  ux      = rtpa(iel, iu(iphas) )
  uy      = rtpa(iel, iv(iphas) )
  uz      = rtpa(iel, iw(iphas) )

  radius  = AD_position(nbelm)%rad
  azim_ang = AD_position(nbelm)%azim_deg
  u_theta = - (uy * dcos(azim_ang)) + (ux * dsin(azim_ang) ) + (omega * radius)
  W_rel2 = (u_theta * u_theta) + (uz * uz)
  !-----Sx source term -----
  if (ivar.eq.iu(1)) then
    k_value      = - AD_position(nbelm)%dFX
!    crvimp(iel) = min(0.0, (- 2.0 * k_value * dsin(azim_ang) * u_theta) )
    crvimp(iel) = - 2.0 * k_value * dsin(azim_ang) * u_theta
    crvexp(iel) = - k_value * ( W_rel2 - (2.0 * dsin(azim_ang) * u_theta * ux) )
!-----Sy source term -----
  else if (ivar.eq.iv(1)) then
    k_value      = - AD_position(nbelm)%dFY
!    crvimp(iel) =  min(0.0, (2.0 * k_value * dcos(azim_ang) * u_theta))
    crvimp(iel) =  2.0 * k_value * dcos(azim_ang) * u_theta
    crvexp(iel) =  - k_value * ( W_rel2 + (2.0 * dcos(azim_ang) * u_theta * uy) )
!-----Sz source term -----
  else if (ivar.eq.iw(1)) then
    k_value      = - AD_position(nbelm)%dFZ
!    crvimp(iel) = min(0.0, (- 2.0 * k_value * uz) )
    crvimp(iel) = - 2.0 * k_value * uz
    crvexp(iel) =  k_value * ( (uz * uz) - (u_theta * u_theta) )
  endif
enddo
! -----
! end of loop for momentum source terms consists of Sx, Sy and Sz
! -----
!if (ntcabs > 137) then
!print*, 'step8'
!endif
! -----
! deallocate dynamic arrays associated with the 2D blade design data base
! the Actuator Disc elements
! -----
if ((ncall == 3).and.( ntcabs >= ntmabs)) then
  do n = 1, n_be
    current => blade_position(n)%ptr_bsection
    do while ( associated( current ) )
      previous => current
    enddo
  enddo
endif

```

```

        current => current%next
        deallocate( previous )
    end do
    enddo ! loop of n_be
    deallocate(blade_position)
    do n = 1, nMax_elms_stop(Nfarmax)
        current => AD_position(n)%ptr_Belement1
        do while ( associated( current ) )
            previous => current
            current => current%next
            deallocate( previous )
        end do
    enddo
    do n = 1, nMax_elms_stop(Nfarmax)
        current => AD_position(n)%ptr_Belement2
        do while ( associated( current ) )
            previous => current
            current => current%next
            deallocate( previous )
        end do
    enddo
    deallocate(AD_position)
    ! -----
    ! Close files at final time step
    ! -----
    !if (irangp.le.0) then

    do ii = 1, 1

        close(impout(ii))

    enddo

    !endif
    ! -----
    ! Close files at final time step
    ! -----
endif
!-----

!-----
! Formats
!-----

1000 format(' User source termes for variable ',A8,/)

!----
! End
!----
if (ncall == 3) then
    print*, ' time step = ', ntcabs
    ncall = 0
endif

```

return
contains

```

subroutine find_cl_cd(alpha,Nrec,ptr_bsect,cl,cd,icheck)
  use turbine_design
  implicit none
  integer      irec,Nrec,n
  double precision cl,cd,cl1,cl2,cd1,cd2,alpha,alpha1,alpha2,interp1,interp
  double precision, parameter :: v_small = 1.0d-6
  double precision, parameter :: alfmin = -3.14
  double precision, parameter :: cd_max = 1.07
  type (b_section), pointer :: ptr_bsect
  logical icheck

  icheck = .true.
  n = Nrec - 1
  if (alpha > alfmin) then
    do irec = 1,n
      alpha1 = ptr_bsect%alpha
      if (alpha1 == -999) call error_message("error1 with find_cl_cd")
      cl1 = ptr_bsect%cl
      cd1 = ptr_bsect%cd
      ptr_bsect => ptr_bsect%next
      alpha2 = ptr_bsect%alpha
      if (alpha2 == -999) call error_message("error2 with find_cl_cd")
      cl2 = ptr_bsect%cl
      cd2 = ptr_bsect%cd
      if ((alpha >= alpha1).and.(alpha <= alpha2)) then
        icheck = .false.
        exit
      endif
    enddo
    interp1 = (alpha2 -alpha1)
    if (dabs(interp1) < v_small)then
      call error_message("error4 with find_cl_cd")
    endif
    interp = (alpha -alpha1)/interp1
    cl = cl1 + interp *(cl2 -cl1)
    cd = cd1 + interp *(cd2 -cd1)
    if (cd > cd_max) cd = cd_max
  else
    alpha1 = ptr_bsect%alpha
    if (alpha1 == -999) call error_message("error1 with find_cl_cd")
    cl1 = ptr_bsect%cl
    cd2 = ptr_bsect%cd
    ptr_bsect => ptr_bsect%next
    alpha2 = ptr_bsect%alpha
    if (alpha1 == -999) call error_message("error2 with find_cl_cd")
    cl2 = ptr_bsect%cl
    cd1 = ptr_bsect%cd
    interp1 = (alpha2 -alpha1)
    if (dabs(interp1) < v_small)then
      call error_message("error4 with find_cl_cd")
    endif
  endif
end subroutine

```

```
endif
  interp = (alpha -alpha1)/interp1
  cl = c11 + interp *(c12 -c11)
  cd = 0.5 * (cd2 + cd1)
endif
return
end subroutine find_cl_cd
end subroutine ustsns
```


Bibliography

- Bryden, I., Couch, S., Owen, A., and Melville, G. (2007). Tidal current resource assessment. *Proceedings of the Institution of Mechanical Engineers, Part A: Journal of Power and Energy*, 221(2):125–154.
- Childs, H., Brugger, E., Bonnell, K., Meredith, J., Miller, M., Whitlock, B., and Max, N. (2005). A contract-based system for large data visualization. In *Proceedings of IEEE Visualization*, pages 190–198.
- Crawley, M. (2007). *The R Book*. John Wiley & Sons, Chichester, England.
- EDF (2012). Code_Saturne version 2.0.6 practical user’s guide. Technical report, Fluid Dynamics, Power Generation and Environment Department, EDF R&D, 6, Quai Watier, F-78401 Chatou CEDEX.
- Foley, J. and Van Dam, A. (1982). *Fundamentals of interactive computer graphics*. Addison-Wesley, Reading, Mass.
- Halse, M., Curtis, C., and McCormick, L. (1991). *IRIS Explorer Users Guide*. Silicon Graphics Inc, Mountain View, California.
- Hansen, M. (2001). *Aerodynamics of Wind Turbines : Rotors, Loads and Structure*. James and James (Science Publishers) Ltd.
- Harrison, M., Batten, W., Myers, L., and Bahaj, A. (2010). Comparison between CFD simulations and experiments for predicting the far wake of horizontal axis tidal turbines. *IET Renewable Power Generation*, 4(6):613–627.
- Horlock, J. (1978). *Actuator disk theory - Discontinuities in thermo-fluid dynamics*. McGraw-Hill International Book Co., New York.
- Ihaka, R. and Gentleman, R. (1996). R: A language for data analysis and graphics. *Journal of Computational and Graphical Statistics*, 5(3):299–314.
- Ingram, D., Gao, F., Causon, D., Mingham, C., and Troch, P. (2005). Numerical wave flume simulations of seawall overtopping. In Smith, J., editor, *Coastal Engineering 2004*, volume 4, pages 4560–4572. World Scientific, Singapore.
- Joy, K., Miller, M., Childs, H., Bethel, E., Clyne, J., Ostrouchov, G., and Ahern, S. (2007). Frameworks for visualization at the extreme scale. *Journal of Physics: Conference Series*, 78:012035.

- Larkin, S. (1992). Evaluation of visualisation systems. Technical report, Advisory Group on Computer Graphics (AGOCG). Available from Dr A Mumford, Computer Centre, Loughborough University of Technology.
- Mikkelsen, R. (2003). *Actuator Disc Methods Applied to Wind Turbines*. PhD thesis, Technical University of Denmark, ISBN 87-7475-296-0.
- Moulinec, C., Denis, C., Pham, C.-T., Rougé, D., Hervouet, J.-M., Razafindrakoto, E., Barber, R., Emerson, D., and Gu, X.-J. (2011). TELEMAC: An efficient hydrodynamics suite for massively parallel architectures. *Computers and Fluids*, 15(1):30–34.
- Nguyen, Q. (2011). k-omega sst is not applicable for roughness study in saturne.
- Prandtl, L. and Betz, A. (1927). Vier abhandlungen zur hydrodynamik und aerodynamic. Technical report, Göttingen.
- Richardson, S., Ingram, D., Mingham, C., and Causon, D. (2002). On the validity of the shallow water equations for violent wave overtopping. In Edge, B., editor, *Ocean Wave Measurement and Analysis*, pages 1112–1125. ASCE, Reston, Virginia.
- Richardson, S., Pullen, T., and Clarke, S. (2003). Jet velocities of overtopping waves on sloping structures: Measurement and computation. In Smith, J., editor, *Proceedings of the 29th International Congress on Coastal Engineering*, volume 2, pages 2239–2250, New Jersey. ASCE, Reston, Virginia, World Scientific.